

## **IARC Technical Report # 2**

# **Report of the NABOS/CABOS 2004 Expeditions in the Arctic Ocean**

With support from the National Science Foundation  
Grant # 0327664



# TABLE OF CONTENTS

	Page #
<b>PREFACE</b> ( <i>I.Polyakov, IARC</i> ).....	7
<b>I. NABOS-04 EXPEDITION IN THE NORTHERN LAPTEV SEA ABOARD THE ICEBREAKER KAPITAN DRANITSYN (SEPTEMBER 2004)</b> .....	<b>9</b>
I.1. INTRODUCTION ( <i>I.Polyakov and I.Dmitrenko, IARC</i> ).....	11
I.2. RESEARCH VESSEL ( <i>I.Dmitrenko, IARC</i> ) .....	11
I.3. CRUISE TRACK ( <i>I.Dmitrenko, IARC, and V.Smolianitsky, AARI</i> ).....	14
I.4. SCIENTIFIC PARTY ( <i>I.Dmitrenko, IARC, and L.Timokhov, AARI</i> ).....	15
I.5. ICE CONDITIONS ( <i>V.Smolianitsky, AARI</i> ).....	16
I.6. METEOROLOGICAL CONDITIONS ( <i>O.Andreev, AARI</i> ).....	20
I.7. OBSERVATIONS ( <i>I.Dmitrenko, IARC, and L.Timokhov, AARI</i> ).....	23
I.7.1. AIR-ICE INTERACTION OBSERVATIONS ( <i>I.Repina, IAF</i> ).....	24
I.7.1.1. Introduction.....	24
I.7.1.2. Objectives.....	24
I.7.1.3. Methods and equipment.....	24
I.7.1.4. Preliminary results.....	25
I.7.2. ICE OBSERVATIONS ( <i>V.Smolianitsky, AARI</i> ).....	27
I.7.2.1. Background information.....	27
I.7.2.2. Objectives.....	28
I.7.2.3. Sea ice observations and processing.....	28
I.7.2.3.1. Shipborne ice observations and processing.....	28
I.7.2.3.2. Satellite ice observations and processing.....	31
I.7.2.3.3. Ice observations during ice stations.....	33
I.7.3. OCEANOGRAPHIC OBSERVATIONS.....	37
I.7.3.1. Background information ( <i>I.Polyakov, IARC, and D.Walsh, NRL</i> ).....	37
I.7.3.2. Routine CTD Measurements and Water Sampling.....	39
I.7.3.2.1. Objectives ( <i>I.Polyakov and I.Dmitrenko, IARC</i> ).....	39
I.7.3.2.2. Methods ( <i>I.Dmitrenko, IARC, and S.Kirillov, AARI</i> ).....	39
I.7.3.2.3. Equipment ( <i>R.Chadwell, IARC, and M.Dempsey, OM</i> ).....	40
I.7.3.2.4. Preliminary Results ( <i>I.Dmitrenko, IARC, S.Kirillov, and L.Timokhov, AARI</i> ).....	41
I.7.3.3. Moorings Observations.....	47
I.7.3.3.1. Objectives ( <i>I.Polyakov and I.Dmitrenko, IARC</i> ).....	47
I.7.3.3.2. Mooring Design and Equipment ( <i>R.Chadwell, IARC, and M.Dempsey, OM</i> ).....	47
I.7.3.3.3. Bottom topography at deployment sites ( <i>O.Churkin, SRNHI</i> ).....	50
I.7.3.3.4. Mooring Deployments ( <i>R.Chadwell, IARC, and M.Dempsey, OM</i> ).....	53
I.7.3.3.5. Mooring Recovery ( <i>R.Chadwell, IARC, and M.Dempsey, OM</i> ).....	56
I.7.3.3.6. Preliminary Results ( <i>I.Dmitrenko, I.Polyakov, IARC, L.Timokhov, AARI, and D.Walsh, NRL</i> ).....	57
I.7.4. CHEMICAL OBSERVATIONS ( <i>M.Nitishinskiy, AARI and A.Vetrov, IO</i> ).....	64
I.7.4.1. Objectives .....	64
I.7.4.2. Methods and Equipment .....	64
I.7.4.3. Preliminary Results.....	66

I.7.5. BIOLOGICAL OBSERVATIONS ( <i>M.Ringuette, C.Bouchard, A.Forest, and L.Fortier, LU</i> ).....	70
I.7.5.1. Objectives.....	70
I.7.5.2. Methods and Equipment.....	71
I.7.5.3. Preliminary Results.....	72
I.7.6. ICE BUOYS DEPLOYMENTS ( <i>I.Dmitrenko, IARC</i> ) .....	73
<b>II. EXPEDITION TO THE WESTERN NANSEN BASIN ABOARD R/V LANCE (SEPTEMBER 2004).....</b>	<b>75</b>
II.1. INTRODUCTION .....	76
II.2. RESEARCH VESSEL .....	76
II.3. CRUISE TRACK .....	77
II.4. SCIENTIFIC PARTY .....	77
II.5. WEATHER AND ICE CONDITIONS .....	78
II.6. OCEANOGRAPHIC OBSERVATIONS .....	78
II.6.1. Background information .....	78
II.6.2. CTD Measurements .....	79
II.6.2.1. Methods .....	80
II.6.2.2. Equipment .....	80
II.6.2.3. Preliminary Results .....	80
II.6.3. Moorings Observations.....	84
II.6.3.1. Mooring Design and Equipment .....	84
II.6.3.2. Mooring Deployment.....	84
<b>III. CRUISE REPORT OF THE CABOS-04 EXPEDITION TO THE BEAUFORT SEA ABOARD CANADIAN COAST GUARD ICEBREAKER <i>Louis S. St-Laurent</i> , SEPTEMBER 2004 .....</b>	<b>87</b>
III.1. INTRODUCTION .....	88
III.2. RESEARCH VESSEL AND CRUISE PLAN.....	89
III.3. MOORING RECOVERY AND DEPLOYMENT.....	89
III.3.1. Mooring Recovery .....	90
III.3.2. Mooring Deployment.....	93
III.4. A PRELIMINARY LOOK AT THE LATEST MMP DATA .....	95
<b>REFERENCE .....</b>	<b>98</b>
Appendix 1: NABOS-04 STATION LIST ( <i>I.Dmitrenko, IARC, and S.Mastrukov, SRNHI</i> ).....	101
Appendix 2: Ship track of icebreaker Kapitan Dranirsyn during NABOS-04 expedition ( <i>V.Smolianitsky, AARI</i> ).....	111
Appendix 3: RV Lance cruise log.....	112
Appendix 4: RV Lance Station List.....	114

## **GLOSSARY:**

**IARC:** International Arctic Research Center, University of Alaska Fairbanks, Alaska, USA

**NLR:** Naval Research Laboratory, USA

**IOS:** Institute of Ocean Sciences, BC, Canada

**OM:** Oceanetic Measurement Ltd., Sidney, BC, Canada

**LU:** Laval University, Quebec City, Quebec, Canada

**NPI** Norwegian Polar Institute, Tromser, Norway

**AARI:** Arctic and Antarctic Research Institute, St.Petersburg, Russia

**IAF:** Institute of Atmospheric Physics, Russian Academy of Science, Moscow, Russia

**IO:** Institute of Oceanology, Russian Academy of Science, Moscow, Russia

**SRNHI:** State Research Navigation and Hydrographic Institute, St.Petersburg, Russia



## PREFACE

Motivated by scarceness of observational data, in 1999 a group of scientists of the International Arctic Research Center (IARC) at the University of Alaska Fairbanks (UAF) initiated a discussion about needs in a large-scale Arctic Ocean mooring-based observational program. By 2000, major features of this program had been shaped. With carefully chosen mooring sites, advanced pioneering technologies, and cooperative spirit this observational program targets long-term large-scale Arctic Ocean climate change and variability. In September 2001, in cooperation with our Canadian colleagues from the Institute of Ocean Sciences (IOS), BC the first mooring was deployed at the Beaufort Sea slope. Since then our growing project called NABOS/CABOS (NABOS=Nansen and Amundsen Basins Observational System and CABOS=Canadian Basin Observational System) became an internationally recognized and scientifically sound Arctic Ocean observational program. For example, our project became a part of major observational programs like the NSF-led SEARCH program and the EU-led DAMOCLES program. The intention is to make the NABOS/CABOS one of the key parts of the international Mooring-based Arctic Ocean Observational System (MAOOS) proposed for the International Polar Year (IPY). Under the stimulus of the IPY, MAOOS will become the most comprehensive mooring-based observational system in the Arctic Ocean.

This Report reflects the fact of the NABOS/CABOS program's growing maturity. It includes three sections in which field operations in three different parts of the Arctic Ocean are described. Section I describes the core NABOS program under which, in cooperation with our Russian, US, Canadian, and German colleagues, we collect data in the eastern part of the Eurasian Basin. The second Section is devoted to our youngest project under which, together with our Norwegian colleagues, we conduct observations in the vicinity of Svalbard. The last Section describes our observations in the Canada Basin where we continue our cooperative work with IOS scientists. These three parts together comprise our cooperative, coordinated approach planned for the growing large-scale mooring-based observational program of the Arctic Ocean.

Igor Polyakov







## SECTION I

### **NABOS-04 Expedition in the Northern Laptev Sea aboard the Icebreaker *Kapitan Dranitsyn* (September 2004)**

Igor Dmitrenko<sup>1</sup>, Leonid Timokhov<sup>2</sup>, Oleg Andreev<sup>2</sup>, Robert Chadwell<sup>1</sup>,  
Oleg Churkin<sup>4</sup>, Michael Dempsey<sup>3</sup>, Sergey Kirillov<sup>2</sup>, Vasiliy Smolianitsky<sup>2</sup>,  
Sergey Mastrukov<sup>4</sup>, Miroslav Nitishinskiy<sup>2</sup>, Igor Polyakov<sup>1</sup>, Irina Repina<sup>5</sup>,  
Marc Ringuette<sup>6</sup>, Alexandr Vetrov<sup>7</sup>, and David Walsh<sup>8</sup>

1 - International Arctic Research Center  
University of Alaska Fairbanks  
Fairbanks, Alaska, USA

2 - Arctic and Antarctic Research Institute  
St.Petersburg, Russia

3 - Oceanetic Measurement Ltd.  
Sidney, BC, Canada

4 - State Research Navigation and Hydrographic Institute,  
St.Petersburg, Russia

5 – Institute of Atmospheric Physics, Russian Academy of Science  
Moscow, Russia

6 – Laval University,  
Québec City, Québec, Canada

7 – Institute of Oceanology, Russian Academy of Science  
Moscow, Russia

8 – Naval Research Laboratory  
USA



Scientific Party of the NABOS-04 Cruise  
to the Laptev Sea

## **I.1. INTRODUCTION** (*I.Polyakov and I.Dmitrenko, IARC*)

NABOS (Nansen and Amundsen Basins Observational System) is one of the major International Arctic Research Center (IARC) initiatives. NABOS is a long-term program aimed to provide a quantitative observationally based assessment of circulation, water mass transformations, and transformation mechanisms along the principal pathways transporting water from the Nordic Seas into the central Arctic Basin. The scope of the field problem clearly calls for international cooperation/coordination, a task commensurate with an international center. NABOS is currently conducted jointly by the IARC, the Institute of Marine Science (IMS), Canada, the Arctic and Antarctic Research Institute (AARI), Russia, and the Norwegian Polar Institute (NPI), Norway in cooperation with University of Washington (International Arctic Buoy Project) and Wilfred Wegener Institute for Polar and Marine Research (AWI), Germany. By now NABOS has become a major IARC initiative.

The primary monitoring tool of the NABOS program is the series of moorings placed at carefully chosen locations around the Arctic Ocean. Time series obtained from these moorings will allow separation of synoptic-scale signal (e.g., eddies, shelf waves) from longer-term climatic signal. Located along the major pathways of water, heat, and salt transport, such moorings capture climatically important changes in oceanic conditions. The NABOS moorings operate for one year at a time, with replacement every year. A gradual increase in the number of moorings is planned, from two deployed in summer 2002, to the full-scale monitoring system after several years.

This report describes field research during the oceanographic cruise NABOS-04 aboard the icebreaker “Kapitan Dranitsyn” in September 2004. It was the third NABOS expedition. The overarching goal of the 2004 field program was to characterize the oceanographic, ice, and biological conditions in the northern part of the Laptev Sea in 2004 along with mooring deployments and recovery.

## **I.2. RESEARCH VESSEL** (*I.Dmitrenko, IARC*)

The Russian icebreaker “Kapitan Dranitsyn” (Figure I.2.1) has been chartered by the University of Alaska Fairbanks to carry out oceanographic research over the continental slope of the Siberian Arctic shelf. The ship is under the operation of the Murmansk Shipping Company located in Murmansk, Russia. I/B “Kapitan Dranitsyn” is a powerful conventional propelled ice breaker, constructed in 1982. It was intended for working in the conditions of the Northern Sea Route and the Baltic Sea. The vessel was built at Wartsila Shipyard, Helsinki, Finland; on December 2, 1980 she was accepted by the crew and registered under Russia’s flag. In 1994 the icebreaker was remodeled in Finland; later she was reequipped for passenger operations. In 1999 she was updated in Norway and got a passenger vessel certificate. The icebreaker’s main technical characteristics are presented in Table I.2.1.

The ship may be navigated from two positions on the bridge and from an aft auxiliary bridge (ice can also be broken when traveling stern-first). An air curtain system is applied to assist ice-breaking (air at  $0.8 \text{ kg cm}^{-2}$  is discharged through vents from forward to midships 2 m above the keel). Ice friction is reduced by polymeric coatings on the ice skirt. A cushioned stern allows close towing when vessels are being assisted through ice. Pumps can move 74 tons of water a minute between ballast and heeling tanks. Fresh water is provided from a vacuum distillation apparatus heated by exhaust gasses, which is supplemented by a reverse osmosis apparatus. A maximum of 80 tons a day can be produced. Two helicopters are carried to assist ice navigation. Safety equipment includes 4 fully enclosed life-boats and 4 inflatable life rafts (total capacity 264 persons). The fuel consumption rate is shown in Table I.2.1. The icebreaker is

equipped with 3 deck cranes. Two forward cranes can lift 3 tons each, and one on the helicopter deck lifts up to 10 tons.



**Figure I.2.1:** Icebreaker “Kapitan Dranitsyn” on NABOS-02 cruise in the northern Laptev Sea.

**Table I.2.1:** The main technical characteristics of I/B “Kapitan Dranitsyn”

Displacement	15000 t (full load)
Draft	8.5 m
Breadth	26.75 m
Length	121 m (waterline), 132.4 m (overall)
Height	48.7 m
Main engines	6 Wärtsilä-Sulzer 9 ZL40/48 Diesel sets developing 18.5MW (24,200 horse power) which drive 6 AC generators
Propulsion	3 twin DC electric motors, each producing 5400 kW in either direction, turn the 22m long propeller shafts (one spare shaft is carried)
Propellers	3, fixed pitch, 4.3 m diameter with 4 hardened steel blades turn at about 110 to 200 r/m. Spare blades are carried which can be deployed at sea
Auxiliary power	5 alternating current generator sets developing 730kW (2200 horse power)
Fuel	IFO-30 for main diesel sets, MGO for auxiliary generator sets
Fuel storage	2800 tons IFO-30 and 600 tons MGO
Hull thickness	45 mm where ice is met (the ice skirt) and 22-35 mm elsewhere
Speed	Full: 19 knots (35.2 km/h) with 6 engines; cruising speed: 16 knots (30 km/h) in calm open water; ice 1.5 m thick may be broken at 1 knot (1.8 km/h), 3 m has been broken by repeated ramming.
Ice class	KM*LL3 A2
Operating range	10 500 nautical miles (19 500 km) at 16 knots (30 km/h)
Anchors	2 weighing 6 tons each, with 300 m chains, and one spare
Crew and passengers	60 and 102

**Table I.2.2:** Fuel consumption of I/B “Kapitan Dranitsyn”. Data provided by Murmansk Shipping Company

Consumption for main diesel sets (IFO-30)		Additional consumption (IFO-30)	
Number of Diesels	Fuel Consumption (tons/day)	Air Temperature (grad. C)	Fuel Consumption (tons/day)
1	15.6	+15	2.5
2	31.2	+5	3.5
3	46.8	-10	5.0
4	62.4	-30	6.0
5	78.0	Site Consumption	Consumption Rate MGO/IFO
6	93.6	4 tons/day	1/25



**Figure I.2.2:** LEBUS double-drum oceanographic winch on the helicopter deck of I/B “Kapitan Dranitsyn” (photo by Robert Chadwell, IARC).

A LEBUS double-drum electric oceanographic winch (Figure I.2.2) manufactured by LEBUS Engineering International Ltd., England was additionally deployed on the helicopter deck of the icebreaker in September 2003 (Figure I.2.4) in order to operate with the CTD profiler, biological nets and trawl, and to deploy/recover the moorings. Winch electric motor power is 7.3 KW. Each drum capacity is 3500 m of 0.3-inch cable. The left drum (Figure I.2.2) is used only for mooring recovery. The right drum with spooling mechanism contains the mechanical cable of 3000 m length to carry CTD probe, nets and trawl. A HAWBOLDT C15-40 horizontal capstan manufactured by HAWBOLDT Industries (1989) Ltd., Canada was placed near the LEBUS winch in September 2004 (Figure I.2.3). The capstan is equipped with a 11.2 KW two speed Toshiba electric motor and is used for mooring deployment/recovery. The horizontal drum diameter is 40”.



**Figure I.2.3:** HAWBOLDT C15-40 horizontal capstan on the helicopter deck of I/B "Kapitan Dranitsyn" (photo by Robert Chadwell, IARC).

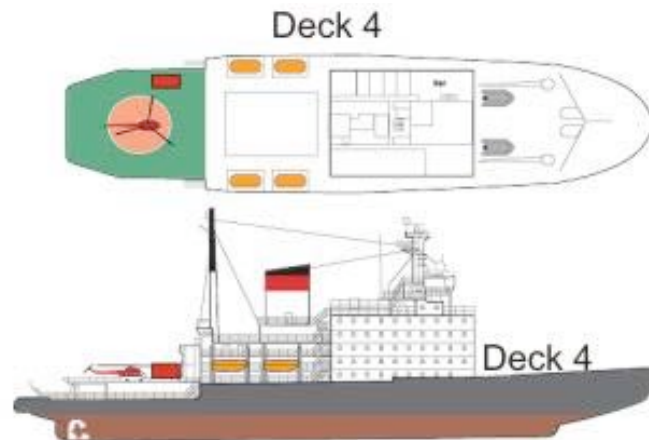


**Figure I.2.4:** CTD/Rosette winch and mooring capstan site position on Deck 4 are shown by a red rectangle.

### **I.3. CRUISE TRACK** (*I.Dmitrenko, IARC, and V.Smolianitsky, AARI*)

I/B "Kapitan Dranitsyn" left Kinkiness Harbor, Norway on 5 September 2004 and returned on 27 September 2004. The research area was over the continental slope of the Laptev Sea and the adjacent Eurasian Basin (Figure I.3.1). CTD profiles were carried out along two transects across the continental slope in the central and eastern Laptev Sea and along another two transects approximately oriented along the continental slope. The survey within the Russian Exclusive Economic Zone was authorized by the Russian Ministry for Education and Science. On the way to the research area the icebreaker passed along the Northern Sea Route through the Barents and Kara seas and entered the Laptev Sea through the Vilkitsky Strait on

September 10, 2004. The scientific operations began on 12 September. Having completed the major goals of the cruise on 20 September, the icebreaker left the Laptev Sea through the Vilkitsky Strait on 23 September (Figure I.3.1). On the way to the Laptev Sea bunkering took place at 20:00 on September 6 near the entrance to Kola Bay in the vicinity of Murmansk Harbor. Due to very heavy ice conditions in the Laptev Sea additional bunkering was done near Vilkitsky Strait on 22 September from the Russian nuclear icebreaker Vaygach.

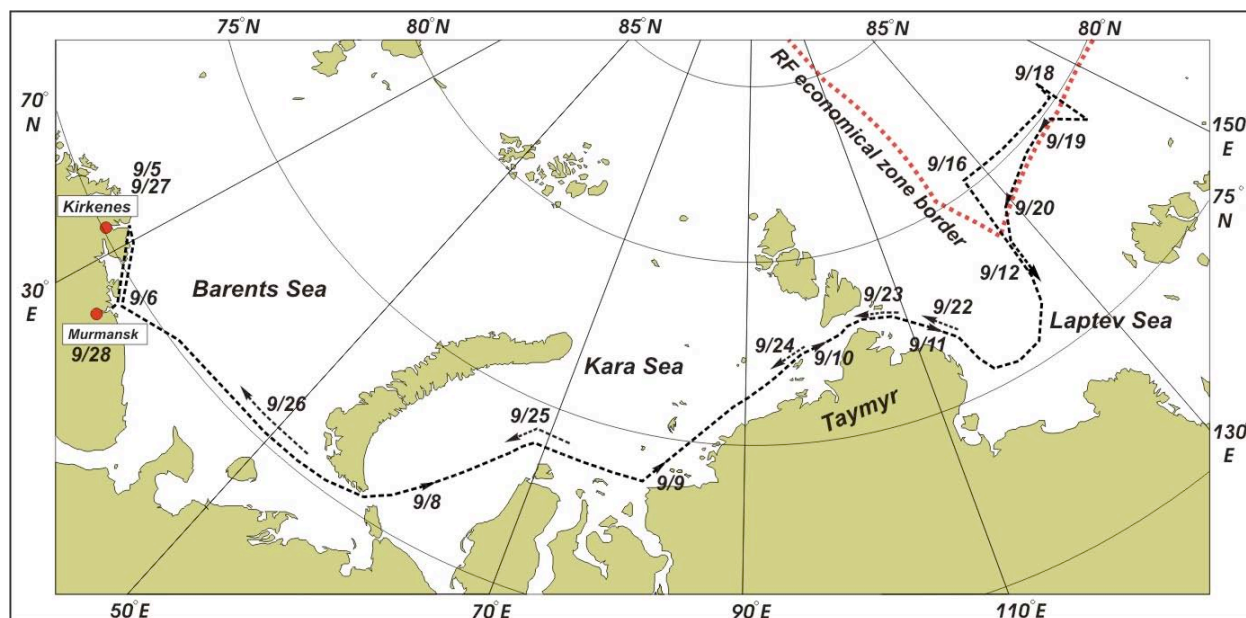


Figure I.3.1: NABOS-04 cruise track, 09/05/2004-09/27/2004.

#### I.4. SCIENTIFIC PARTY (*I.Dmitrenko, IARC, and L.Timokhov, AARI*)

Name	Country	Position	Affiliation
Igor Dmitrenko	USA	Co-Chief Scientist	University of Alaska Fairbanks
Marc Ringuette	Canada	Scientist	Laval University
Caroline Bouchard	Canada	Master Student	Laval University
Robert Chadwell	USA	Mooring Technician	University of Alaska Fairbanks
Michael Dempsey	Canada	Mooring Technician	Oceanetic Measurement Ltd.
Mark Parrott	USA	Film Maker	Ascan Video Productions Co.
Jess Anto	USA	Technician	Ascan Video Productions Co.
Leonid Timokhov	Russia	Co-Chief Scientist	Arctic and Antarctic Research Institute
Sergey Kirillov	Russia	Scientist	Arctic and Antarctic Research Institute
Victor Vizitov	Russia	Scientist	Arctic and Antarctic Research Institute
Miroslav Nitishinsky	Russia	Scientist	Arctic and Antarctic Research Institute
Vasiliy Smolianitsky	Russia	Scientist	Arctic and Antarctic Research Institute
Alexandr Smirnov	Russia	Scientist	Arctic and Antarctic Research Institute
Oleg Andreev	Russia	Scientist	Arctic and Antarctic Research Institute
Elena Dobrotina	Russia	Scientist	Arctic and Antarctic Research Institute
Anna Akimova	Russia	Scientist	Arctic and Antarctic Research Institute
Tatyana Alexeeva	Russia	Scientist	Arctic and Antarctic Research Institute
Olga Morozova	Russia	Scientist	Arctic and Antarctic Research Institute
Nikolay Koldunov	Russia	Scientist	Arctic and Antarctic Research Institute

Mikhail Makhotin	Russia	Scientist	Arctic and Antarctic Research Institute
Sergey Mastruykov	Russia	Scientist	
Oleg Churkin	Russia	Scientist	State Research Navigation and Hydrographic Institute
Irina Repina	Russia	Scientist	State Research Navigation and Hydrographic Institute
Alexandr Petrov	Russia	Engineer	Obukhov Institute of Atmospheric Physics
Nikolay Belaev	Russia	Scientist	Obukhov Institute of Atmospheric Physics
Alexandr Vetrov	Russia	Scientist	Shirshov Institute of Oceanology
Natalya Markova	Russia	Scientist	Shirshov Institute of Oceanology
Irina Borzaeva	Russia	Interpreter	St.Petersburg State University
			St.Petersburg State University

### **I.5. ICE CONDITIONS** (*V. Smolianitsky, AARI*)

Heavy ice conditions which predominated during and within the area of the NABOS-04 expedition were caused by a number of factors, including a) vast areas of residual ice within the northeast part of the Kara Sea and northeast part of the Laptev Sea at the end of summer 2003, and b) predominance of northern winds during summer 2004. Conditions favored conservation and further development of the Taimir Ice Massif (TIM) and intensive transfer of old ice and icebergs from the Arctic Ocean and northwestern Laptev Sea southward, and the observed shift of the ice formation date towards the beginning of September. Typical ice forms were residual one-year and multi-year ice with inclusion of new and young ice, with significant snow cover and hummock concentrations. The ice conditions of the 2004 expedition were therefore significantly different from those in 2003 and even more different from those in 2002, allowing us to define 2004 ice conditions as heavier than 75% quantile ice conditions, both by total ice concentration and by concentration of multi-year ice.

To present a simplified description, the cruise track was divided into 6 more or less uniform sections noted A1 – A6 for the cruise towards the northeastern-most point, and as B1 – B6 for the cruise back. The position of the sections is given in Figure I.5.1.

*Section A1: Northeastern part of the Kara Sea.* The first-year ice was observed on September 9 at 94°29'E. Further, within the Nordenskiöld Archipelago and in the vicinity of Vilkitsky Strait stripes and patches of residual one-year and multi-year ice were observed (Figure I.5.2).

*Section A2: Vilkitsky Strait.* Only patches and stripes of residual one-year and multi-year ice with a floe width up to 300 meters were observed.

*Section A3: Western periphery of TIM.* The first-year ice (cakes of residual ice) were encountered just after the exit from Vilkitsky Strait at 77°39'N 106°45'E. Further along the route the ice with total concentration of 8-10/10 was predominant, composed of 9/10 residual first-year ice (70-140 cm) mixed with multi-year ice (150-300 cm) with inclusions of new and young ice (15-20 cm) with some grey-white ice, and 10-20% hummocks (Figure I.5.3). A typical feature of this section is the presence of significant quantities of icebergs, including tabular-form icebergs. Information on icebergs is summarized in the next paragraph. Periodic occurrence of leads facilitated the ship's movement; however in the southern part of the section at 76°04'N 115°51'E, where a higher (up to 40%) level of hummocks was found, the ship was beset by ice for the first time.

*Section \_4-\_4: Ice boundary.* These sections correspond to the southern compact boundary of TIM, composed of residual cakes, dark nilas and grease ice (Figure I.5.4). Ice conditions for A4 and B4 varied insignificantly.

*Section A5: Eastern periphery of TIM.* The ship was moving northward along the 126°E meridian surrounded by compact, partly consolidated, melted residual one-year (50-120 cm)



and multi-year (150-300 cm) ice with inclusion of young ice (Figure I.5.6). There were significant quantities of icebergs (Figure I.5.5). Increase of ice thickness and concentration resulted in the ship being periodically beset.

**Section A6:** This section adjacent to the Arctic Ocean was dominated by big and vast floes of multi-year ice (150-300 cm) and residual one-year ice (80-120 cm) with high snow concentration (Figure I.5.7), as well as continuous leads covered by dark nilas which made navigation easier in comparison with the previous section.

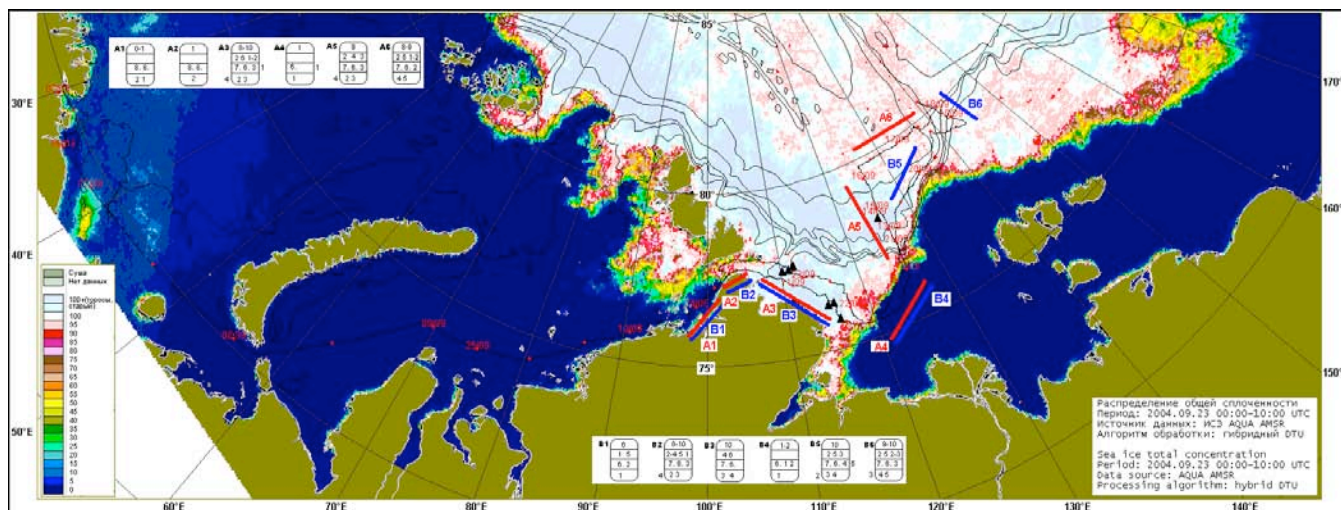


**Figure I.5.1:** Ice extent along the NABOS-04 cruise track. Total sea-ice concentration on September 23, 2004 shown by color. The ice chart was prepared using AMSR AQUA data from <http://www.seaice.dk>. Ice conditions were analyzed along the red lines (1...6) on the eastward expedition track, and blue lines (6...1) along the westward cruise track. The corresponding ice conditions along these lines are shown by standard World Meteorological Organization (WMO) symbols. Iceberg positions are depicted by black triangles. Black lines show 200, 500, 1000, 2000, 3000, and 4000 m bathymetry contours.

**Section B6:** This section was similar in ice composition to the previous A6 section but was situated within the limits of a vast quasi-stationary opening in the northeastern part of the Laptev Sea.

**Section B5:** *The northeastern part of the Laptev Sea.* This section was characterized by residual one-year and multi-year melted ice. Due to predominance of northern winds and the relative vicinity of the ice boundary, vast leads covered by grey and grey-white ice were observed.

**Section B3:** *Western periphery of TIM.* This section appeared to be the most difficult for navigation of the whole expedition. Despite the general similarity of ice composition to that of section A3, due to impact of northern and northeastern winds and negative temperatures this section was characterized by higher values of total ice concentration, with 20% hummocks and ridges and 20% snow; this section actually represented consolidated floes and cakes of residual one-year and multi-year ice (Figure I.5.9). For old ice (250-300 cm) the high concentration of hillocks was also typical. Many icebergs were also observed. Heavy ice conditions dramatically decreased the ship's average velocity to 5-6 knots; following the convoy led by nuclear icebreakers Sovetskii Soyuz and Arktika (Figure I.5.10) allowed the icebreaker to stay within the planned schedule.

**Section B2:** *Vilkitsky Strait.* On the way back the strait was filled by residual one-year and multi-year ice with total concentration of 80-100%. A typical feature was the presence of ice

stripes composed of multi-year ice. A timely ice chart together with shipborne radar imagery (Figure I.5.11) allowed the icebreaker captain to make a bypass maneuver and enter the Kara Sea.

*Section B1. Northeastern part of the Kara Sea.* In general, ice conditions were similar to those observed at section A1. Presence of vast areas of dark nilas was typical for the section. The icebreaker exited ice on 24.09 at 10:10 MSK at 76°12'N 93°47'E.

Meteorological conditions in summer 2003/2004 favored transport of significant masses of old ice from the area of Severnaya Zemlya to the Laptev Sea and extension of the Taimir Ice Massif by 75%, resulting in a large number of icebergs amongst consolidated one-year and multi-year ice in the western part of the Laptev Sea. Table I.5.1 summarizes all cases of iceberg occurrence during the expedition. Geographical distribution of the icebergs is shown in Figure I.5.1. Note that poor visibility, mist, and high concentration of hummocks hampered visual and radar observations; thus the actual number of icebergs should be significantly greater.

**Table I.5.1:** Parameters of the icebergs observed during the expedition NABOS-04.

#	Latitude and Longitude	Date	Time, UTC	Type	Dimensions, m length/width/height
1	76.892°N 113.284° (v)	11.09.2004	02:20	growler	15//4 (v)
2	76.647°N 114.195° (v)	11.09.2004	04:05	tabular	100//8 (v)
3	76.627°N 114.641° (v)	11.09.2004	04:32	tabular	70//6-7 (v)
4	76.532°N 115.244° (v)	11.09.2004	05:40	tabular	100-150//8-10 (v)
5	75.759°N 116.408° (r)	11.09.2004	11:17	growler	25//5 (v)
6	78.094°N 126.051° (r)	13.09.2004	03:47	tabular	100/20/8 (r)
7	77.251°N 112.810° (v)	23.09.2004	03:22	tabular	100-130//6 (v)
8	77.249°N 112.811° (v)	23.09.2004	04:05	tabular	200//10-15 (v)
9	77.292°N 112.653° (v)	23.09.2004	05:00	growler	5//2 (v)
10	77.412°N 111.974° (v)	23.09.2004	06:10	tabular	200//15 (v)
11	77.464°N 111.592° (v)	23.09.2004	06:35	tabular	300//8 (v)

Note: v – dimensions/position determined visually relatively to the ship, r - dimensions/position determined by shipborne radar.

Note also that position of iceberg # 6 is rather close to the location of the lost mooring station M2. This iceberg is shown in Figure I.5.5. Using data from Table I.5.1 and the size ratio, possible draft H for icebergs # 6 and 8 was 40 m and 75 m. Maximum potential draft may be defined more precisely on the basis of glacier tongues on Severnaya Zemlya. Therefore, displacement of a tabular berg similar to iceberg # 8 over the point of mooring station M2 could be the reason for its loss if its upper buoy was less than 75 m deep.



**Figure I.5.2:** Sections A1 – B1. Northeastern part of the Kara Sea – new ice and open water.



**Figure I.5.3:** Section \_3. Western periphery of TIM – heavily hummocked compacted old and residual ice with high snow concentration.



**Figure I.5.4:** Sections A4 – B4. Southern compact ice limit of TIM – cakes of residual ice.



**Figure I.5.5:** Section A5. Eastern periphery of TIM – typical tabular iceberg (100\_20\_8m).

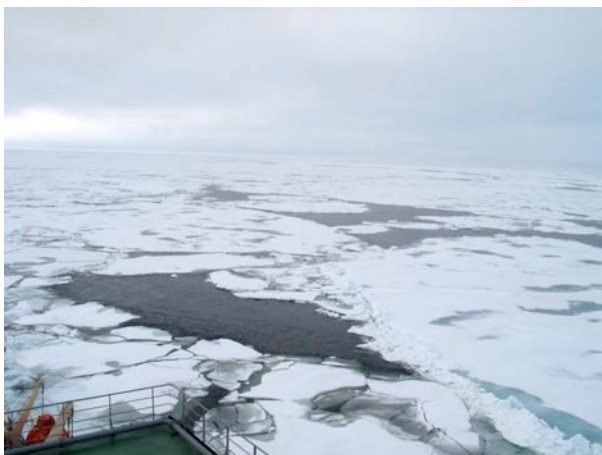


**Figure I.5.6:** Section A5. Eastern periphery of TIM – heavily melted residual and old ice with new ice.



**Figure I.5.7:** Section B6. Adjacent to the Arctic Ocean – close heavily snowed floes of old and residual ice and leads covered by dark nilas.



**Figure I.5.8:** Section B5. Northeastern part of the Laptev Sea – residual and old ice, and leads, covered by grey and grey-white ice.



**Figure I.5.9:** Section B3. Western periphery of TIM – consolidated ice floes of old and residual ice with heavy snow and fresh ridges, ice pressure 10-20%.



**Figure I.5.10:** Section B3. NW part of TIM – navigation in the channel within the convoy.

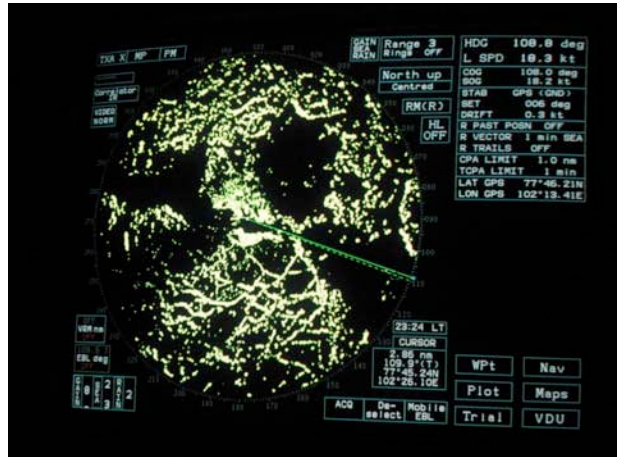


**Figure I.5.11:** Section B2. Shipborne radar imagery of old ice belt in the Vilkitsky Strait.

## I.6. METEOROLOGICAL CONDITIONS (O.Andreev, AARI)

The analysis of synoptic and meteorological conditions ranges from September 11, 2004 (the beginning of work at the first oceanographic station) to September 21, 2004, when the last station was done and the icebreaker left the area of research. The synoptic regime over the Laptev Sea was characterized by high cyclonic activity (Figure I.6.1). Within the Icelandic Low the intensive processes of cyclogenesis occurred. The hollow of low pressure was stretched from Iceland along Greenland to the south of Archipelago Spitsbergen to Novaya Zemlya Island. The cyclones passed along this direction. As they approached the Laptev Sea across the Taimyr Peninsula, the cyclones were amplified by local synoptic conditions.

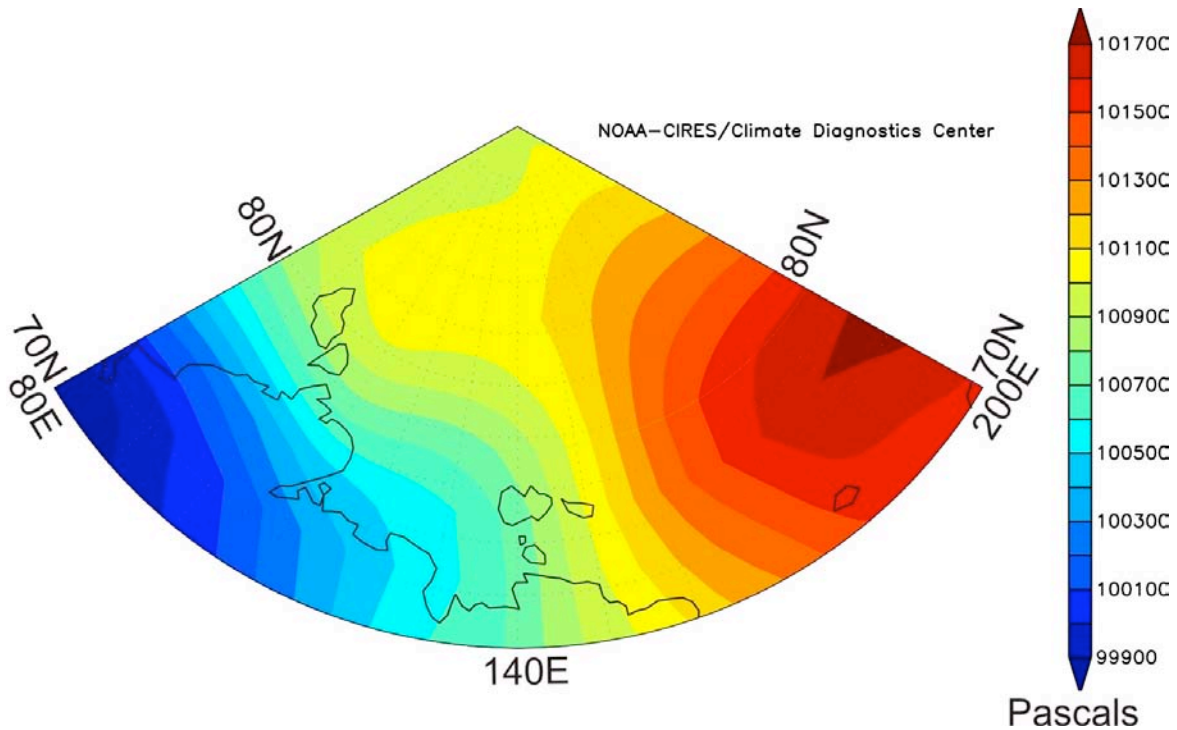


**Figure I.6.1:** NCEP/NCAR Sea level pressure averaged over September 12-20, 2004.

During September 9–11 the weather conditions on the route towards and within the research area were defined by cyclone movement from the Taimyr Peninsular across the western Laptev Sea towards Severnaya Zemlya Island. Atmospheric pressure varied within 982-995 mb. The weather was characterized by overcast and northern and northeastern gusty winds of 6-17 m/s. The air temperature decreased from +4.0°C at Vilkitski Strait, down to 0.0°C in the research area (Figure I.6.2).

Further, during September 12-13, while the cyclone was weakening and leaving the region, the area of research was located out in the pressure saddle, and then at the boundaries of a small local cyclone (1002-1007 mb). The weather conditions on September 12-13 were still determined by overcast and gusty winds primarily of southwest and then north and northwestern directions. Occasionally it was snowing. The air temperature in the area of research slightly increased up to 1 ÷ 2°C.

On September 14-17 the next cyclone appeared in the Laptev Sea. A cyclonic track was laid across the Laptev Sea to the east. Atmospheric pressure decreased down to 996-1005 mb. The weather was cloudy with precipitation and very often heavy fogs were observed. The wind was mainly southeastern, and then of stable northeastern direction with a speed of 5-12 m/s. Air temperature dropped down to -3 to -5°C.

On September 18-21 the weather was determined by the influence of an atmospheric pressure crest stretched across the Laptev Sea from the east. Atmospheric pressure was 1008-1013 mb. The cloud cover became broken; however snowfall took place a couple of times. The wind was generally stable and from a northern and northeastern direction with a speed of 7-14 m/s. Air temperature first dropped down to -7 to -10°C; however later on when it was overcast again (September 21) the temperature rose to 0 -3°C.

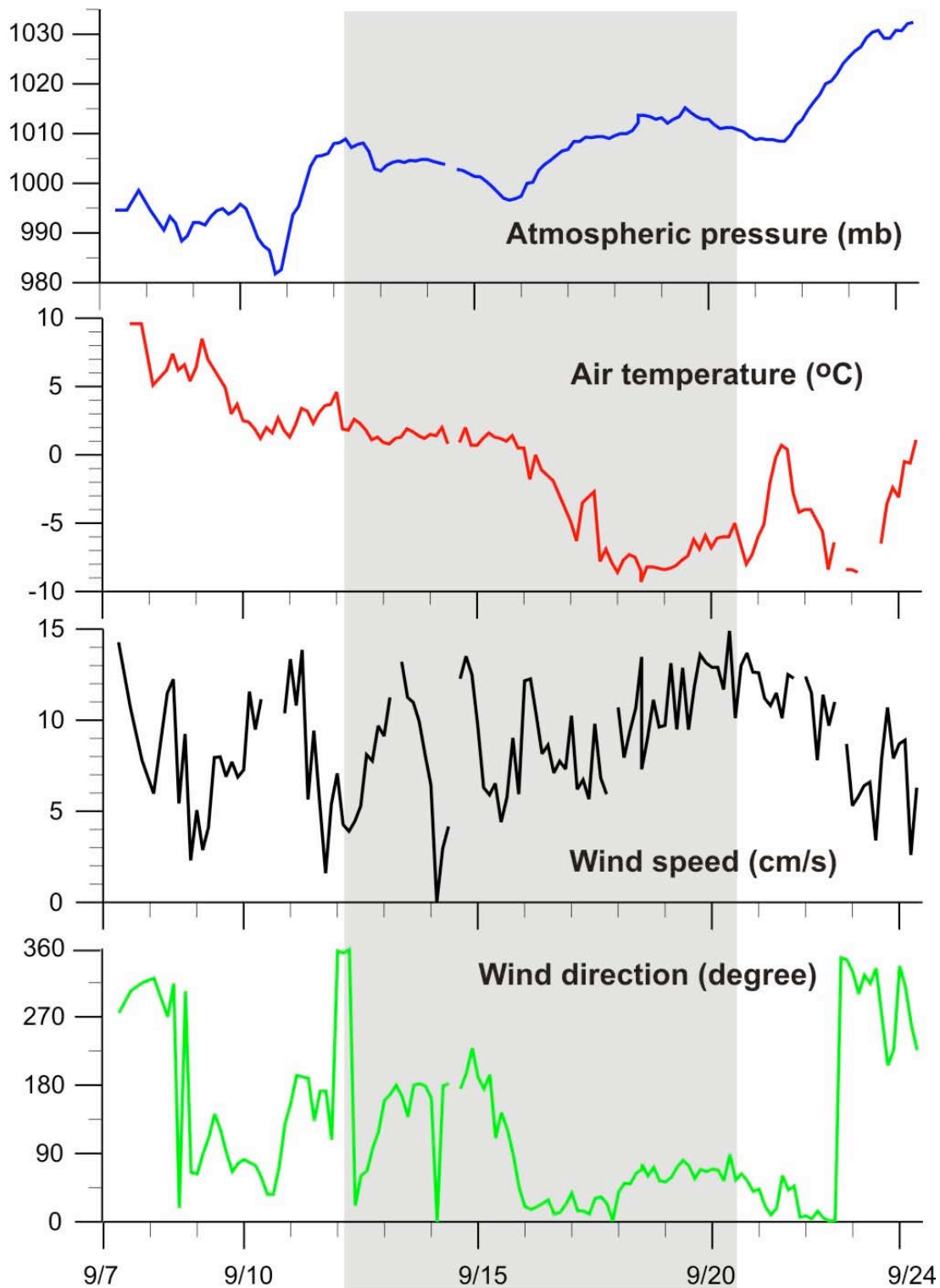


**Figure I.6.2:** Variation of the main meteorological parameters along the NABOS 2004 cruise track. The measurements were carried out from the upper deck of the icebreaker by the WM-918 weather station. The gray strip corresponds to the time of operation within the area of oceanographic research.

## 1.7. OBSERVATIONS *(I.Dmitrenko, IARC, and L.Timokhov, AARI)*

The NABOS-04 program included routine CTD observations and water sampling, recovery and deployment of oceanographic moorings, ARGOS ice buoy deployments, biological observations, and ice sampling along with routine ice and meteorological observations. Measurements made during the cruise NABOS-04 on the I/B “Kapitan Dranitsyn” are described in Table I.7.1. The complete information about all research activities during the cruise is summarized in Appendix 2. The information in Table I.7.1 and Appendix 1 is presented in chronological order.

**Table I.7.1:** Observations during NABOS-04 cruise of the I/B “Kapitan Dranitsyn”

Station #	Date Dd/mm	Time GMT	Lat	Lon	Depth m	CTD	Water sampl.	Net	ADCP	Mooring Dep.	Mooring Rec.	Ice Buoy Dep.	Ice Sampl.
KD0104	12/09	4:00	76°44.6'	125°59.8'	67	X							
KD0204	12/09	6:25	77°03.2'	125°59.6'	112	X		X					
KD0304	12/09	16:00	77°19.3'	126°04.4'	1420	X		X					
KD0404	12/09	19:56	77°30.7'	125°58.7'	1810	X		X					
KD0504	12/09	23:45	77°44.4'	126°00.6'	1700	X		X					
KD0604	13/09	4:08	78°06.2'	126°04.5'	2400	X		X					
KD0704	13/09	12:14	78°26.4'	125°38.6'	2700	X		X		X	X		
ICE0104	14/09	08:06	78°25.9'	125°38.4'	>2000							AWI	X
KD0804	15/09	16:10	78°56.9'	126°03.6'	>3000	X	X	X					
KD0904	15/09	23:04	79°23.2'	125°47.6'	>3000	X	X	X	X				
KD1004	16/09	05:57	79°49.6'	126°05.2'	>3000	X	X	X	X				
KD1104	16/09	13:30	79°48.8'	129°19.5'	3280	X	X	X	X				
KD1204	16/09	22:10	79°49.8'	133°23.8'	>3000	X	X	X					
ICE0204	17/09	04:10	79°50.2'	134°50.0'	>2000							AWI	X
KD1304	17/09	10:53	79°50.1'	137°48.3'	2825	X	X	X					
KD1404	17/09	18:55	79°55.4'	142°20.2'	1300	X	X	X		X			
KD1504	18/09	10:00	80°25.8'	140°26.2'	1600	X	X	X					
KD1604	18/09	14:55	80°14.1'	140°58.4'	1700	X							
KD1704	18/09	17:34	80°01.7'	141°27.9'	1600	X							
KD1804	18/09	20:51	79°35.3'	142°24.0'	1170	X							
KD1904	18/09	23:10	79°25.4'	143°01.1'	500	X	X	X					
KD2004	19/09	02:07	79°15.2'	143°29.2'	218	X							
KD2104	19/09	04:22	79°00.0'	143°59.8'	98	X	X	X					
KD2204	19/09	10:30	79°30.4'	138°59.4'	>2000	X	X	X					
KD2304	19/09	16:45	78°59.7'	137°02.0'	1980	X	X	X					
KD2404	19/09	22:45	78°45.2'	133°53.3'	>2000	X	X	X					
KD2504	20/09	06:18	78°30.1'	131°00.0'	2500	X	X	X					
KD2604	20/09	14:33	78°09.7'	127°59.9'	>2000	X	X	X					

## **I.7.1. AIR-ICE INTERACTION OBSERVATIONS (I.Repina, IAF)**

### **I.7.1.1. Introduction**

The interaction between the ocean and the atmosphere in the polar regions is specific, first of all, due to the presence of ice at the ocean surface and, thus, due to the properties of the boundary layers in the two media. The mechanism of energy exchange between the atmosphere and the underlying surface in the polar basin is very complicated. During experimental study of the thermal balance of the Arctic region, especially in the case of polynyas, leads and young ice surrounded by an extensive ice field, the main difficulty is determining vertical sensible and latent heat fluxes.

There are many methods reliable enough to determine the components of the energy balance for an old ice cover [Makshtas, 1991]. However, over the areas of young thin ice and especially over the open water areas in polynyas and leads, the conditions of heat exchange change. All the components of heat balance increase rapidly, and the turbulent heat flux changes its sign [Repina and Smirnov, 2000]. Until now there have been no reliable parameterizations of these processes [Andreas and Cash, 1999]. It is even more difficult to parameterize for the cases of non-uniform ice fields [Ivanov et al. 2003].

### **I.7.1.2. Objectives**

The following tasks were carried out:

- Investigation of energy exchange between atmosphere and surface (open water, ice) by measurements of turbulent heat and momentum fluxes in the subsurface layer of atmosphere.
- Determination of the coefficient for parametric methods of calculating turbulent fluxes.

### **I.7.1.3. Methods and equipment**

The following kinds of observations were carried out during the cruise:

- Direct measurements of temperature, horizontal and vertical components of wind speed, and humidity fluctuations above surfaces of various types (open water, ice of various structure and age, polynya). The data are used for determinations of heat and momentum fluxes, as well as to obtain the roughness parameter of a surface. The measurements were carried out both from the cruising vessel, and at ice stations; and
- measurement of the spatial distribution of surface temperature in the IR-range.

For measurements the following equipment was employed:

- A sonic thermo-anemometer USA-1 (made by METEK Co.) that allows the measurement of fluctuations of the three wind speed components (X, Y, Z) and temperature fluctuations with frequency of 20-50 Hz.
- A high frequency hygrometer (analyzer of air humidity) HMP-233 that allows relative humidity and air temperature to be measured. Frequency of measurements is 6 Hz.

For measurements of surface temperature the following instrumentation was applied:

- A GTH-175 digital thermometer with a range of measurements from -199.9 up to +199.9 °C with accuracy of 0.1 °C.
- An IR thermometer for remote temperature measurement with a range of measurements from -10 °C up to 300 °C with resolution of 0.1 °C and accuracy of 3 % from measured values.

During movement of a vessel the equipment was placed on the bow by meter boom (height of measurements is 8 meters) to minimize the effect of being onboard the vessel. At ice stations the measurements were carried out from a 2 m high stationary platform.



For calculation of fluxes two methods were used: a direct method and an inertial-dissipation method. In the direct method the heat and momentum fluxes are determined from direct measurements of horizontal and vertical wind speed component fluctuations and temperature. The fluxes are calculated from their covariations. The inertial-dissipation method is based on the assumption of local isotropy and existence of an inertial interval. The fluxes are estimated based on turbulent energy balance and budget dispersions of temperature and specific humidity [Fairall and Larsen, 1986]. The roughness parameter was calculated by the technique presented in Grachev et al. [1998] with the usage of an atmospheric stability parameter. Universal function parameterizations for different types of stability were used [Andreas, 2002].

#### I.7.1.4. Preliminary results

Measurements of the atmospheric turbulence characteristics directly from ice allow accurate results to be obtained, especially for small values of turbulent fluxes. In Table I.7.1.1 the measurement results of the atmospheric turbulence characteristics, obtained at two ice stations on September 17 and 14, 2004 are shown. In Table 1.7.1.1 V is wind speed; D is wind direction; f is relative humidity; T air - is air temperature; T sur - is surface temperature; H is sensible heat flux; all at a height of 2 m above the surface. LE is latent heat flux; is momentum flux; u\* is friction velocity; T\* is temperature scale; z/L is stability, z is height of measurements, L is Monin-Obukhov length scale; z<sub>0</sub> is roughness length;  $\sigma_u$  is standard deviation of wind speed (u-component);  $\sigma_v$  is standard deviation of wind speed (v-component);  $\sigma_w$  is standard deviation of wind speed (w-component);  $\sigma_t$  is standard deviation of temperature; C<sub>D</sub> is Drag coefficient; C<sub>H</sub> is sensible heat transfer coefficient; C<sub>E</sub> is latent heat transfer coefficient.

At the first station a positive stratification of atmosphere close to neutral was observed. The surface was composed of 90% one-year ice and 10% hummocks (average hummock height was 0.5 m). On the airflow (upwind) side there was a hummock ridge. The sensible and latent heat fluxes were small; the sensible heat flux was directed to the surface. At the second station the atmosphere was negatively stratified, resulting in the presence of a positive sensible heat flux. The ice surface was 100% covered by snow. There were no hummocks preventing free airflow. The ice was covered with a lot of puddles, which probably determined the negative stratification of the atmosphere.

**Table I.7.1.1:** Characteristics of turbulence in the lower atmosphere at ice stations (direct measurements). Height of measurements is 2 m.

Station #	time (GMT)	$V m s^{-1}$	D grad	f %	T air -	T sur -		
ICE0104	9:30-10:30	6.5	178	98.4	-0.3	-0.5		
ICE0204	5:20-6:30	4.6	338	95.4	-5.7	-4.7		
		$H W m^{-2}$	$LE W m^{-2}$	-	$u_* m s^{-1}$	$T^*$	$z/L$	$z_0 m$
ICE0104	-3	1.9	0.115	0.3	0.005	0.006	$6.7 \cdot 10^{-4}$	
ICE0204	5.7	3.7	0.04	0.17	-0.07	-0.014	$1.6 \cdot 10^{-5}$	
		$\sigma_u / u_*$	$\sigma_v / u_*$	$\sigma_w / u_*$	$\sigma_t / T^*$	C <sub>D</sub>	C <sub>H</sub>	C <sub>E</sub>
ICE0104	2.6	1.9	1.08	2.25	$2.25 \cdot 10^{-3}$	$2.2 \cdot 10^{-3}$	$2.64 \cdot 10^{-3}$	
ICE0204	2.6	2.3	1.05	2.53	$1.4 \cdot 10^{-3}$	$2 \cdot 10^{-3}$	$2.51 \cdot 10^{-3}$	

The transport of airflow through a small hummock ridge resulted in an increase of the surface roughness parameter at the first station in comparison with the second one. Accordingly, drag coefficient was also increased. The values of exchange coefficients are roughly equal to the mean values typical for snow-covered ice [Repina et al., 2002].

The onboard measurements were carried out on all routes of the icebreaker. Based on the measurement data the fluxes of both sensible heat and momentum and the surface roughness parameter were calculated. During measurements, basically, weak - stable, weak - unstable and neutral stratifications were observed. The strong - unstable stratification was observed over open water. The highest level of atmosphere stability parameter noise is observed at small speeds of wind (Figure I.7.1.1). At high wind speeds, in general the neutral stratifications were observed. The exceptions are the cases when the surface is much warmer than the air, which was observed since September 18, 2004 at low air temperatures and in the presence of open water.

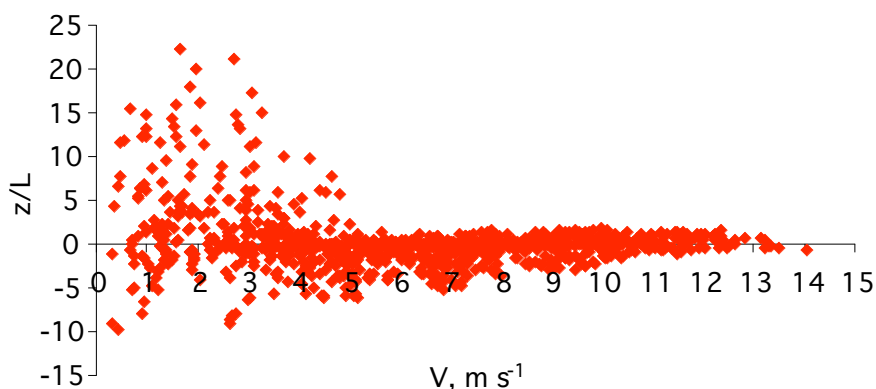


**Figure I.7.1.1:** Relationship between the stability parameter and wind speed.

Sensible heat flux was very small, almost zero. After entry into the ice fields (Figure I.7.1.2), the variations of heat flux increased, related to ice type and age variations, and also to the presence of open water.

On September 18, during the oceanographic station, there was a wide area of open water under the devices that determined an increase of flux associated with a temperature drop. The friction velocity  $u^*$ , determining momentum flux, changed from 0.1 up to 0.7  $\text{m s}^{-1}$  (Figure I.7.1.6). Practically all values had equal probability and depended on wind speed.

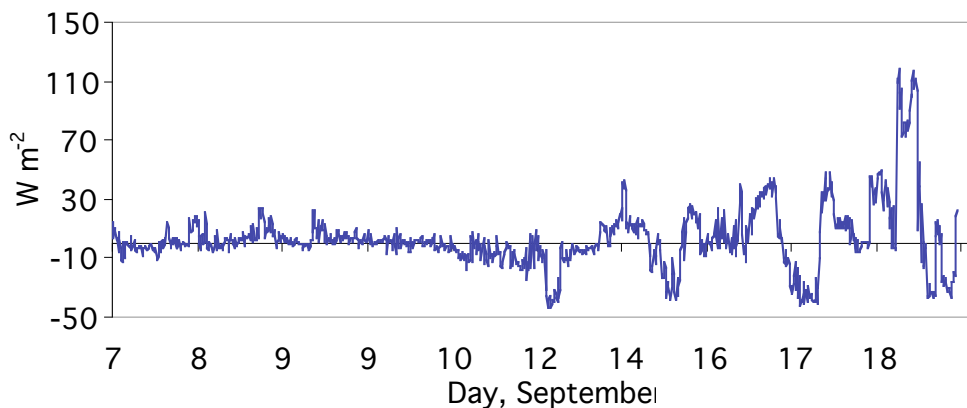


**Figure I.7.1.2:** Heat flux variations along the NABOS-04 cruise in the Laptev Sea.

In Figure I.7.1.3 the distribution of roughness parameter is shown for measurements carried out above ice and open water. Above ice a wider spectrum of values is possible. Two peaks correspond to equal snow-covered surface and surface with hummocks. The exchange coefficient values above ice vary in a narrow range.

For constant flux the following ratio for the second moments of turbulent fluctuations is applicable:

$$\sigma_u^2 = \overline{(u')^2} = A_u^2 u_*^2, \quad \sigma_v^2 = \overline{(v')^2} = A_v^2 u_*^2, \quad \sigma_w^2 = \overline{(w')^2} = A_w^2 u_*^2$$

$$\sigma_T^2 = \overline{(T')^2} = A_T^2 T_*^2, \quad \overline{u'T'} = A_{uT} u_* T_*$$

These coefficients are calculated using NABOS observational data and are shown in Table I.7.1.2.

**Table I.7.1.2:** Coefficient numbers of similarity theory for different types of surface.

Surface	$\overline{u}$	$\overline{w}$	$\overline{T}$	$\overline{uT}$
Open water	2.5	1.24	2.5	3.43
Leads	2.29	1.22	2.53	3.5
Ice	2.2	1.9	2.64	3.21

More systematic data processing will allow us to determine dependence of energy exchange parameters from the ice type and age.

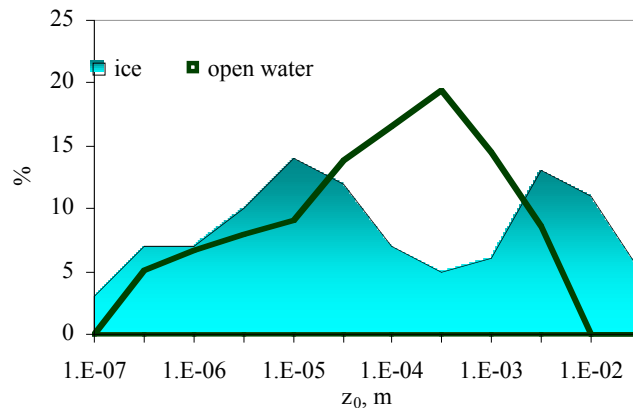


**Figure I.7.1.3:** The relative occurrence of roughness parameter ( $z_0$ ) from the measurements taken over ice fields and open water.

## I.7.2. ICE OBSERVATIONS (V.Smolianitsky, AARI)

### I.7.2.1. Background information

Mean climatic total ice concentration and old ice partial concentration for September are given in Figures I.7.2.1 and I.7.2.2. Statistics is based on processing of 10-days averaged AARI

air reconnaissance ice charts for 1950-1992 from the archive of the WMO project “Global Digital Sea Ice Data Bank” [Smolyanitsky, 2000].

These maps show that the first 10 days of September is a period of minimum ice extent and in 50% of cases (median) practically the entire Laptev Sea is ice-free except for the northern part and the part adjacent to Vilkitsky Strait. At the same time, the second 10-day period of September is, in 50% of cases, the starting period of ice formation. During the years with heavy ice conditions (quintile 75%) the Taimyr Ice Massif (TIM) is observed in the western part of the sea throughout the whole summer, and start of ice formation is shifted to the beginning of September. For the old ice the normal conditions are those with no significant extent of old ice in the Laptev Sea until the third 10-day period of September. For the years with heavy ice conditions old ice expands towards the central part of the sea in the first 10-day period of September, and within the area of TIM during the second and third 10-day periods.

### **I.7.2.2. Objectives**

Objectives of ice observations during the expedition were:

- Obtain sea-ice data which is necessary to interpret oceanographic and meteorological observations gained during the expedition and to describe sea-ice variability including that affecting ice navigation;
- Map ice conditions on the basis of satellite passive microwave data from AQUA AMSR and shipborne data;
- Sample and describe ice kerns.

### **I.7.2.3. Sea ice observations and data processing**

#### ***I.7.2.3.1. Shipborne ice observations and data processing***

Continued (11-24 September, 2004) ice observations included area observations (within the range of horizontal visibility and screen area of regular radar) and en-route observations (within the zone 1.5-2 hull lengths ahead and 3 hull widths from each side) (Figure I.5.1). Quantitative and symbolic description of the main ice parameters (concentration, stages of development, forms) follows “WMO Sea Ice Nomenclature” [WMO, 1989]. For such parameters as stages of melting, hummock and ridge concentrations, and snow concentration standard WMO symbols and scales are not enough; therefore Russian national scales and symbols were also used according to the national manual.

For a visual definition of en-route ice thickness, a 2 meter stick installed starboard was used (Figure I.7.2.3, left). Regular shipborne radar was used to estimate configuration of ice zones within the area of navigation (Figure I.7.2.3, right). Ship speed, course angle, time and geographical coordinates were read from the radar screen.

The following ice cover parameters were observed:

- concentration (total and partial for all stages of development);
- stages of development and forms (according to stages or predominant);
- stages of melting;
- hummock and ridge concentrations;
- ice pressure;
- surface contamination concentration;
- predominant ice thickness (en route only);
- predominant snow height (en route only) and concentration;
- existence and orientation of openings (leads, cracks) in the ice cover.

Ice conditions observed during oceanographic stations are given in Table I.7.2.1.

September, 1-10

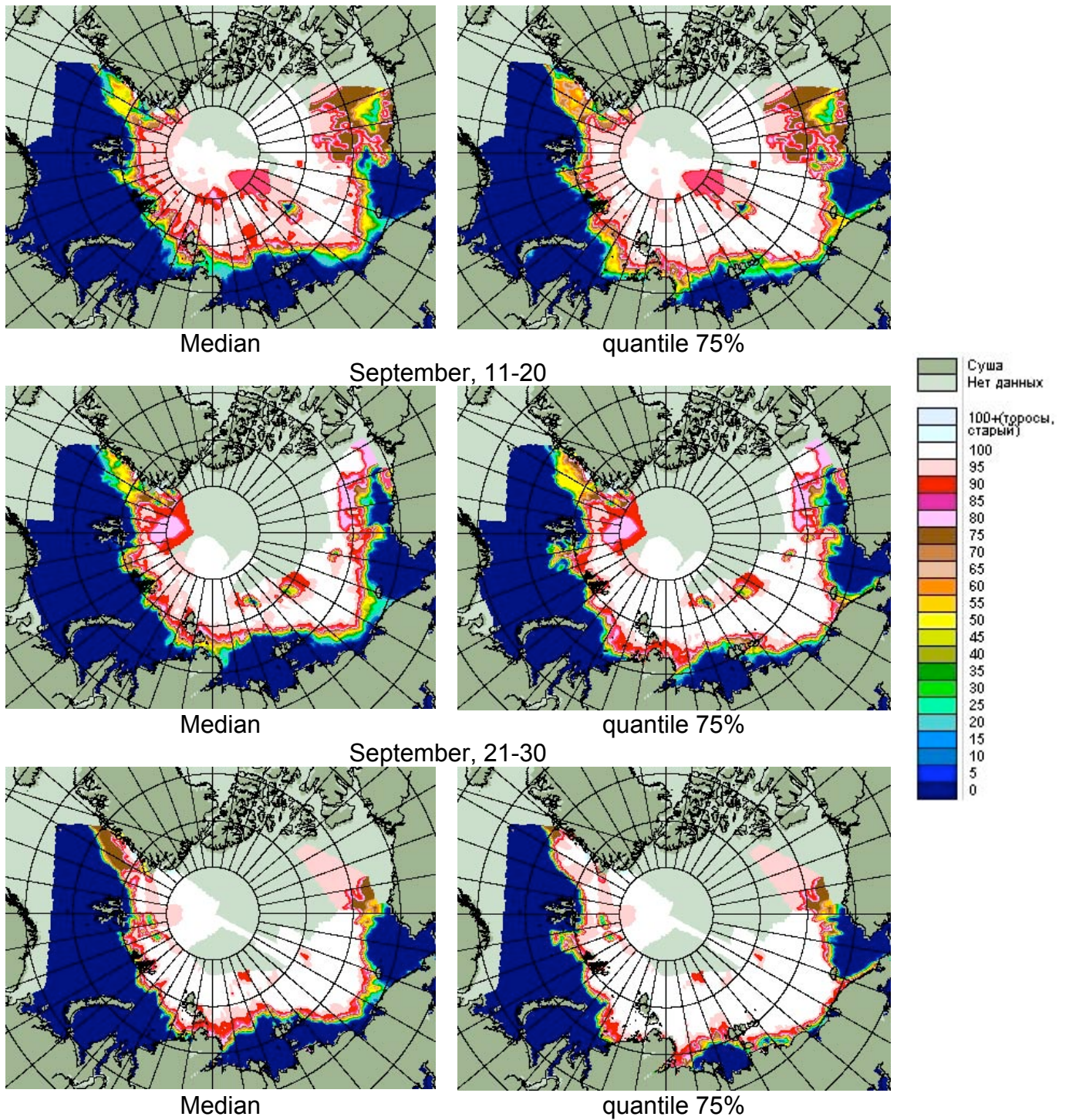
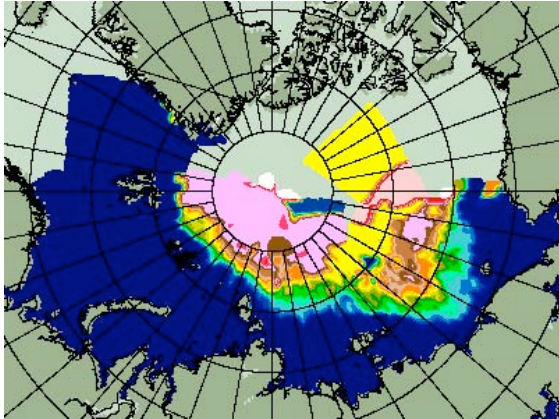
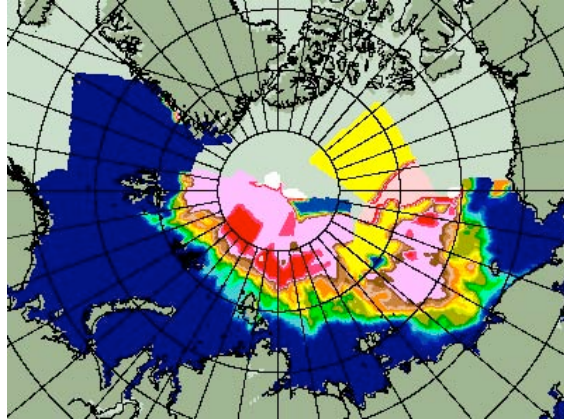


**Figure I.7.2.1:** Mean climatic sea ice total concentration in three 10-day periods of September based on AARI air reconnaissance ice charts for 1950-1992.

September, 1-10

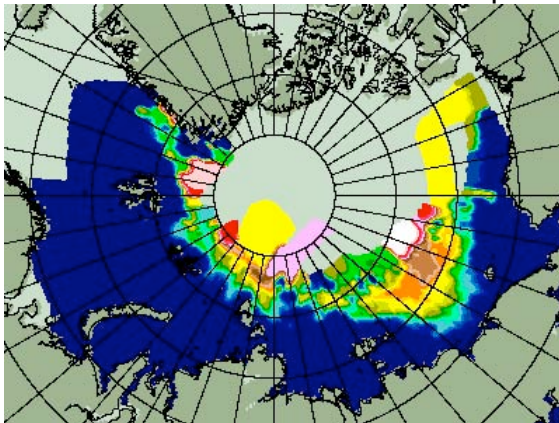


Median

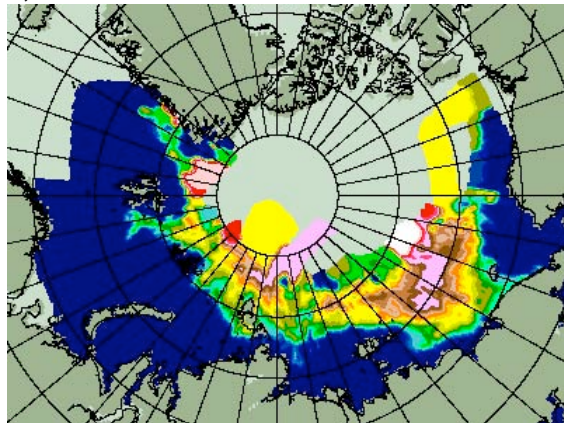


quantile 75%

September, 11-20

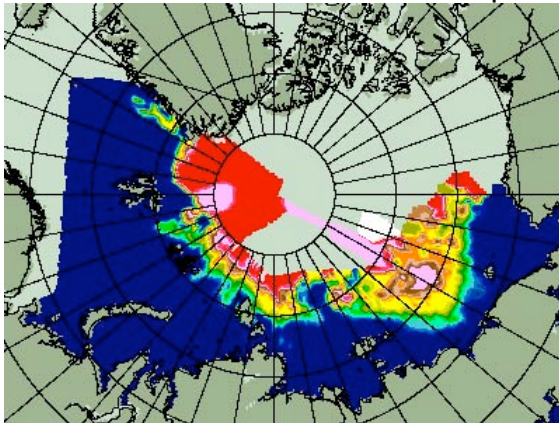


Median

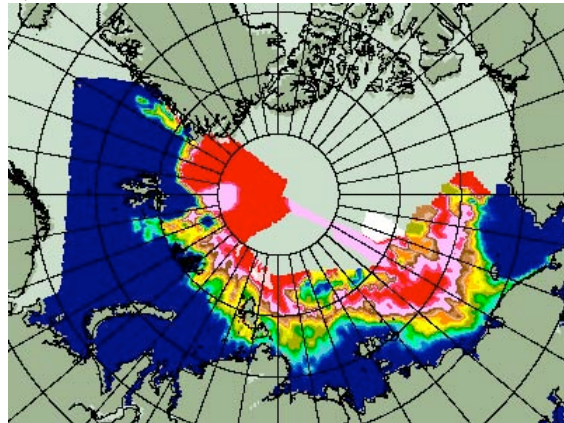


quantile 75%

September, 21-30



Median



quantile 75%

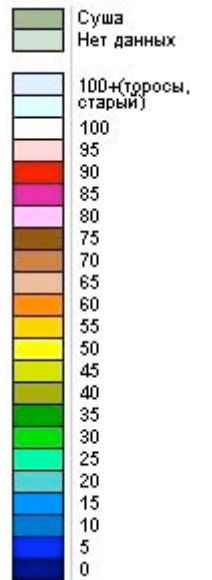


**Figure I.7.2.2:** Mean climatic old ice partial concentration in three 10-day periods of September based on AARI air reconnaissance ice charts for 1950-1992.

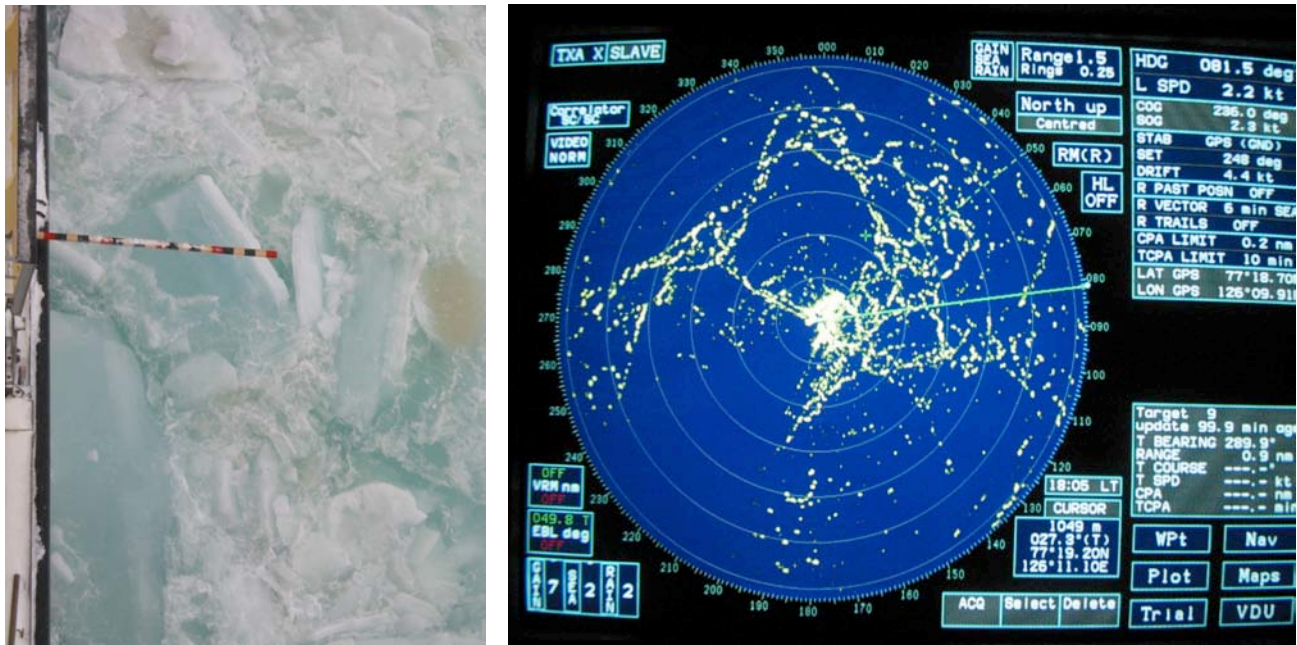


**Figure I.7.2.3:** Photos of ice measurement stick (left) and regular radar (right).

### **I.7.2.3.2. Satellite ice observations and data processing**

Mapping of ice conditions was carried out using satellite AQUA AMSR, DMSP SSM/I and ENVISAT data, obtained daily from the Danish Technical University (DTU, <http://www.seaice.dk>). Twenty-one ice charts were compiled during the period 7-23 September, 2004. Twelve ice charts were compiled using 6 km resolution ice concentration imagery from AQUA AMSR (9-16.09, 19-23.09), and 4 charts were compiled using DMSP SSM/I 12.5 km resolution ice concentration imagery (7 and 8.09); for all given cases a hybrid DTU algorithm to retrieve the ice total was used. Four charts were compiled using 1 km resolution GMM SAR ENVISAT imagery (mosaics for 18 and 19.09 and single orbit for 2:28UTC 18.09 and 01:38UTC 19.09), which also depicted ice roughness, allowing ice genesis to be traced.

Coloring and geographical transformation of initial imagery downloaded from the DTU server were carried out using the author's software, while visualization and additional geographical location were accomplished using DTU-developed Java software available at the URLs <http://www.seaice.dk> and <http://www.dcrs.dtu.dk>.

Compiled charts may be divided into 3 groups:

- general-purpose ice charts for expeditionary planning within the sea area (Figure I.7.2.4a);
- special-purpose ice charts allowing navigational planning within the sections of the cruise (Figure I.7.2.4b);
- detailed ice charts, which may be used for active navigation within the area of oceanographic research (Figure I.7.2.4c).

In our experience there is a high demand for ice information on the part of ship navigators and administrators for the purpose of active navigation and planning. Situations where such a need was particularly striking occurred on 19-20.09 while navigating around the southern boundary of the Taimyr Ice Massif, and on 23.09 while bypassing a strong ice belt in Vilkitsky Strait.

A Globalsat B-307 GPS receiver and SeaClear II freeware (<http://www.sping.com>) were used for registration of ship coordinates. Geographical coordinates and vectors of ship displacement for 5 – 24 September 2004 interpolated for 00, 06, 12 and 18 UTC are given in Appendix 2.

**Table I.7.2.1:** Ice conditions observed during oceanographic stations.

Station	Date	Time (GMT)	Ice cover parameters						
			CT	CA	CB	CC	SM	TR	SN
KD0104	12/09	4:00	90	50 6• 3	40 4 2	-	3	0-1	1
KD0204	12/09	6:25	90	50 6• 3	40 4 2	-	3	1	1
KD0304	12/09	16:00	91	20 7• 3	50 6• 2	23 4 2	3	1	1
KD0404	12/09	19:56	91	20 7• 3	50 6• 3	23 4 2	3	1	1
KD0504	12/09	23:45	90	30 7• 3	40 6• 2	20 4 2	3	1	1
KD0604	13/09	4:08	91	01 7• 3	60 6• 2	30 3 2	3	0-1	2
KD0704	13/09	12:14	90	10 7• 3	50 6• 2	40 5 2	3	0-1	2
ICE0104	14/09	08:06	91	10 7• 3	50 6• 4	34 3 3	3-4	0-1	1-2
KD0804	15/09	16:10	91	01 7• 3	70 6• 5	20 3 2	3-4	0-1	2
KD0904	15/09	23:04	91	30 7• 3	56 6• 5	10 3 1	3	2	2
KD1004	16/09	05:57	92	30 7• 6	50; 6• 5	20 3 4	3	1	2
KD1104	16/09	13:30	92	92 7• 6 5	-	-	2	1	2
KD1204	16/09	22:10	91	89 7• 5	10 3 x	-	2	1	2
ICE0204	17/09	04:10	91	10 7• 4 3	80 6• 5	01 2 x	2	0-1	2
KD1304	17/09	10:53	91	20 7• 4	67 6• 5	10 3 2	-	2	2
KD1404	17/09	18:55	92	80 6• 4 5	20 3 2	-	-	1-2	2
KD1504	18/09	10:00	90	20 8• 2	60 6• 4 3	10 2 x	2	1	2
KD1604	18/09	14:55	92	20 7• 4 5	60 6• 4	20 2 x	3-4	2	2
KD1704	18/09	17:34	92	10 7• 6	80 6• 5	10 5 3	2-3	1	2
KD1804	18/09	20:51	90	20 7• 4	40 6• 3	30 2 x	3	1	2
KD1904	18/09	23:10	89	23 8• 2	6 6• 5	20 3 3	3	1	2
KD2004	19/09	02:07	90	20 7• 4	40 6• 3	30 3 2 2	3	2	2
KD2104	19/09	04:22	92	30 7• 3	40 6• 3 4	30 3 2	3	2-3	2
KD2204	19/09	10:30	90	20 7• 2 3	40 6• 4	30 4 3	2	1	2
KD2304	19/09	16:45	90	70 6• 2	10 4 2	10 2 x	-	0-1	-
KD2404	19/09	22:45	92	40 6• 3 5	50 5 3	10 1 x	2	1	2
KD2504	20/09	06:18	92	20 7• 4	60 6• 2	20 4 3 1	2-3	1	1
KD2604	20/09	14:33	92	90 6• 5	10 5 2	-	2	2	1

Note: C \_ – total concentration; \_\_, \_\_, \_\_ – partial parameters (partial concentration, stage of development, ice form); SM – stage of melting (Russian national 5-point scale); TR – hummock and ridge concentrations (Russian national 5-point scale); SN – snow concentration (Russian national 3-point scale)

Total concentration of ice (C)		Stage of development and thickness (S <sub>a</sub> S <sub>b</sub> S <sub>c</sub> S <sub>o</sub> S <sub>d</sub> )		
Concentration	Symbol	Element	Thickness	Symbol
Ice free	00	No stage of development	-	0
Less than one tenth	01	New ice	-	1
1/10, 2/10 .... 9/10	10, 20, ..., 90	Nilas; ice rind	< 10 cm	2
10/10	92	Young ice	10-30 cm	3
1/10 – 2/10, 1/10 – 3/10, ... 8/10 – 9/10	12, 13 ... 89	Gray ice	10-15 cm	4
9/10 – 10/10	91	Gray-white ice	15-30 cm	5
Undetermined or unknown	x	First-year ice	30-200 cm	6
Table 3. Form of ice (F <sub>a</sub> F <sub>b</sub> F <sub>c</sub> F <sub>p</sub> F <sub>s</sub> )		Thin first-year ice	30-70 cm	7
Element	Floe size	Thin first-year ice, first stage	30-50 cm	8
Pancake ice	-	Thin first-year ice, second stage	50-70 cm	9
Small ice cake; brash ice	< 2 m	Medium first-year ice	70-120 cm	1•
Ice cake	2-20 m	Thick first-year ice	> 120 cm	4•
Small floe	20-100 m	Old ice		7•
Medium floe	100-500 m	Second-year ice		8•
Big floe	500 m-2 km	Multi-year ice		9•
Vast floe	2-10 km	Ice of land origin		•
Giant floe	> 10 km	Undetermined or unknown		x
Fast ice	-			
Icebergs, growlers or floebergs	-			
Undetermined or unknown	-			



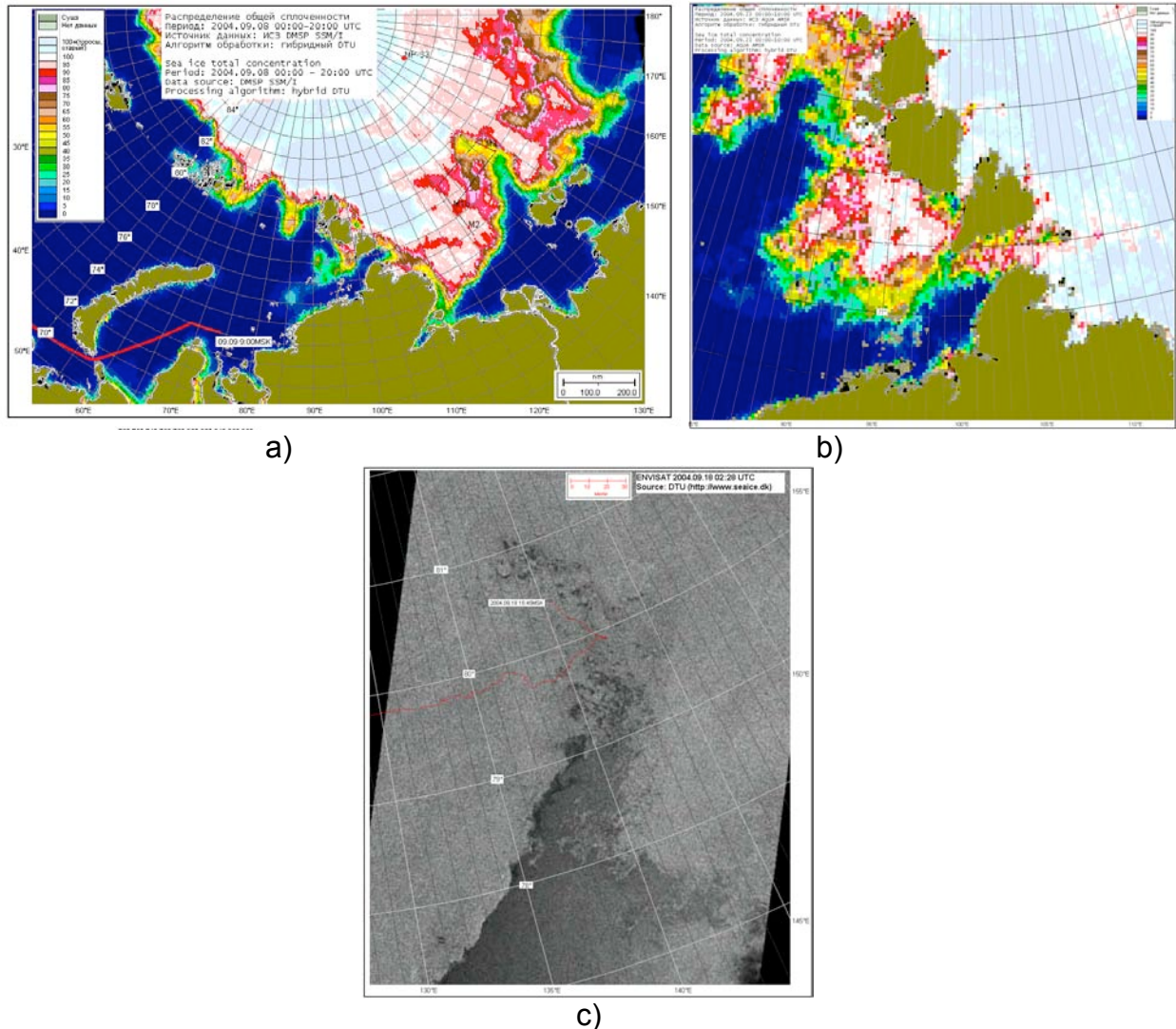


**Figure 1.7.2.4:** Ice charts: a – general-purpose ice chart along the Northern Sea Route for 8 September 2004 based on AMSR AQUA data, b – detailed ice chart for Vilkitsky Strait for 23 September 2004 based on AMSR AQUA data, c – detailed ice chart for the area of oceanographic stations for 18 September 2004 based on GMM SAR ENVISAT (source of initial data for a-c – DTU, <http://www.seaice.dk>).

### 7.2.3.3. Ice data observations during ice stations.

During two ice stations 7 ice cores were cut and their texture and structure were described. Photos of two of them are shown in Figures 1.7.2.5 and 1.7.2.6 along with results of their texture and structure analysis presented in Tables 1.7.2.2 and 1.7.2.3.

There are some differences in ice composition observed during the ice stations. Generally, the ice core structure is characterized by the last stage of melting and beginning of recrystallization. During the second ice station placed on a medium ice floe, a third core was drilled in the thick (255 cm) multi-year ice. Puddles with saturated ice crumbs were observed in all cores at different layers. Usually the ice had white color, solid structure with small bubbles in the upper layers, and porous structure with 5 mm diameter brine channels in the lower layers.

**Table I.7.2.2:** General characteristics of the ice cores, drilled in the first ice station.

**Core 1.** Thickness = 126 cm (the lowest border of the ice floe was not reached)

Layer depth (cm)	Description
0-22	Snow. Density increases with depth.
22-38	White muddy ice. Small bubbles 1 mm in diameter.
38-60	Puddle with saturated ice crumbs.
60-126	Monolithic ice. Ice crumbs were found at the 93-98 cm depth.

**Core 2.** Thickness = 97 cm (the lowest border of the ice floe was not reached)

Layer depth (cm)	Description
0-8	Puddle.
8-14	White muddy ice with small bubbles.
14-34	Puddle.
34-97	White muddy ice. Porous, spongy ice with big brine channels.

**Core 3.** Thickness = 139 cm

Layer depth (cm)	Description
0-10	Snow.
10-31	White muddy ice. Monolithic structure of the ice with small bubbles.
31-39	Puddle.
39-76	White muddy ice. Porous, spongy ice with deep brine channels in various directions. Density of ice increased with depth.
76-139	White muddy ice with vertical brine channels.

**Core 4** (Figure 7.2.5). Thickness = 112 cm (the lowest border of the ice floe was not reached)

	Layer depth (cm)	Description
1	0-10	Snow.
2	10-19	White transparent ice with a small amount of bubbles (1-1.5 mm diameter).
3	19-38	Puddle.
4	38-41	Porous, spongy ice with brine channels (5 mm diameter) in various directions.
5	41-63	Ice crumbs.
6	63-87	Porous, spongy ice with brine channels (5 mm diameter) in various directions.
7	87-112	Density of the ice is higher than upper layer. Brine channels (2 mm diameter).



**Figure I.7.2.5:** Core 4. Ice station ICE0104. This photo shows the lowest part of the 6<sup>th</sup> layer and the whole 7<sup>th</sup> layer (vertical profile).

**Table I.7.2.3:** General characteristics of the ice cores, drilled in the second ice station.

**Core 1** (Figure I.7.2.6). Thickness = 125 cm (the lowest border of the ice floe was not reached). Snow - 27 cm.

Layer depth (cm)	Description
0-27	White monolithic ice with 2-3 mm diameter bubbles.
27-34	Puddle.
34-37	Porous rotten ice.
37-53	White porous ice with brine channels (5-7 mm diameter) in various directions.
53-125	Porous ice with brine channels (5-7 mm diameter) in horizontal directions.

**Core 2.** Thickness = 105 cm. Snow - 18 cm.

Layer depth (cm)	Description
0-4	White porous ice with brine channels (3-4 mm diameter) in various directions.
4-29	Puddle.
29-36	White transparent monolithic ice with small amount of bubbles (2 mm diameter).
36-105	Saturated ice crumbs.

**Core 3.** Thickness = 255 cm. Snow 20 m.

Layer depth (cm)	Description
0-29	White transparent ice with small amounts of bubbles (2-3 mm diameter).
29-49	Puddle.
49-255	Porous ice with brine channels (0.5 cm diameter) in various directions.

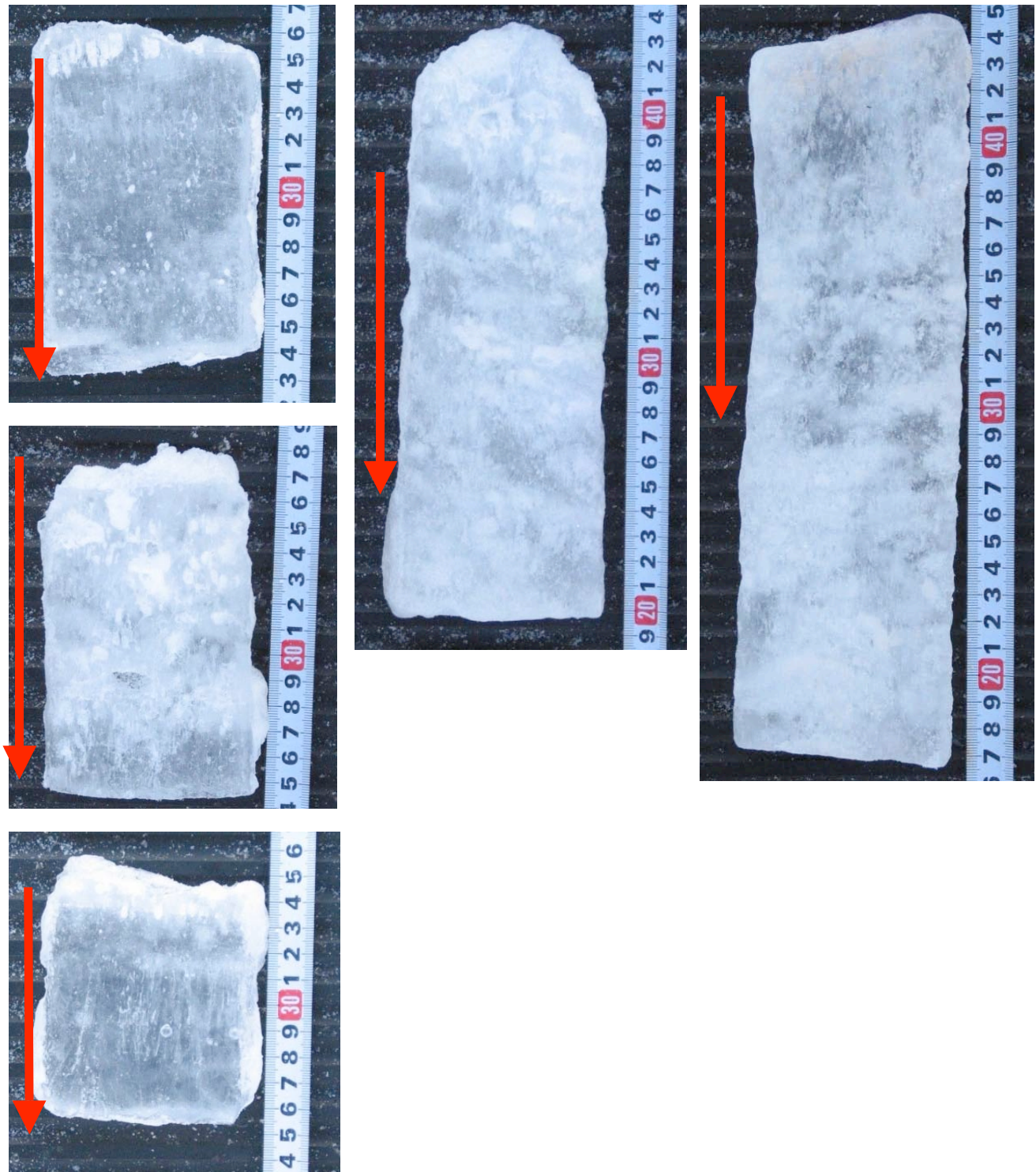
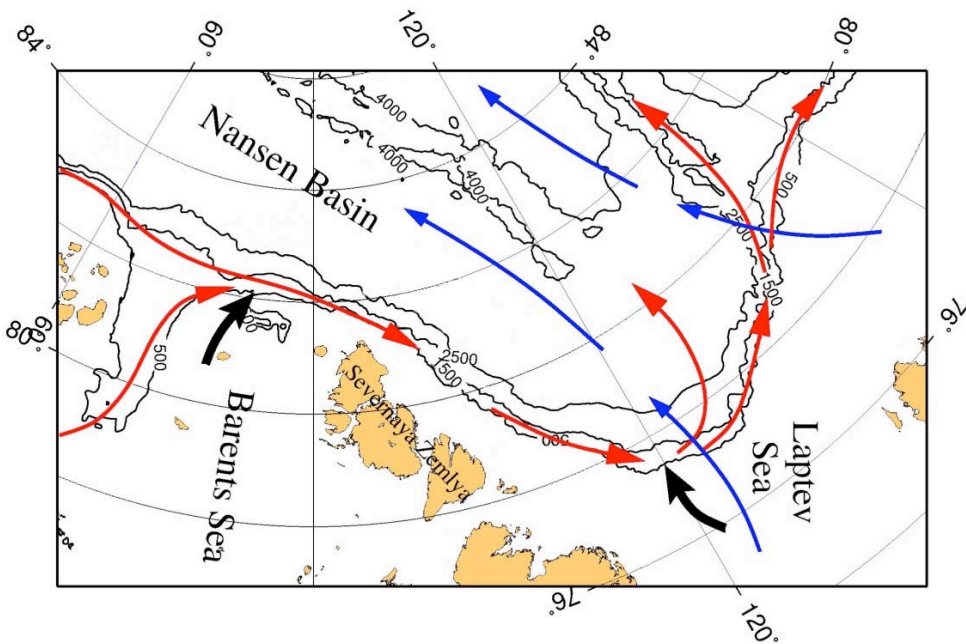


Figure I.7.2.6: Core 1. Ice station ICE0204.

### I.7.3. OCEANOGRAPHIC OBSERVATIONS

#### I.7.3.1. Background information (*I.Polyakov, IARC, and D.Walsh, NRL*)

Observations made from ice buoys, manned drifting stations, and satellites show that near-freezing surface waters, driven by surface winds and ice drift, exhibit a trans-polar drift from the Siberian Arctic toward Fram Strait [Rigor et al., 2002]. In the eastern part of the Eurasian Basin this flow merges with several branches coming from marginal arctic seas (the East Siberian and Laptev Sea branches, and further west the Barents Sea branch). The basic features of the circulation in the Nansen and Amundsen Basins are shown by blue arrows in Figure I.7.3.1. Nansen was the first to identify Atlantic Water (AW) in the Arctic Ocean during his drift on board the Fram in 1893-1896. Later observations provided evidence that the AW spreads cyclonically around the Arctic Basin and is its major source of heat [Timofeev, 1960; Coachman and Barnes, 1963], and clarified the properties of AW circulation. Aagaard [1989] used moored current measurements and hypothesized that major subsurface water transports occur in the form of narrow near-slope cyclonic boundary currents (Figure I.7.3.1, red arrows). Two major inflows supply the polar basins with AW - the Fram Strait AW branch and the Barents Sea AW branch [Rudels et al., 1994].



**Figure I.7.3.1:** Water mass circulation patterns in the Nansen Basin and adjacent arctic seas. Surface and subsurface circulation shown by blue and red arrows respectively.

The Fram Strait branch enters the Nansen Basin through Fram Strait and follows the slope until it encounters the Barents Sea branch north of the Kara Sea, an area characterized by strong water-mass mixing and thermohaline interleaving. The two merged branches follow the Eurasian Basin bathymetry in a cyclonic sense, forming a narrow topographically trapped boundary current which flows at about 5 cm/s [Woodgate et al., 2001]. Near the Lomonosov Ridge the flow bifurcates, with part turning north and following the Lomonosov Ridge and another part entering the Canadian Basin [Woodgate et al., 2001]. Jones [2001] stresses that the circulation in the deep waters (>1700m) has not been well determined.

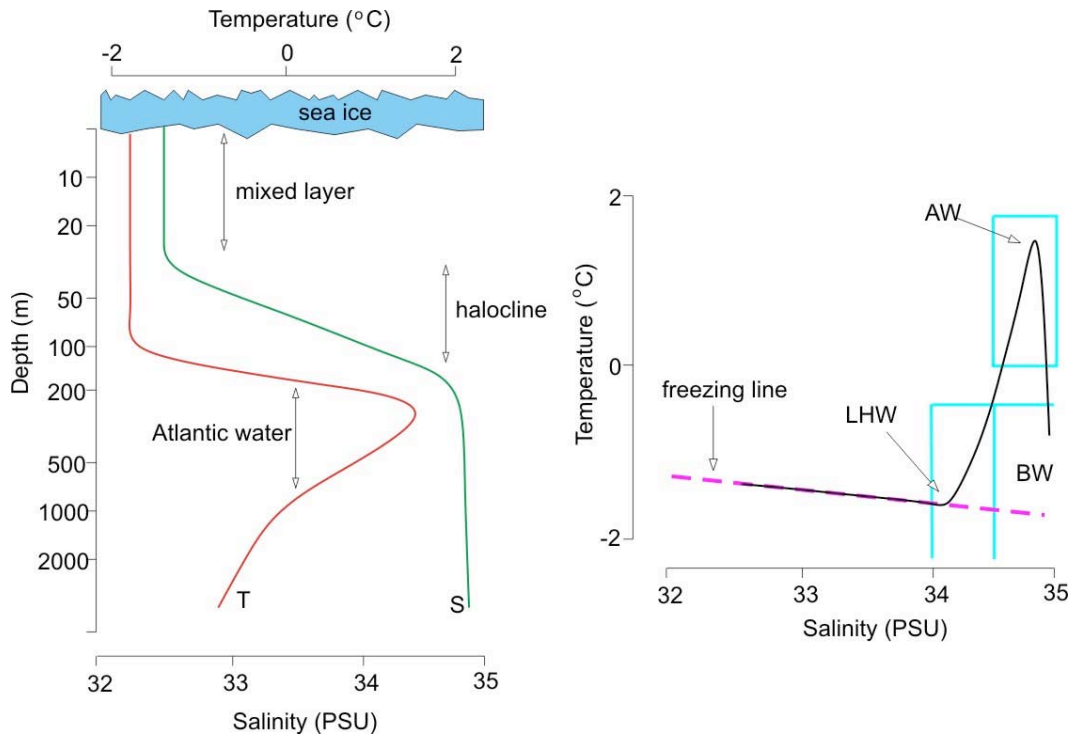


**Figure I.7.3.2:** Low Halocline Water (LHW), Atlantic Water (AW), and Bottom Water (BW) on the typical vertical temperature and salinity (T-S) distribution and T-S curve in the research area.

The area of the northern Laptev Sea and adjacent Eurasian basin has complex water-mass characteristics [Pfirman et al., 1994; Schauer et al., 1997; Schauer et al., 2002]. Atlantic Waters originating in Fram Strait are found between 150 and 800 m depth in this region (Figure I.7.3.2, left panel). Lower Halocline Water (LHW) lies at the base of the permanent halocline, occupying the region of temperature-salinity (T-S) space defined by  $34.0 < S < 34.5$  psu and temperature less than  $-1.0$  °C [Woodgate et al., 2001]. Below the Atlantic Water layer are the Bottom Waters (BW) layers, with potential temperatures down to  $-0.95$ °C. The locations of these water masses in the T-S plane are shown in Figure I.7.3.2, right panel.

Little is known about temporal variability of thermohaline structure in the Eurasian Basin. An early attempt to quantify interannual variability of water-mass structure in this region is due to Quadfasel et al. [1993], who compared measurements from cruises in different years, finding significant year-to-year variability in the core temperature of the AW layer. However, because Quadfasel et al. compared measurements taken in different years and at different locations in the Nansen Basin, it is difficult to determine the extent to which their conclusions were influenced by aliasing of spatial and temporal variability, especially as the AW layer is known to cool dramatically as it flows through the Nansen Basin [Polyakov et al., 2003], emphasizing that quantifying interannual variability in this region is substantially complicated by the large spatial gradients in the area. Processes which affect fresh water content (e.g., freezing, melting, and riverine inflow) are of first-order importance to Arctic Ocean dynamics [Aagaard, 1989]. Large amounts of ice form in winter on the wide continental shelves on the periphery of the Arctic Ocean, in some cases producing dense, briny waters which flow off the shelves and significantly influence the T-S structure in the interior.

### I.7.3.2. Routine CTD measurements and water sampling

#### I.7.3.2.1. Objectives (I.Polyakov and I.Dmitrenko, IARC)

The major objectives of the 2004 field experiment were:

- quantify the structure and spatial variability of the main water masses over the continental shelf of the Laptev Sea and adjoined Eurasian Basin in 2004; and
- enhance understanding of mechanisms by which the Atlantic Water is transformed across and along the continental slope of the Eurasian Basin.

The hydrographic survey also provides important background information for processing of the long-term mooring data.

#### I.7.3.2.2. Methods (I.Dmitrenko, IARC, and S.Kirillov, AARI)

Over the 9-day period 26 CTD casts were made. Location and sampling time for the CTD casts are listed in Table I.7.1 and the locations are also depicted in Figure I.7.3.3.

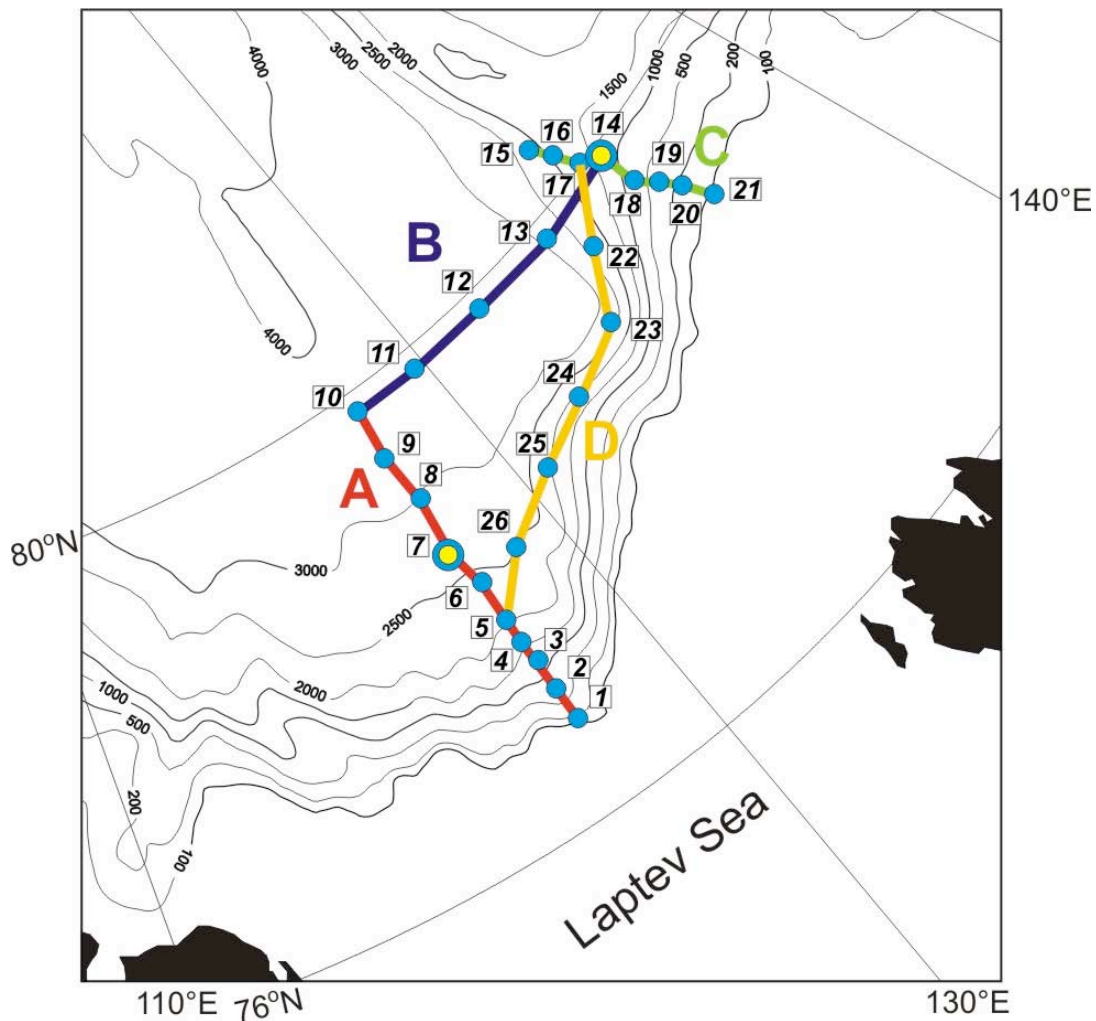


**Figure I.7.3.3:** CTD cross-sections on the NABOS-04 cruise. Blue circles represent CTD and CTD/Niskin bottle stations; yellow circles are mooring sites. Bathymetry is from IBCAO.

Cross-section A (Figure I.7.3.3) extended across the Russian Exclusive Economic Zone (REEZ) and the Laptev Sea continental slope to the Arctic Ocean. The southern part of transect A is located within the REEZ and measurements at this part of the transect were carried out at the beginning of observations during September 12-13. Stations KD0104-0304 were completed before unsuccessful attempts to recover mooring M2a, and stations KD0404-0604 were carried out after the extensive search for mooring M2a on the way to mooring M1b. The measurements along the northern part of this transect outside the REEZ (stations KD0704-1004) were carried out after successful recovery of mooring M2b on September 14 near the position of station KD0704. Mooring M1c was deployed at the same position a couple of hours after the CTD cast (station KD0704). Cross-section B (stations KD1004-1404) connected the observational area in the central Laptev Sea with the region of mooring M3a deployment northward of the New Siberian Islands where cross-section C (stations KD1404-2104) crossed the continental slope. Cross-section D (KD1404, KD2204-2604, and KD0504) was carried out along the continental slope of the Laptev Sea (Figure 1.7.3.3).

Most CTD casts were made from the sea surface to a depth of 2000 m. Continuous CTD profiles were made on the downcast. Due to the technical problems with the rosettes the water sampling at most stations (Table I.7.1) was carried out only within 50 m of the surface water layer. Five-liter Niskin bottles were fixed on the cable and tripped at the sampling level. Sampling depth was determined by winch counter. Sampling levels are shown in Appendix 1.

The CTD winch was located on the helicopter deck of the icebreaker approximately 17 m forward of the three icebreaker propellers (Figure I.2.3). The icebreaker draft at the position of the CTD winch varies between 8.5 and 9.5 m. In order to maintain correct ship position relative to the ice floes, during CTD sounding the propellers were not switched off.

The SBE SEASOFT software package for Windows was used for data collection and processing. Derived variables include pressure (in db), water temperature (in °C), and conductivity (S/m). Poor quality data from the upper water layer (usually 10-20 m) were removed. Poor quality was mainly determined by higher than normal noise levels, spikes or jumps in the data due to the strong impact from the rotating icebreaker propellers in the upper water layer. To avoid the spikes in the calculated salinity (which depends on measured temperature, conductivity, and pressure) caused by misalignment of temperature and conductivity with each other we used an alignment procedure. The best alignment of conductivity with respect to temperature was obtained when the salinity spikes were minimized. Some experimentation with different advances was required to find the best alignment; ultimately the advance of conductivity relative to temperature was determined to be -0.4 sec.

Although in some cases the data were considered reliable one should take into account that the noise from propellers and ship draft can affect the data within the upper 20 m layer. The ocean depth was reliably measured by an Odom Hydrographic System dual frequency 12 and 210 KHz Eco-Sounder only within the range of 2000 m (see also section I.7.3.3.3). Otherwise the depth information was obtained from the navigation charts.

### I.7.3.2.3. Equipment (R.Chadwell, IARC, and M.Dempsey, OM)

Continuous CTD profiles were made using the SEACAT Profiler SBE19plus. This system continuously measures conductivity, temperature and pressure at 0.25 m intervals in the vertical. The Seacat was calibrated just prior to the expedition (June, 2004) and will not be recalibrated again until just before next year's scheduled NABOS cruise. The technical description of sensors is presented in Table I.7.3.1. Information in Table I.7.3.1 is presented according to the specifications of Sea-Bird Electronics, Inc. The full information can be downloaded from: [http://www.seabird.com/products/spec\\_sheets/19plusdata.htm](http://www.seabird.com/products/spec_sheets/19plusdata.htm).

**Table I.7.3.1:** SEACAT Profiler SBE19plus technical information.

	Measure-	Initial	Typical	
--	----------	---------	---------	--



Sensors	ment Range	Accuracy	Stability (per month)	Resolution
Conductivity (S/m)	0 – 9	0.0005	0.0003	0.00005 (most oceanic waters) 0.00007 (high salinity waters) 0.00001 (fresh waters)
Temperature (°C)	-5 to +35	0.005	0.0002	0.0001
Pressure	3500 m	0.1% of full scale range	0.004% of full scale range	0.002% of full scale range

#### I.7.3.2.4. Preliminary Results (I.Dmitrenko, IARC, S.Kirillov, and L.Timokhov, both AARI)

Early fall water-column structure in the area of the oceanographic survey is characterized by a cold (-1.8°C), and fresh (28-32 psu) surface layer, overlying a halocline in which salinity increases to 34.85 psu at about 230 m (Figures I.7.3.4 - 7.3.6). The surface mixed layer is about 20 m thick (Figures I.7.3.5, and I.7.3.6). The shallow halocline centered at about 100-105 m depth is found above the thermocline (centered at 180 m); this layer is believed to play a crucial role in insulating near-surface waters and overlying ice from upward heat fluxes.

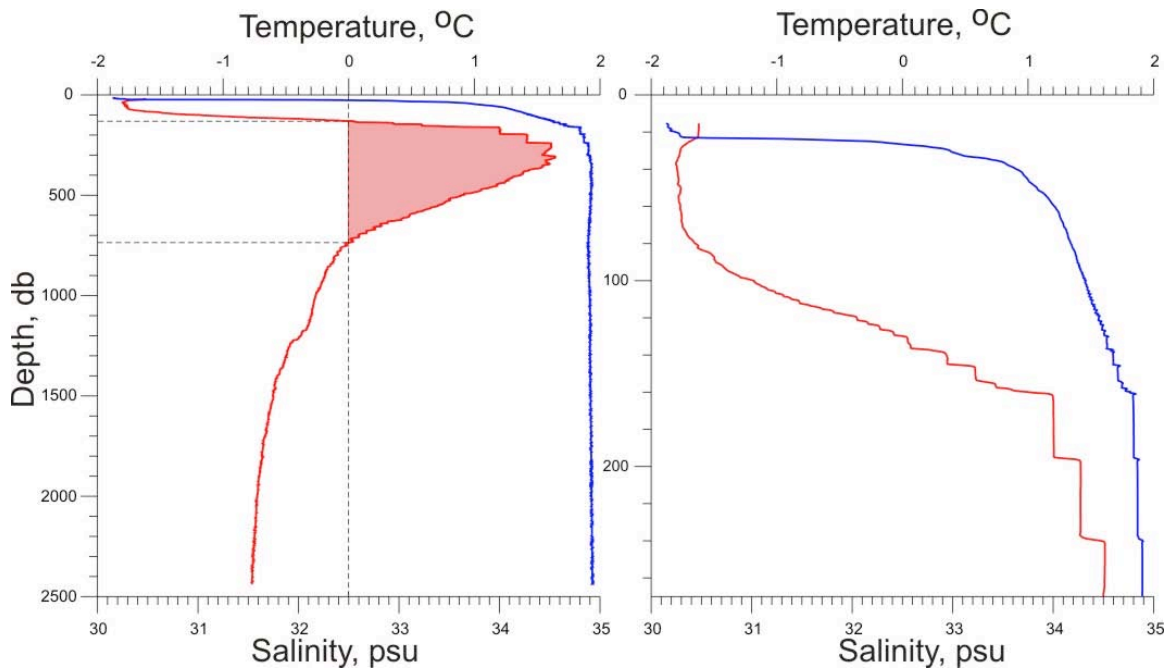


**Figure I.7.3.4:** Salinity (blue) and temperature (red) vertical distribution at station KD0704. Data from CTD SBE19plus. Right panel presents the zoomed upper 270 db of the left panel.

In most cases the surface temperature is close to the freezing point down to the depth of 80 m. The exceptions are represented only by stations situated in the vicinity of the continental shelf break (KD0104-KD0404, and KD2104), where increase of temperature by 0.35°C was observed right beneath the surface mixed layer down to the depth of 80 m (Figure I.7.3.5, left and right). This year we did not record the increase of temperature by 0.2 ÷ 0.5 °C at the depth of 20-30 m that was commonly observed in 2003 and was associated with heating of the surface water layer by summer solar radiation [Dmitrenko et al., 2004]. Apparently, compact ice observed in summer 2004 (Figure I.5.1) prevented solar radiation penetration downward and surface water heating during the summer period.

Farther downward within the thermocline layer the temperature increase was observed reaching the depth of 240-280 m, where a prominent temperature maximum of  $0.85 \pm 1.82$  °C is found (Figure I.7.3.5). This vertical structure corresponds well to the previous studies ([EWG, 1997], see also Figure I.7.3.2). This mid-depth temperature maximum marks the core of the Atlantic Water (AW), typically found between 150 and 800 m depth in this region (Figures I.7.3.4, I.7.3.7, I.7.3.9, see also Schauer et al., [1997] for more details). AW core salinity varies between 34.85 and 34.91 psu (Figures I.7.3.6, I.7.3.11–I.7.3.14). Beneath the AW core the temperature decreases to about -0.8 °C close to the bottom while salinity slightly increases to 34.92 psu.

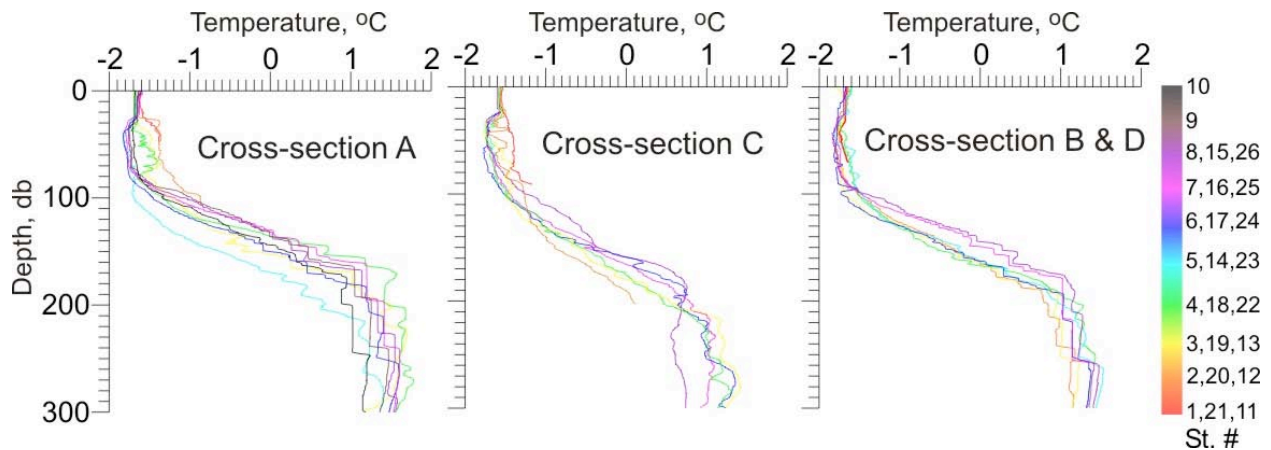


**Figure I.7.3.5:** Vertical temperature (°C) distribution in the upper 300 m layer.

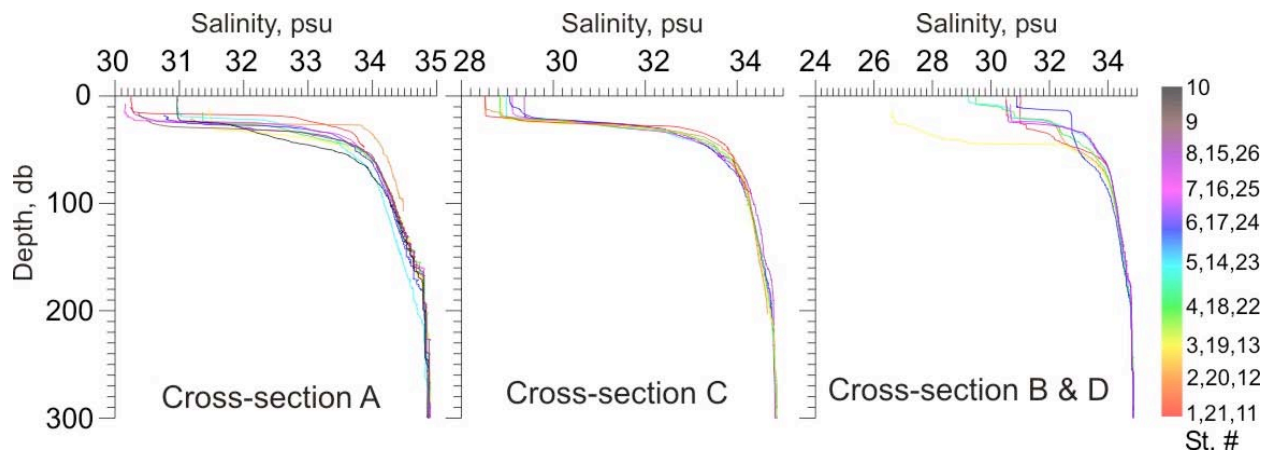


**Figure I.7.3.6:** Vertical salinity (psu) distribution in the upper 300 m layer.

The spatial variations of water temperature and salinity along the transects across the continental slope (marked as A and C in Figure I.7.3.3) are presented in Figures I.7.3.7 and I.7.3.9. Ice melting southward of cross-section C and eastward of cross-sections B and D (Figure I.7.3.3) resulted in freshening of the surface water layer up to 26-30 psu at stations KD1304-KD2304 (Figures I.7.3.6, I.7.3.8 right panel, I.7.3.10). Although this freshening could also be caused by the input of river runoff water, the pack ice edge coincides very well with the zone of freshening (Figure I.7.2.4, panel c).

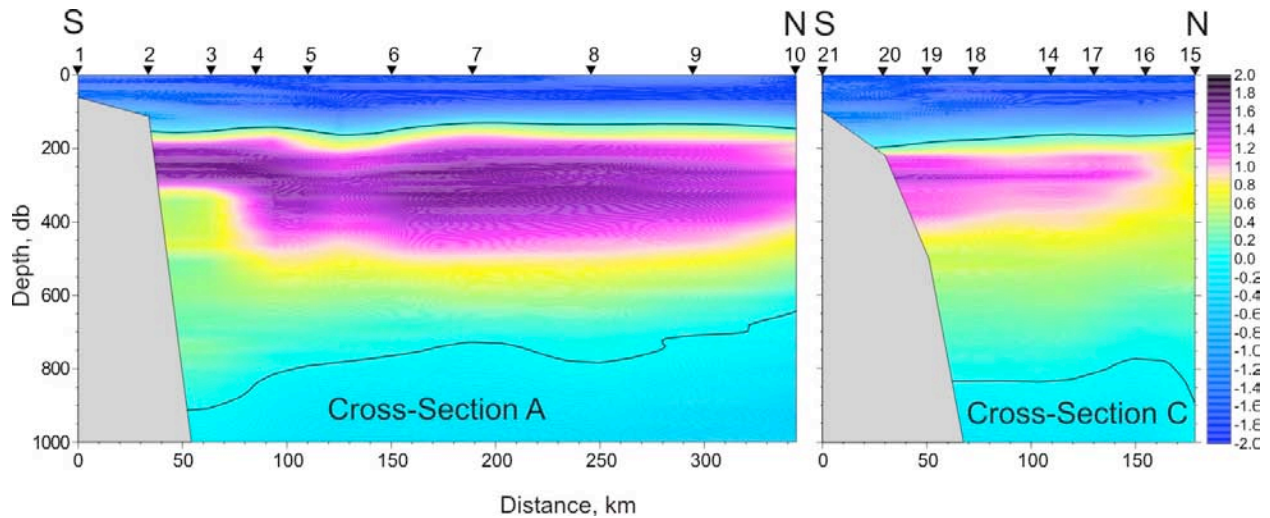


**Figure I.7.3.7:** Temperature ( $^{\circ}\text{C}$ ) distribution across the continental slope of the Laptev Sea along cross-sections A and C.  $0^{\circ}\text{C}$  isotherm (black line) traces the boundaries of the AW layer.

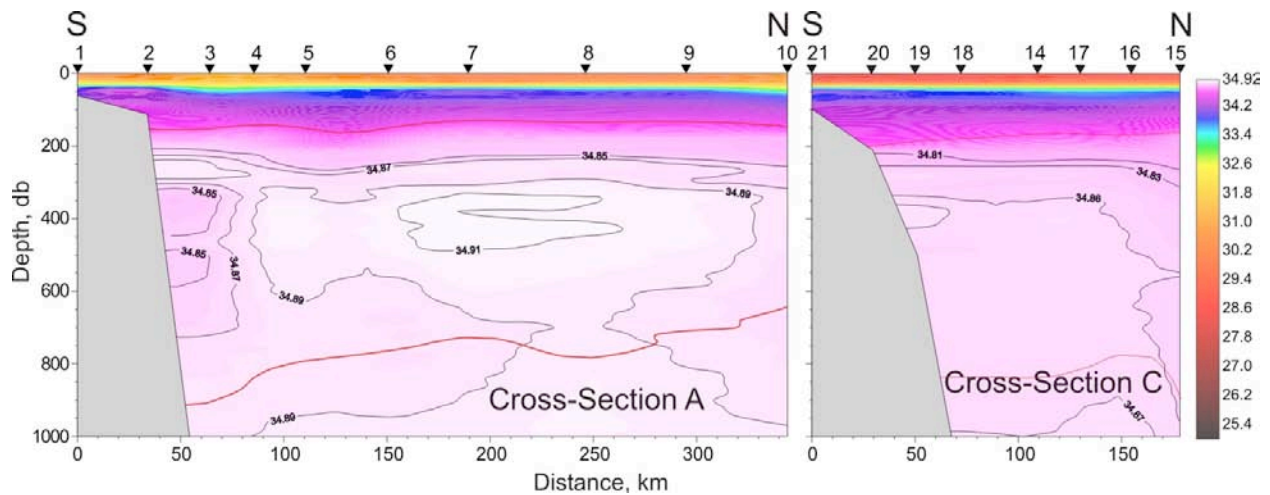


**Figure I.7.3.8:** Salinity (psu) distribution across the continental slope of the Laptev Sea along cross-sections A and C.  $0^{\circ}\text{C}$  isotherm (black line) traces the boundaries of the AW layer.

The thickness of the AW layer, traced by the zero temperature isotherm, varies from 750 m (KD0304, KD1504, Figure I.7.3.7 left) to 425 m (KD1304, Figure I.7.3.9, left). The AW core in the central Laptev Sea (cross-section A) is situated approximately 150 km north of the shelf break in the area of station KD0704, although the second AW core with the maximum-recorded temperature of  $1.82^{\circ}\text{C}$  was traced about 50 km northward from the continental shelf break at station KD0404 (Figure I.7.3.7 left). At the same time, along cross-section C located to the east of cross-section A the thickness of the AW layer was very similar to that from the central part of the sea; however the recorded temperature of the AW core was only as high as  $1.42^{\circ}\text{C}$  (Figure I.7.3.5, central panel, Figure I.7.3.7 right). Similar to the central Laptev Sea, the AW core was located 50 km northward of the shelf break. Note that in 2002 (NABOS-02 expedition) and 1993 (ARK IX/4 Polarstern expedition [Schauer et al., 1997]) in the central Laptev Sea the maximum temperature in the AW core was about 250-300 km northward from the edge of the continental shelf, while in 2003 (NABOS-03 expedition) two maxima of the AW temperature were recorded, one located 30-50 km and the other one 300 km northward from the shelf edge [Dmitrenko et

al., 2004]. A northward decrease of the AW upper boundary depth by 25 and 45 m was observed along cross-section A (Figure I.7.3.7 left) and cross-section D (Figure I.7.3.9 right), respectively. The same features were observed in the westward direction along section B (31 m, Figure I.7.3.9 left).

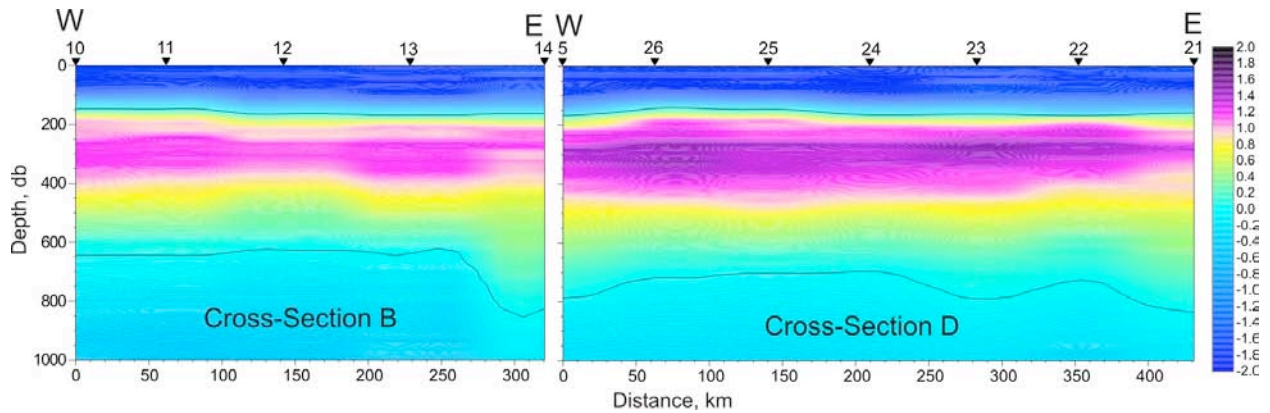


**Figure I.7.3.9:** Temperature ( $^{\circ}\text{C}$ ) distribution along the continental slope of the Laptev Sea on cross-sections B and D.  $0^{\circ}\text{C}$  isotherm (black line) traces the boundaries of the AW layer.

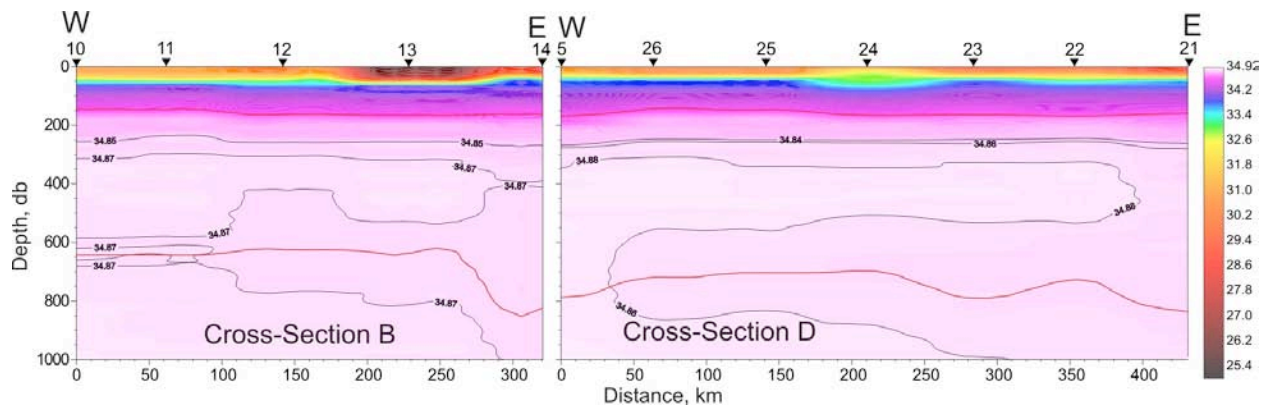


**Figure I.7.3.10:** Salinity (psu) distribution along the continental slope of the Laptev Sea on cross-sections B and D.  $0^{\circ}\text{C}$  isotherm (black line) traces the boundaries of the AW layer.

The AW core temperature found in the southern and central parts of cross-section A is  $0.5\text{--}0.8^{\circ}\text{C}$  higher compared with data collected in 2002 and 2003 [Dmitrenko et al., 2004] (Figure I.7.3.11). At the same time at the western part of cross-section B and northern part of cross-section A the AW temperature and salinity were comparable with 2003 and 2002 data (Figure I.7.3.11 and I.7.3.12), while warming by  $0.3^{\circ}\text{C}$  was measured at the eastern part of cross-section B (Figure I.7.3.12 right) and northern part of cross-section C (Figure I.7.3.13 left). The AW warming by  $0.7^{\circ}\text{C}$  was also measured in the southern part of cross-section C (Figure I.7.3.13 right). Based on the above, we speculate that the main pathway of the warm AW event in 2004 was along the continental slope northeastward within a 100–250 km range off the shelf edge in the central and eastern part of the Laptev Sea, respectively. The warmer temperature of the AW layer along cross-section D compared with cross-section B also supports this conclusion (Figure I.7.3.9).

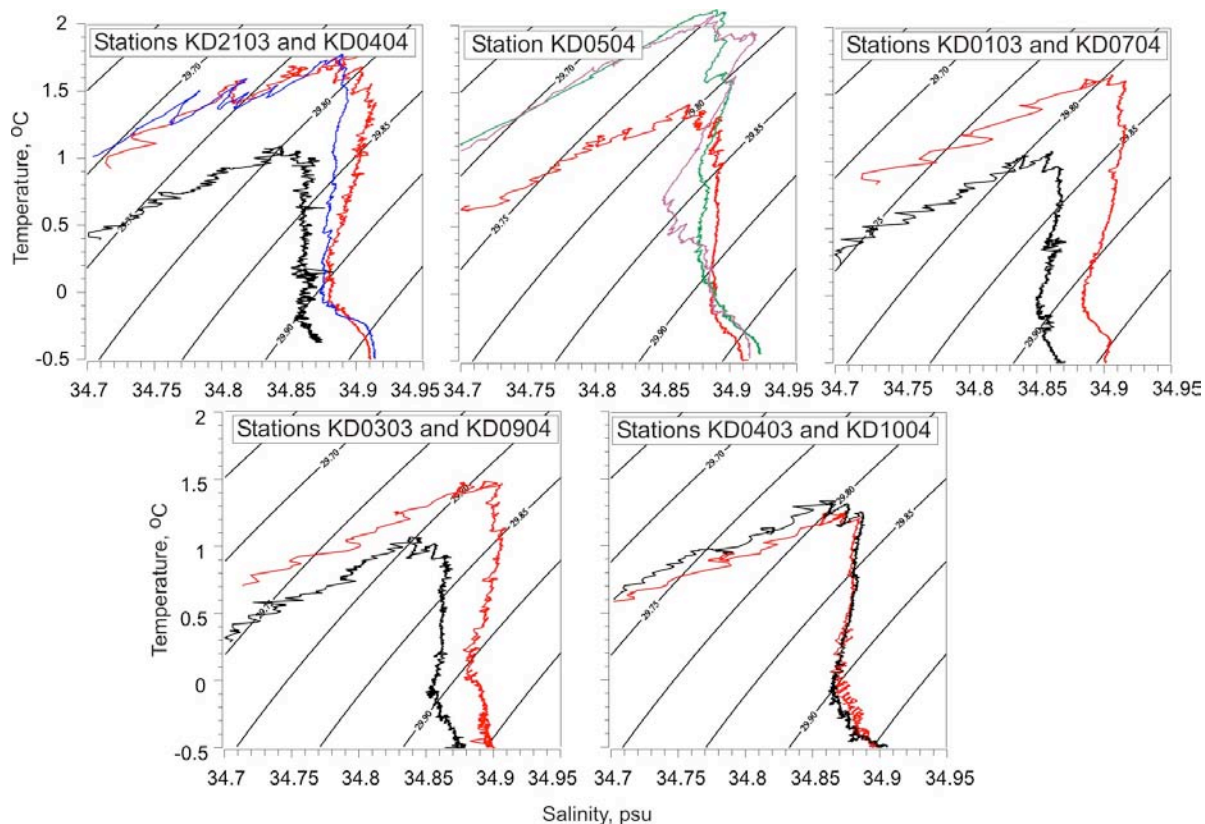


**Figure I.7.3.11:** Temperature versus salinity from (black) NABOS-03, (red) NABOS-04, (blue) Polarstern ARK IX/4 (1993), (green) Polarstern ARK XI/I (1995), and (violet) Polarstern ARK XIII/II (1997) cruises at cross-section A. The measurements were carried out approximately at the same positions. Thin solid black lines are isopycnals referenced to 300 db.

The AW temperature measured in September 2004 was up to 1.0°C higher than the AW climatic mean [EWG, 1997]. At the same time, the AW temperature in 2004 corresponds well to the AW core temperature of 1.7°C recorded at the continental slope north of the Novosibirskiye Islands in August 1995 – January 1996 [Woodgate et al., 2001]. At station KD0404 the AW core temperature was slightly higher than in 1993 (Figure I.7.3.11, upper left panel). Our measurements showed the AW temperature cooler by 0.3-0.5°C along cross-section D compared with Polarstern 1995 cruise data (Figure I.7.3.14). In the central Laptev Sea (station KD0504) it was also cooler by 0.32°C compared with a record-high temperature of 2.15°C observed during the 1995 and 1997 Polarstern cruises [Schauer et al., 1997; Rudels et al., 2000] (Figure I.7.3.11).

A period of cooler AW inflow through Fram Strait began after 1995 [e.g. Karcher et al., 2003]. Apparently, later on this inflow resulted in cooler and fresher water at the continental slope in the northern Laptev Sea. The recent 2000-2001 temperature data from the North Pole Environmental Observatory downstream flank of the Lomonosov Ridge still show increased Atlantic Water temperature inherited from the 1990s [Morison et al., 2002]. Data from 2002 and 2003 NABOS cruises confirm that for the area of the Laptev Sea continental slope the large warming event of the late 1980s – early 1990s is gone. This also corresponds well to other observations and modeling studies [e.g. Karcher et al., 2003]. Observations carried out in 2004 provided strong evidence that a new warming event entered the northern Laptev Sea. Our year-long CTD record from mooring M1B (Figure I.7.3.25) strongly supports this conclusion.

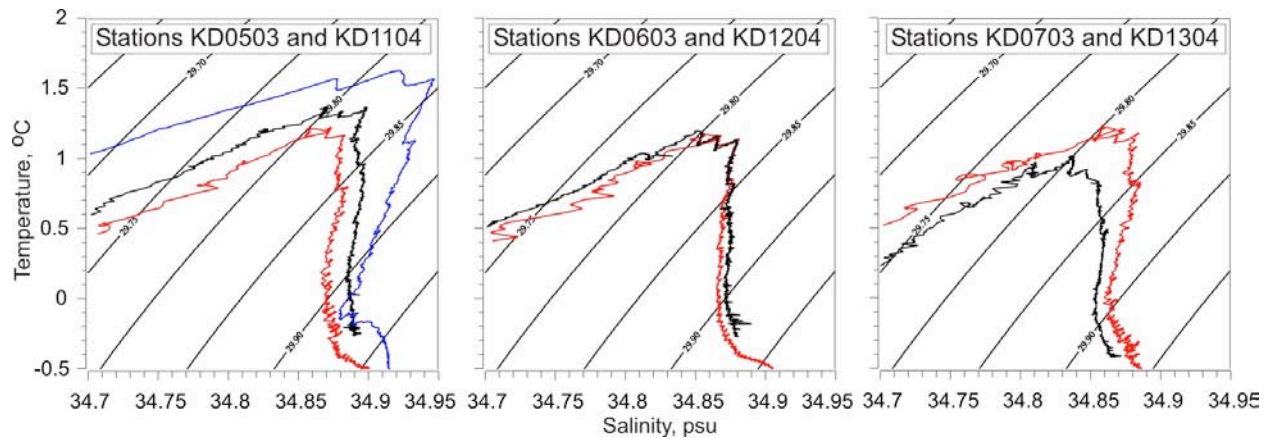


**Figure I.7.3.12:** Temperature versus salinity from NABOS-02 (black), NABOS-03 (red), and (blue) Polarstern ARK IX/4 (1993) cruises along cross-section B. The measurements were carried out approximately at the same positions. Thin solid black lines are isopycnals referenced to 300 db.

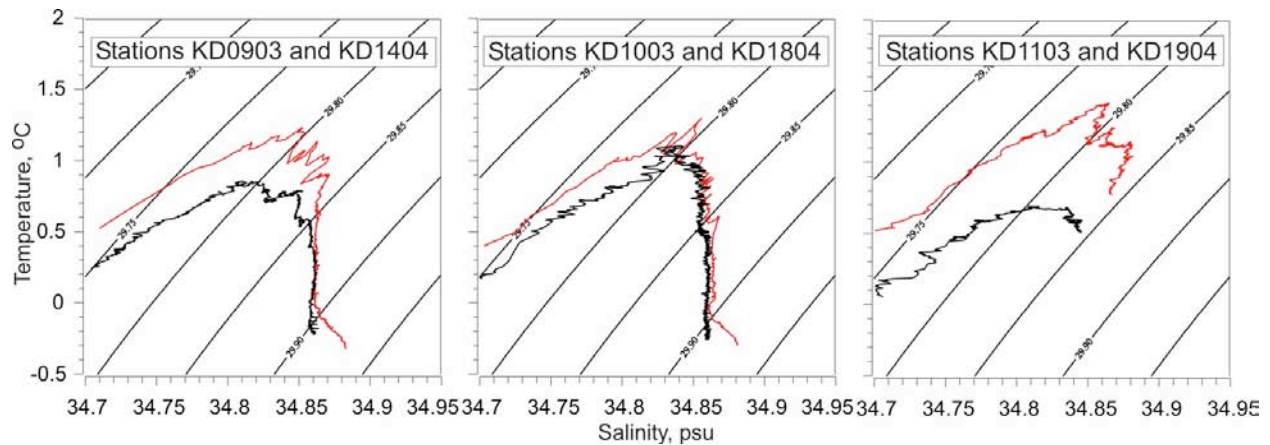


**Figure I.7.3.13:** Temperature versus salinity from NABOS-02 (black) and NABOS-03 (red) expeditions along cross-section C. The measurements were carried out approximately at the same positions. Thin solid black lines are isopycnals referenced to 300 db.

A step-like structure of vertical temperature distribution was observed within the AW layer in 2002, 2003, and 2004. Typical thickness of temperature steps is about 20-25 m (Figure I.7.3.4, right). Similar steps were observed by Rudels et al. [1999]. It was hypothesized that these steps are formed as a result of evolution of temperature isopycnal intrusions. These intrusions represented by small-scale temperature inversions are widely observed in the AW layer (Figure I.7.3.4, see also Rudels et al. [1999]). One may suggest that instability of the boundary separating water masses of the same density but with different temperature and salinity may result in these intrusions. Most interesting is that these intrusions were often located at the same isopycnal surfaces in 2002, 2003, and 2004 [Dmitrenko et al., 2004] (Figures I.7.3.11 lower right and I.7.3.12 central).

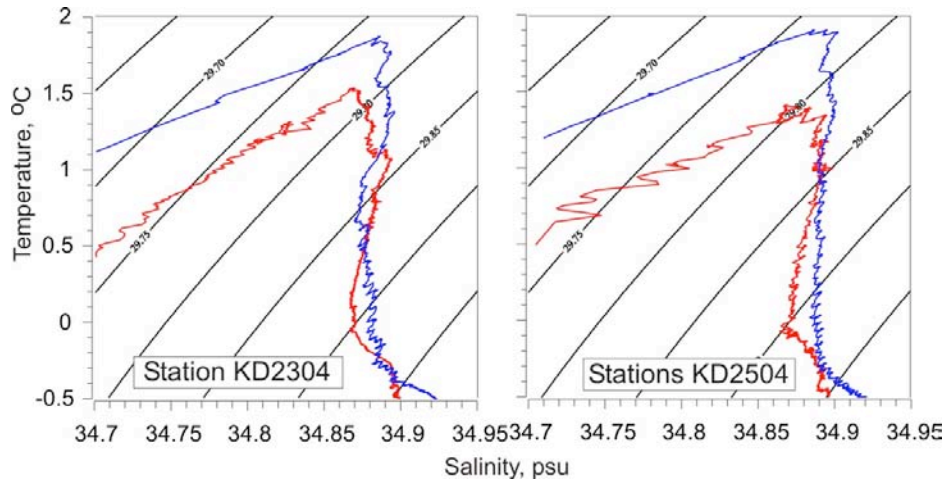


**Figure I.7.3.14:** Temperature versus salinity from NABOS-04 (red) and (blue) Polarstern ARK XI/I (1995) cruise along cross-section D. The measurements were carried out approximately at the same positions. Thin solid black lines are isopycnals referenced to 300 db.

### I.7.1.3. Moorings observations

#### I.7.1.3.1. Objectives (*I.Polyakov and I.Dmitrenko, IARC*)

The overall purpose of mooring observations is to provide observationally based information on temporal variability of water circulation and water mass transformation on the continental slope of the Laptev Sea.

The major objectives are:

- quantify the structure and temporal variability of main water masses over the continental shelf of the Laptev Sea; and
- obtain detailed information about AW layer dynamics and seasonal variations.

#### I.7.1.3.2. Mooring design and equipment (*R.Chadwell, IARC, and M.Dempsey, OM*)

Mooring design and oceanographic equipment is presented in Figure 7.3.15. The most notable feature of these moorings is the specially modified avalanche beacons (Figure I.7.3.16) used for recovery if the mooring is released in ice covered waters. The beacons are modified with mercury tilt switches and three additional batteries to ensure sufficient battery life during the expected one year deployment. The beacons are placed in a heavy gauge Schedule 80 PVC housing with rounded slip caps. Squared slip caps have had a tendency to succumb to the pressure in past experience. The PVC housing is then ballasted to remain upright while buoyant which in turn leaves the mercury tilt switch deactivated to conserve power. When the mooring is released and the beacon reaches the keel of the ice covering, the beacon will then self-right and wait in the receive mode. Searchers on the ice can then use a non-modified avalanche beacon to locate the mooring trapped below.

It is, however, becoming apparent that the NABOS expedition is operating somewhere outside the traditional criteria for selecting mooring locations. It seems that previous locations were selected either because they were in areas where there was a reliable clearance of sea ice for a few months each summer, or because the moorings could be recovered through holes melted in the drifting pack ice in the winter. Considering that recovering through a hole in the pack ice is an equipment- and manpower-intensive operation for which NABOS does not have the necessary resources, NABOS is considering shifting its recovery strategy. Avalanche beacons will be removed and releases and locating transponders will be fitted with more

expensive but longer duration batteries to allow flexibility in recoveries deferred to the second or even third years of deployment.

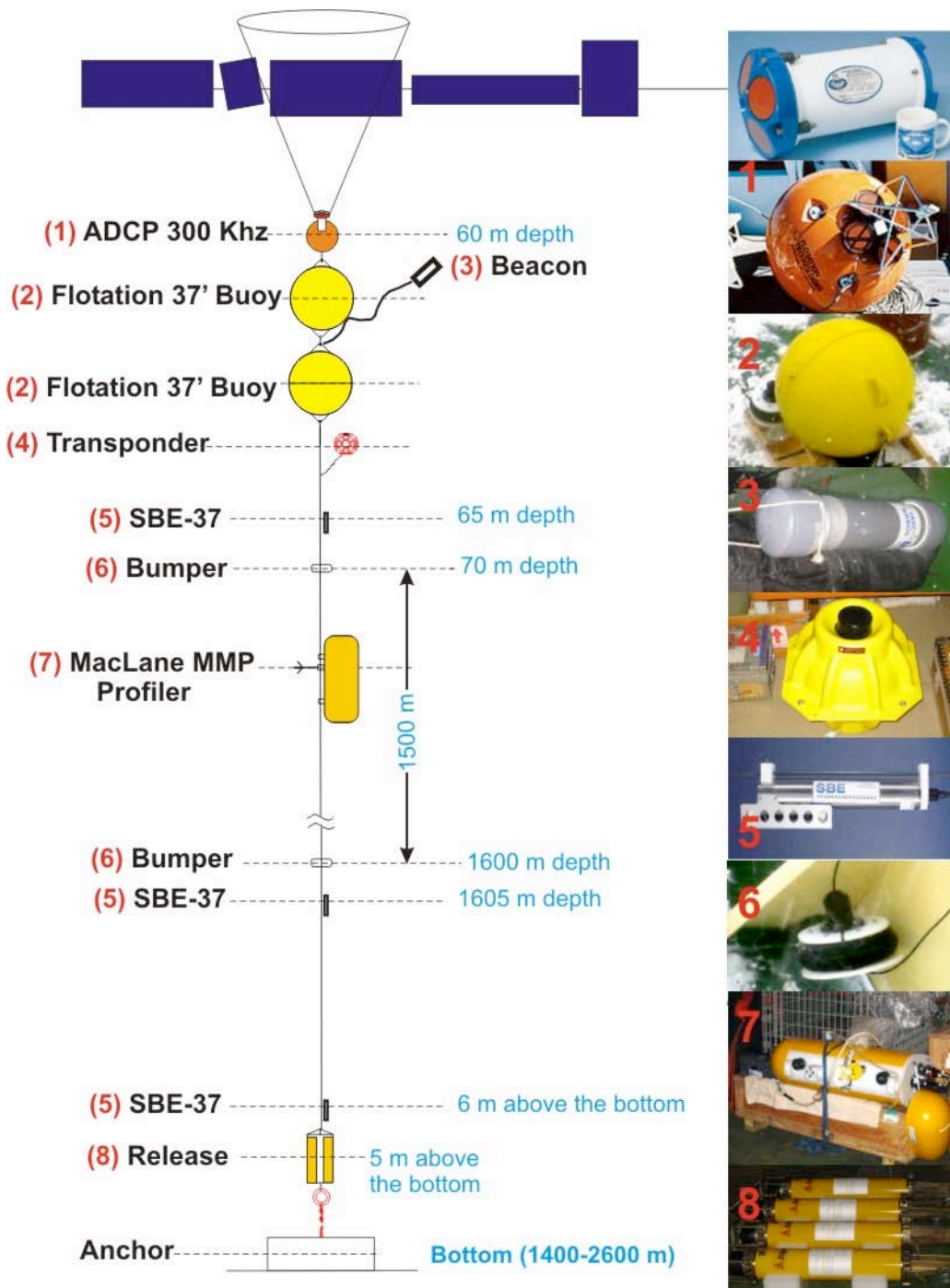


Figure I.7.3.15: NABOS moorings basic design and equipment.





**Figure I.7.3.16:** Beacon (left) and beacon placed in a heavy gauge Schedule 80 PVC housing with rounded slip caps (right).

The transponders positioned on the mooring nearest to the surface are necessary to locate the mooring with greater accuracy, as opposed to using the release transponders located on the bottom, due to the need to recover through small openings in the icepack. Ocean currents can cause horizontal deviation and increase the mooring's watch circle. The acoustic transponder location was modified from the previous years and relocated to just below the lower flotation in order to allow the transponder to be used in the event the mooring surfaced under an ice flow. The new location will help alleviate acoustic shielding from ice keels after release. In the future transponders should be fitted with pressure sensors to help generate more accurate position fixes that will allow recovery through icebreaker-created openings in the ice.

The McLane Moored Profiler (MMP) (Figure I.7.3.17) designed and manufactured by McLane Research Laboratories, Inc. is the main component of NABOS moorings. The full technical information and description are available on <http://www.mclanelabs.com>. The new MMP installed on Mooring M1C was fitted with a Seabird 41CP CTD sensor. The sensor data from the profiler along with other mooring equipment information is presented in Tables I.7.3.2 and I.7.3.3 and Figures I.7.3.21 and I.7.3.22.

**Table I.7.3.2:** Sensors for Mooring M1B recovered 14 September, 2004.

Equipment	Serial #	Parameters	Last Calibration	Sampling Rate	Depth (db)	Comments
Top Microcat CTD SBE-37SM	1672	Conductivity Temperature Pressure	July 16, 2003	15 Minutes	96	Post Cruise Calibration Conducted October 2004
McLane Moored Profiler (MMP)	11474	Current Conductivity Temperature Pressure	N/A	One profile per day	65 to 1500	
MMP FSI ACM Sensor	1661	Current	April 2003	-	N/A	MMP sub-sensor
MMP FSI EMCTD Sensors	1360	Conductivity Temperature Pressure	June 2003	-	N/A	MMP sub-sensor Post Cruise Calibration November 2004

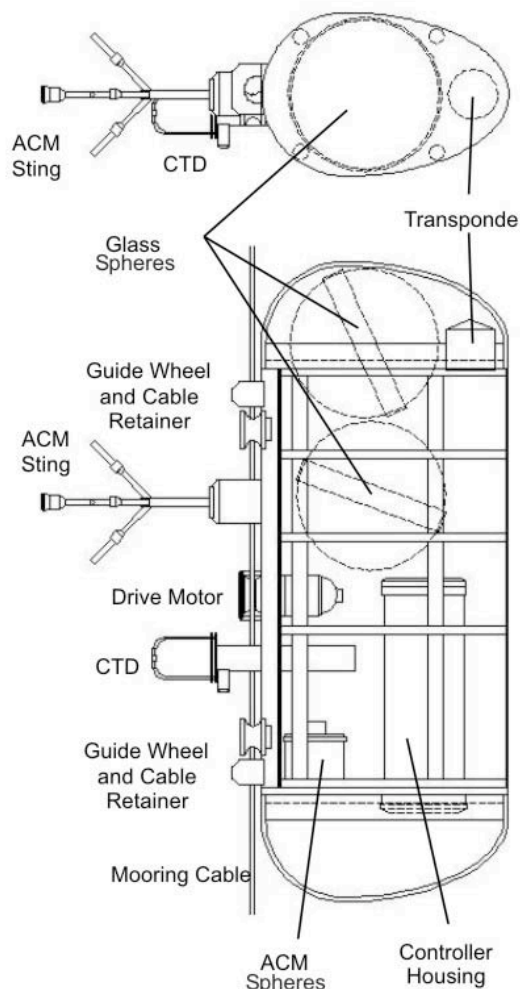


**Figure I.7.3.17:** Sketch of McLane Moored Profiler, © of McLane Research Laboratories, Inc.

**Table I.7.3.3:** Sensors for Mooring M1C Deployed 14 September, 2004.

Equipment	Serial #	Parameters	Last Calibration	Sampling Rate	Target depth (db)	Comments
RDI ADCP		Current			54	
Top Microcat CTD SBE 37 SM	1759	Conductivity Temperature Pressure	Oct 2003	15 Minutes	60	Pressure Sensor 100 dbar
McLane Moored Profiler	116765	Current Conductivity Temperature Pressure	N/A	One profile per day	90 to 1390	
MMP FSI ACM Sensor	1756	Current		-	N/A	MMP sub-sensor
MMP Seabird 41CPs	856	Conductivity Temperature Pressure	June 2004	-	N/A	MMP sub-sensor

**Table I.7.3.4:** Sensors for Mooring M3A Deployed 18 September, 2004.

Equipment	Serial #	Parameters	Last Calibration	Sampling Rate	Estimated depth (db)	Comments
Top Microcat CTD SBE-37SM	1653	Conductivity Temperature Pressure	2001	15 Minutes	37	Owned by LU
Microcat 37SM CTD	1615	Conductivity Temperature Pressure	2001	15 Minutes	136	Owned by LU
RDI ADCP	3845	Current			136	Owned by LU
PPS Sediment Trap	687		N/A	Variable	157	Owned by LU
Microcat 37SM CTD	3049	Conductivity Temperature Pressure	Oct 2003	15 Minutes	243	
RCM 11	270	Current Temperature Fluorometer Conductivity		1 Hour	244	Owned by LU
Microcat 37SM CTD	2864	Conductivity Temperature Pressure	Oct 2003	15 Minutes	344	New Purchase IARC October 2003
RCM11	267	Current Temperature Fluorometer Conductivity		1 Hour	810	Owned by LU
PPS Sediment Trap	0021		N/A	Variable	813	Owned by LU

#### **1.7.3.3.3. Bottom topography at deployment sites (O.Churkin, SRNHI)**

Bottom topography and specific depths at presumable sites of mooring deployment were assessed using available navigation charts before the expedition. For this region both depths and character of bottom topography can be determined only approximately. At present, the bathymetric map of the Arctic Ocean plotted in 2002 (Admiralty # 91115, scale of 1:2 500 000) is the most detailed map for this region. This map is based on acoustic sounding from 1961-1999 conducted during the Russian high-latitude "Sever" expeditions under the project carried out by the Russian Main Administration for Navigation and Oceanography (GUNiO MO RF) together with the Russian Hydrographic enterprise, the Arctic and Antarctic Research Institute (AARI), and the Scientific Research Institute of Arctic Geology. Distance between measured depths ranges from 5 to 15 km, location error ranges from 0.6 to 2 km, and depth determination error comprises 0.5%. Unfortunately, such accuracy and regularity of depth measurements is insufficient to use this chart for navigation and oceanographic research. Mooring deployment requires knowledge of exact depth and slopes at the deployment site; consequently, depth measurements in the surrounding area are required.

The depths down to 2000 m have been measured by the icebreaker's hole-mounted single-beam echo sounder NEL-10 (USSR) (Figure 7.3.18) in standard mode. The transducer depth of 8 m has been taken into account for the depth measurements.



Depths below 2000 m have been measured by the single-beam echo sounder EchoTrack Mark II (USA). The measurements were carried out during drift in open water or in water openings. The echo sounder transducer was held 2-3 m above the deck using a crane (Figure I.7.3.19). It was impossible to fix the transducer to the icebreaker because the presence of ice resulted in an unforeseen declination of the ship's axis from vertical. As a result the difference in depth values during measurement reached 20-25 m. Taking into account this deviation, preference was given to minimal depth values. Compatibility of EchoTrack Mark II operation with other acoustic instruments used for mooring deployment is under consideration. Sometimes the echo sounder operation was interlocked by the acoustic release deck unit and by other devices emitting an acoustic signal in close frequency range.

The depth measurements have been carried out for each of the three regions of mooring deployment. Depth values measured in these regions in 2002 and 2003 have also been included in the data set. Figure I.7.3.20 shows the bathymetric maps of mooring sites M1, 2, and 3; these maps were created using all data obtained during 2002-2004 NABOS cruises.

These maps allowed selection of mooring sites. Bottom topography in these regions is characterized by a gentle slope not exceeding 2-3°. Such topography is well suited for mooring deployment.

#### **I.7.3.3.4. Mooring deployments (R.Chadwell, IARC, and M.Dempley, OM)**

Two subsurface moorings were deployed during the NABOS-04 expedition. Moorings are designated first by location, for example M1, followed by the chronological order designated by a letter i.e, M1A, followed by M1B the subsequent year. The first mooring (M1C, Figure I.7.3.21) was deployed and replaced the recently recovered mooring M1B. The second mooring, M3A (Figure I.7.3.22), was deployed north of the New Siberian Islands. A third mooring was planned to be deployed at location M2; however, it was dependent on the recovery of mooring M2A which was absent on arrival. Mooring deployments in the ice-covered waters is problematic. We used anchor-first deployment in order to avoid towing the mooring through floating ice floes, which would place the towed array in danger of fouling on ice obstacles while the vessel maneuvers toward the target deployment site. Similarly, our moorings were designed with buoyancy located only at the top to prevent the array from surfacing during recovery with floats stranded under the ice on opposite sides of ice keels, thereby complicating retrieval.

Unfortunately, anchor-first operation also has disadvantages. Anchor-first deployments require that the crane and rigging bear the weight of both the anchor and 0.25-inch galvanized Nilspin wire. The tension on the wire hanging vertically over the side makes it more difficult to manipulate the wire while attaching instruments. Additionally, the tension poses greater risk of damaging the plastic wire jacket which is essential for the unencumbered vertical movement of our primary instrument, the McLane Moored Profiler.

Switching to Kevlar line in components not needed by the MMP has proved to be advantageous so far. Kevlar can be used for several years whereas the recommended procedure for wire is to remove it from service after one year's deployment. There are reduced costs associated with using Kevlar in both replacement and shipping. Also, Kevlar line is relatively neutrally buoyant and significantly reduces the tension on deeper moorings. Disadvantages for Kevlar are vulnerability to fish bites which are generally acknowledged as low risk in Arctic environments and the possibility of the line being severed on sharp edges of pack ice during recoveries and deployments.

The purchase of a specially designed Hawboldt capstan (Figure I.2.3) alleviated the problems experienced with "pull down" or "cutting in" of the mooring wire during attempted deployments from our Lebus winch (Figure I.2.2) during last year's NABOS-03 voyage.

# Mooring M1C As Deployed

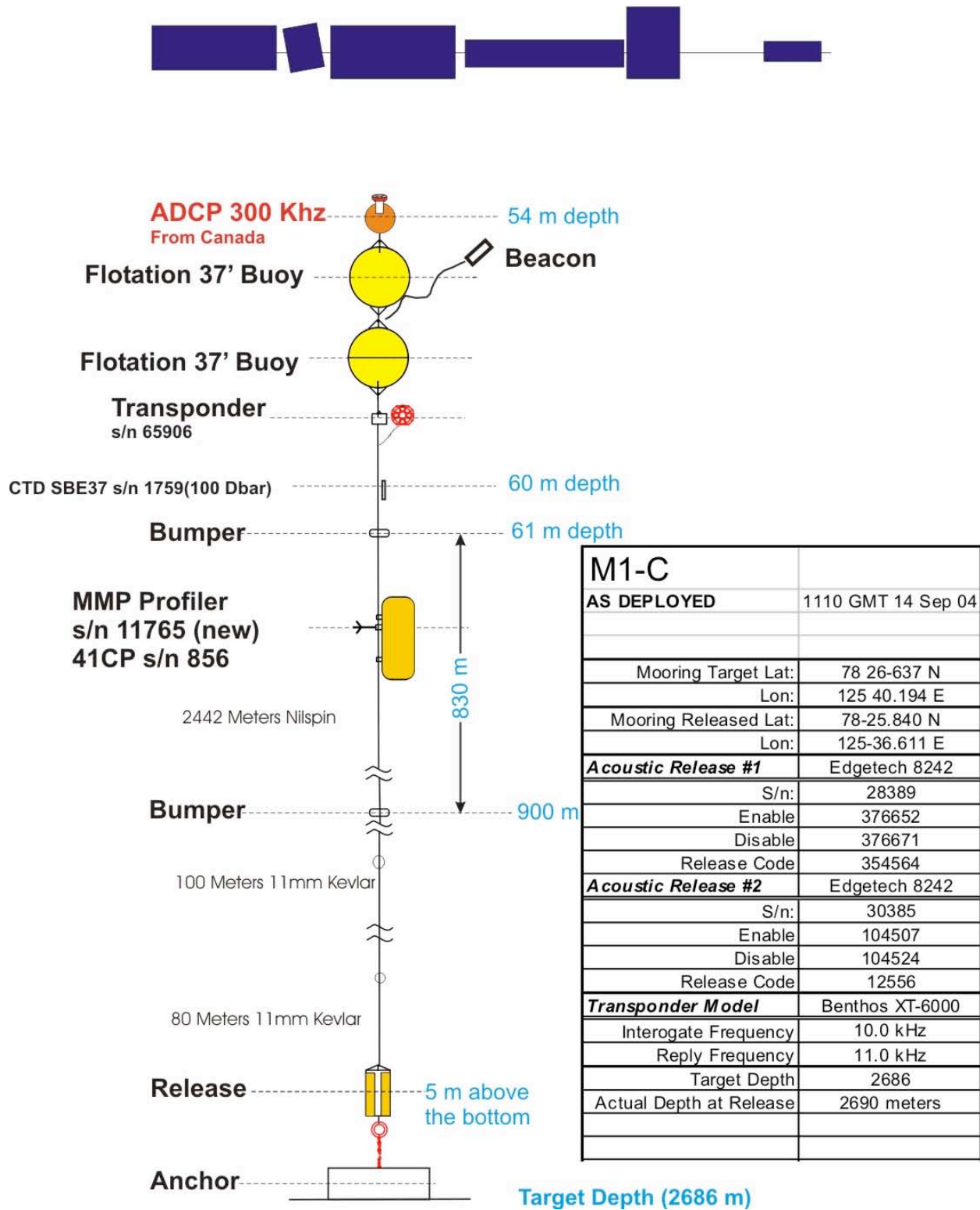


Figure I.7.3.21: NABOS-04 M1C mooring design and equipment.

## Mooring M3A As Deployed

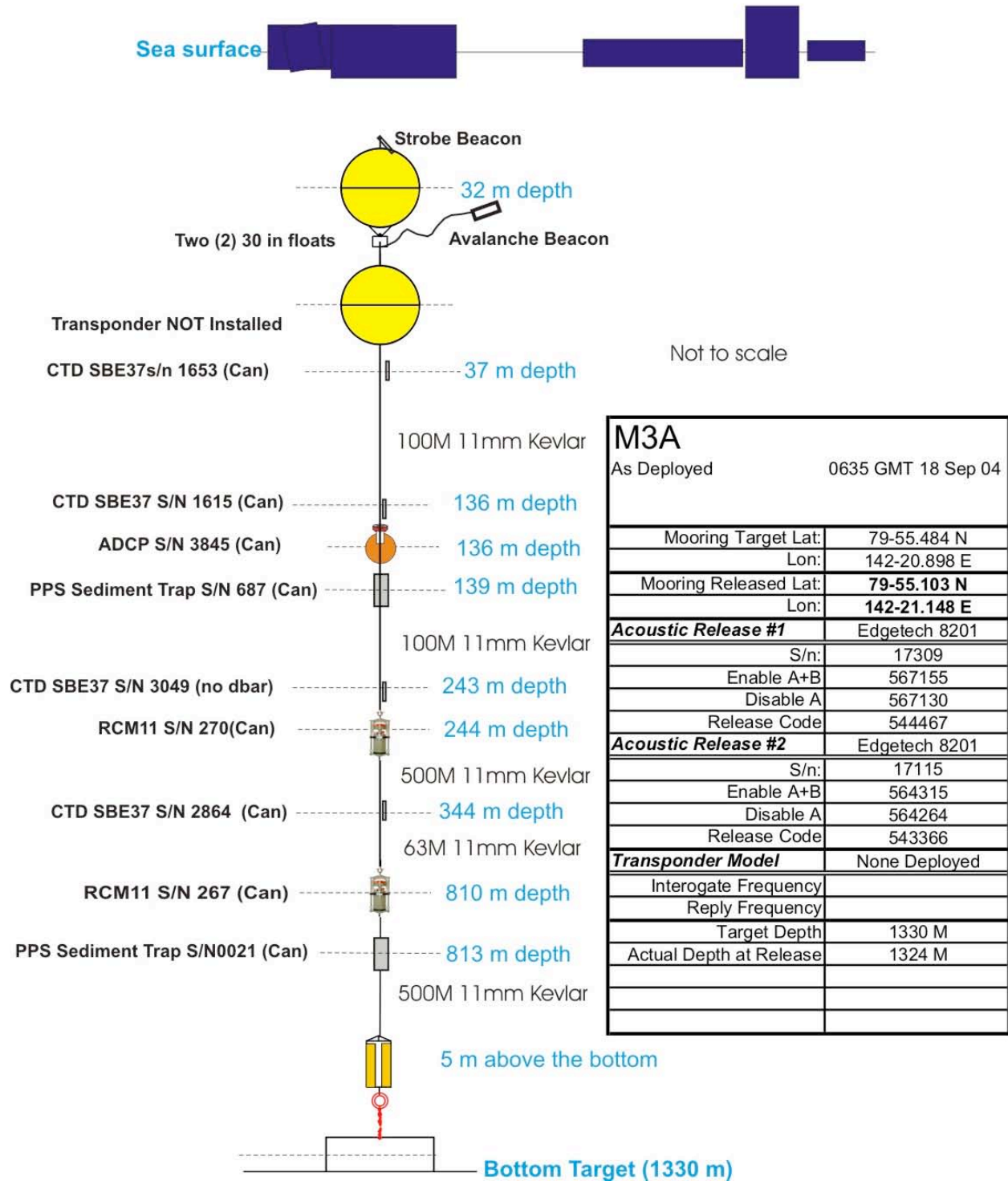


Figure I.7.3.22: NABOS-04 M3A mooring design and equipment.

### I.7.3.3.5. Mooring recovery (R.Chadwell, IARC, and M.Dempley, OM)

Mooring M1B was recovered on September 14<sup>th</sup>, 2004 and turned around for redeployment. Limited visibility upon arrival delayed the recovery for several hours and the time was used to allow the ship to break ice due to heavy ice coverage. The following morning an opening in the ice was sufficient to send a release command.

Mooring M2A was absent upon arrival. A search was conducted expanding from the last known position but no replies were heard from interrogating all three transponders on the mooring at each stop. Ice conditions somewhat inhibited a more thorough search because of the need to clear a small ice free opening at each stop to provide transducer access to the ocean.

The movement of the M1B moored MMP profiler along the cable is depicted in Figure I.7.3.23. Data obtained from this mooring are summarized in Table I.7.3.5.

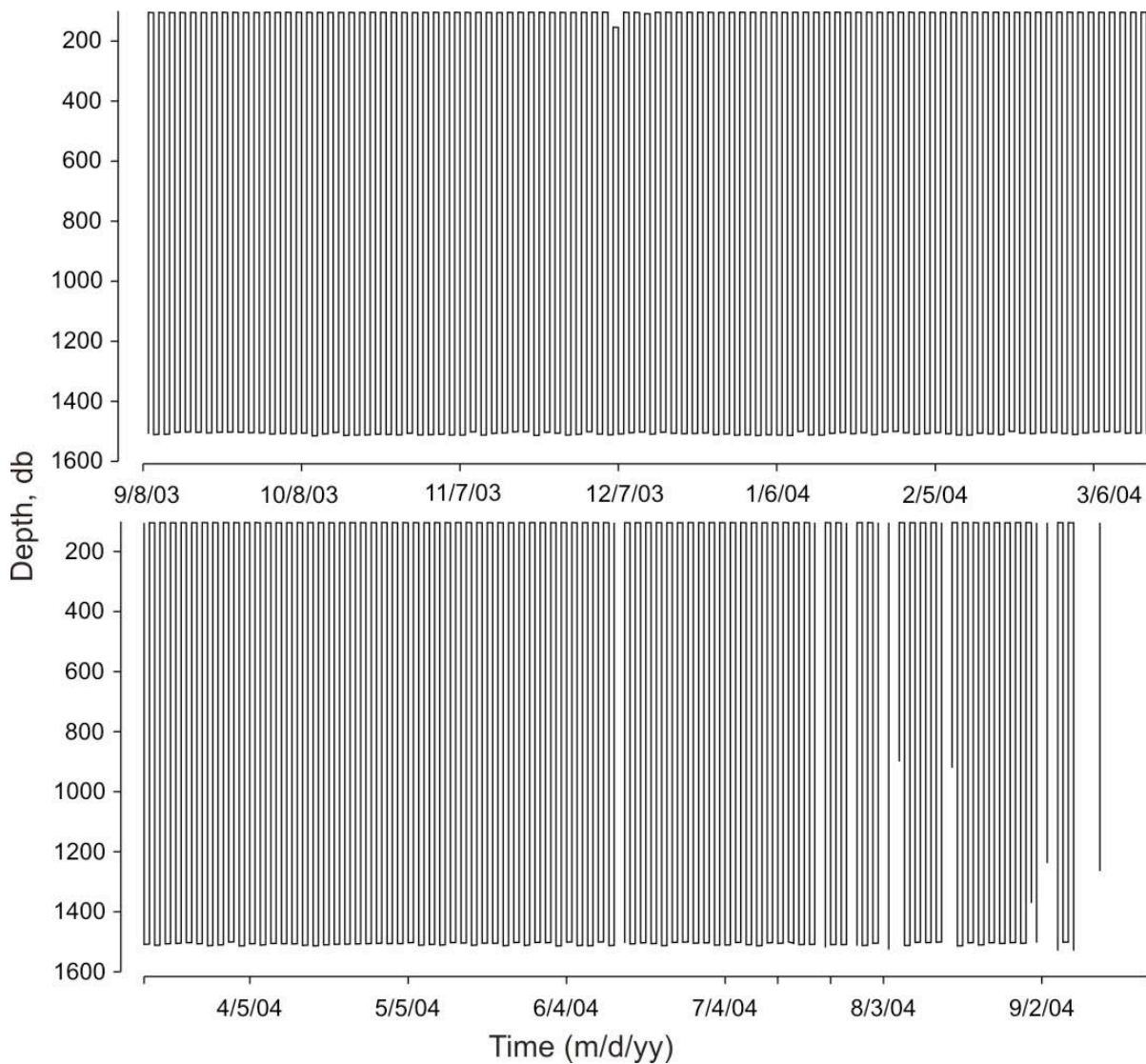


**Figure I.7.3.23:** Actual profiling track of NABOS-03 moored McLANE MMP Profiler (station M1B) according to pressure sensor data.



**Table I.7.3.5:** Data from NABOS-03 (mooring M1B).

Equipment	Serial #	Parameters	Data recovered	Time of observations mm/dd/yy	Actual depth (db)	Comments
Surface Floating CTD SBE-37	1672	Conductivity Temperature Pressure	Yes	09/08/03 – 09/14/04	96	
McLane Profiler	11474	Profiles of: Conductivity Temperature Currents	Yes	See Figure 7.3.22	from 105 to 1509	

**I.7.3.3.6. Preliminary Results** (*I.Dimitrenko, I. Polyakov, IARC, D.Walsh, NRL, and L.Timokhov, AARI*)

High-quality MMP data is demonstrated by good agreement between the SBE19plus CTD record at station KD0704 carried out before mooring recovery on September 13, 2004 and the last successful MMP profile carried out three days before mooring recovery (Figure I.7.3.24).

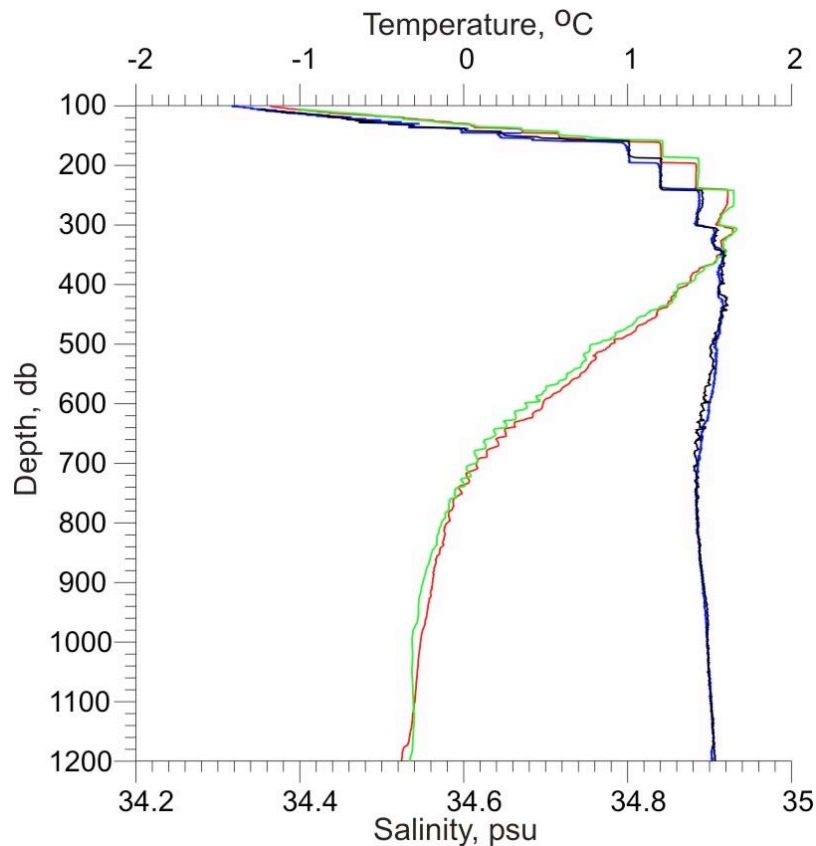


**Figure I.7.3.23:** Vertical temperature (°C) and salinity (psu) distribution at station KD0704 (temperature – red, salinity – blue curves, CTD SBE19plus data, 09/13/04) and MMP last successful run on 09/09/04 (temperature – green, salinity – black curves).

The temperature and salinity continuous MMP records allow temporal variability of the entire AW layer over 366 days of observation (September 8, 2003 – September 9, 2004, Figure I.7.3.25) to be examined.

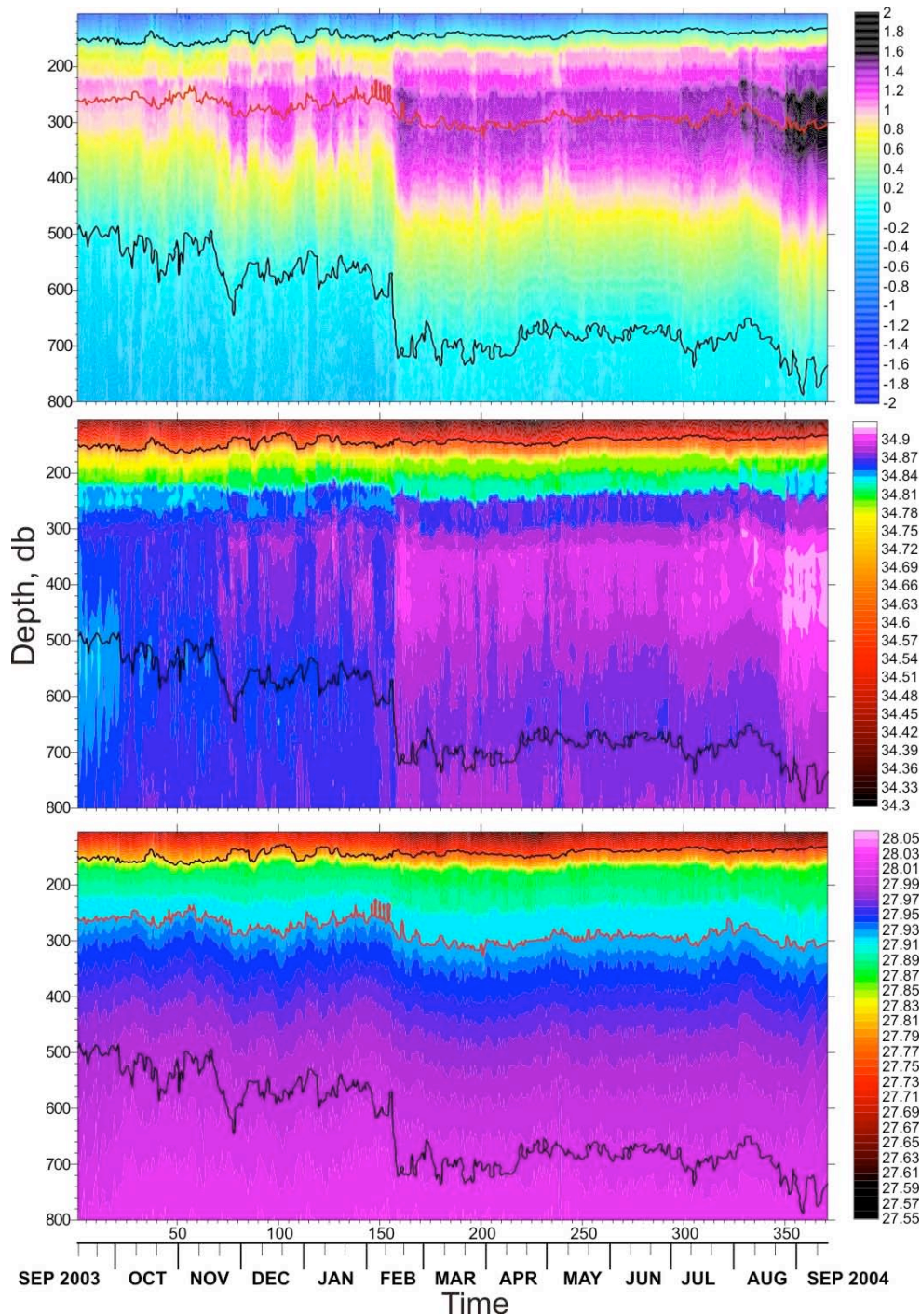


**Figure I.7.3.25:** Temperature ( $^{\circ}\text{C}$ , upper panel), salinity (psu), and potential density (conv. units, lower panel) within the Atlantic Water layer from September 8, 2003 to September 14, 2004, from McLane MMP Profiler CTD data. Isotherm  $0^{\circ}\text{C}$  (black line) shows the boundaries of the AW layer. Water density level of 27.92 that marks the core of AW is shown by a red line.

In terms of temperature, salinity and current variability, two considerably different regimes were observed. The first regime started at the beginning of the record on September 8, 2003 (day #1) and ended on February 11, 2004 (day #157). It is characterized by significant temperature and salinity variations within the core of the AW caused by warm and saltier intrusions. The typical scale of temperature and salinity variations associated with these intrusions is about 0.4-0.7°C (Figure I.7.3.26) and 0.02-0.08 psu (Figure I.7.3.27), respectively.

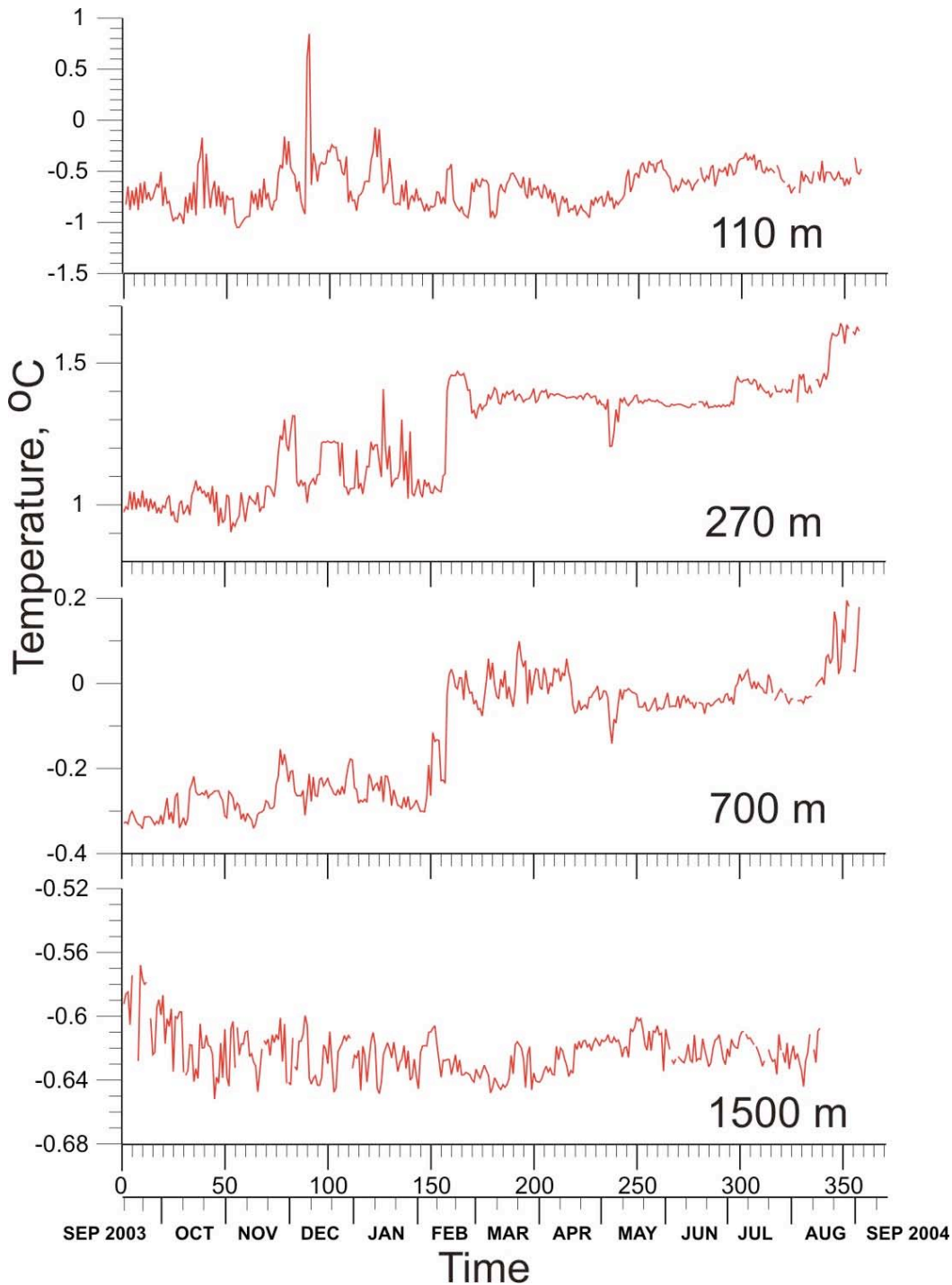


**Figure I.7.3.26:** Time series of daily temperature from 110, 270, 700 and 1500 m depths from McLane MMP Profiler CTD, mooring M1b.

This period is similar to the MMP records from mooring M1a deployed at the same location between September 2002 and February 2003 [Dmitrenko et al., 2004]. The 2002-03 record is characterized by an AW increase interrupted by four intrusions of warm and salty water. Like in 2002-2003, warm salty anomalies decrease with depth downward from the AW core.

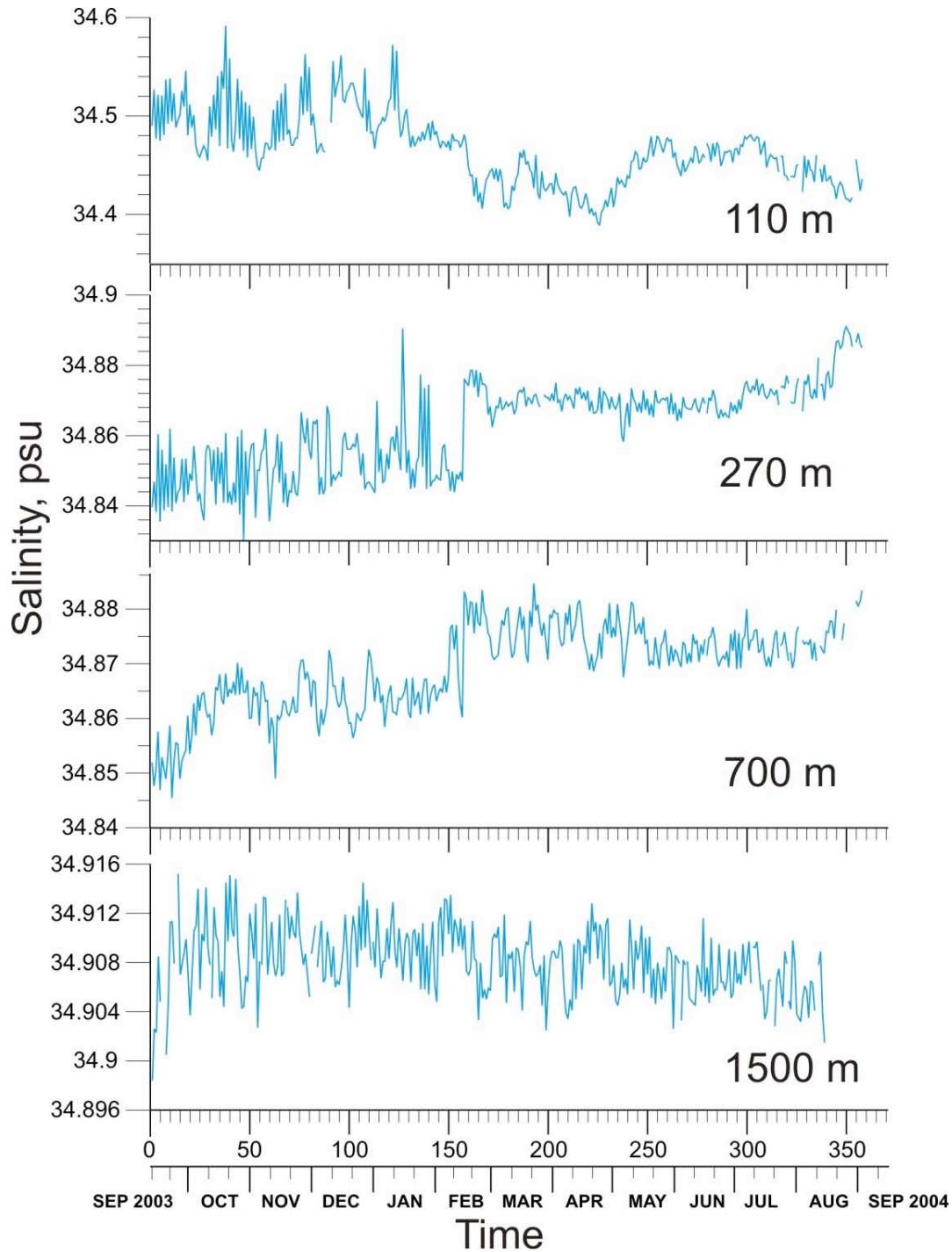


**Figure I.7.3.27:** Time series of daily salinity from 110, 270, 700 and 1500 m depths from McLane MMP Profiler CTD, mooring M1b.

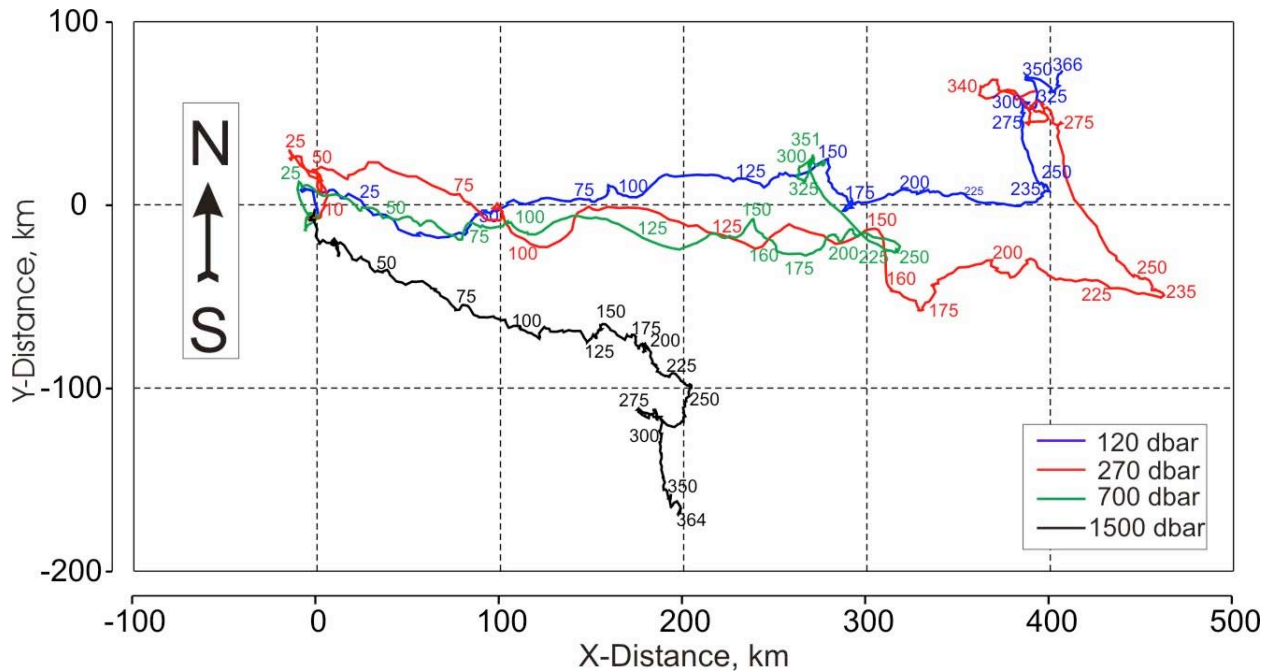


**Figure I.7.3.28:** Progressive vector of daily currents from 110, 270, 700 and 1500 m depths from McLane MMP Profiler FSI current meter, mooring M1b.

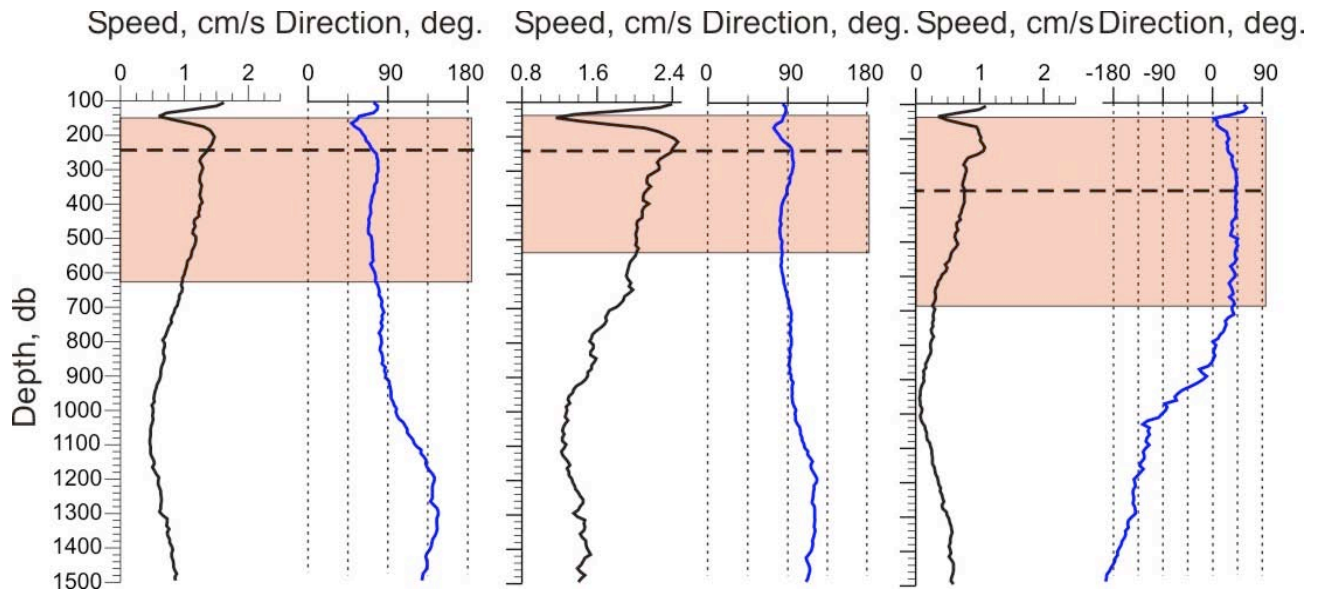


**Figure I.7.3.29:** Vertical profiles of currents (speed and direction) averaged over the whole period of observations (left), from September 8, 2003 to February 11, 2004 (central) and from February 11 to September 9, 2004. Data from the MMP profiler were averaged over 10 m thick bins. Red areas show the depth of AW layer.

During the first period of time the mean current with a speed of 2-2.4 cm/s was relatively stable and orientated toward the east with the exception of the period between days #1 and 25 (Figures I.7.3.28 and I.7.3.29).

The beginning of the second period starting on February 12, 2004 is marked by a sharp temperature and salinity increase within the AW layer by about 0.4 °C and 0.04 psu (Figures I.7.3.25-I.7.3.27, I.7.3.30), and deepening of the AW core by about 50 m. This deepening was first recorded 5 days prior to the exceptional warming. Another deepening of both the AW core and the AW layer lower boundary was recorded at the end of the observational period on August 6, 2004. Similar to the first deepening, it was observed five days prior to the second strong warming event starting August 11, 2004 (MMP profile # 342, Figure I.7.3.25). For both warming events the AW core kept approximately constant density of about 29.82 (Figure I.7.3.30). Rapid warming of the AW layer was accompanied by dramatic increase of the AW layer thickness downward from 550 to 720 m during the first (February) warming and down to 800 m during second warming (August 2004, Figure I.7.3.25).

A considerable salinity decrease by about 0.7 psu was observed in the 100-140 m layer (Figures I.7.3.25 and I.7.3.27, upper panel) during the second half of the record, which is well supported by the SBE-37 record from the 96 dbar depth level (Figure I.7.3.32). Surprisingly, this freshening occurred in winter when we may expect salinification due to brine rejection during ice formation.

The average current speed in the AW core was about 0.8 cm/s, three times weaker compared with the first half of the record. Unlike the first (cold) period, from February to September 2004 current direction varied considerably. A strong southward water current with a speed of up to 8 cm/s was recorded within the AW layer during the 6 days before the warm event of February 12, 2004 (Figure I.7.3.28, period of time between MMP profiles #150 and 160). The current kept a stable eastward orientation until day #235 (April 30, 2004) when a strong stable barotropic northwestward current event with a maximum speed of 9 cm/s was observed through day #280 from 100 m down to the depth of profiling. Afterward the counter-current dominated the water dynamic below 1000 m, while the upper layer current was much suppressed and demonstrated no substantial variability through the end of the record in September 2004 (Figure I.7.3.28).

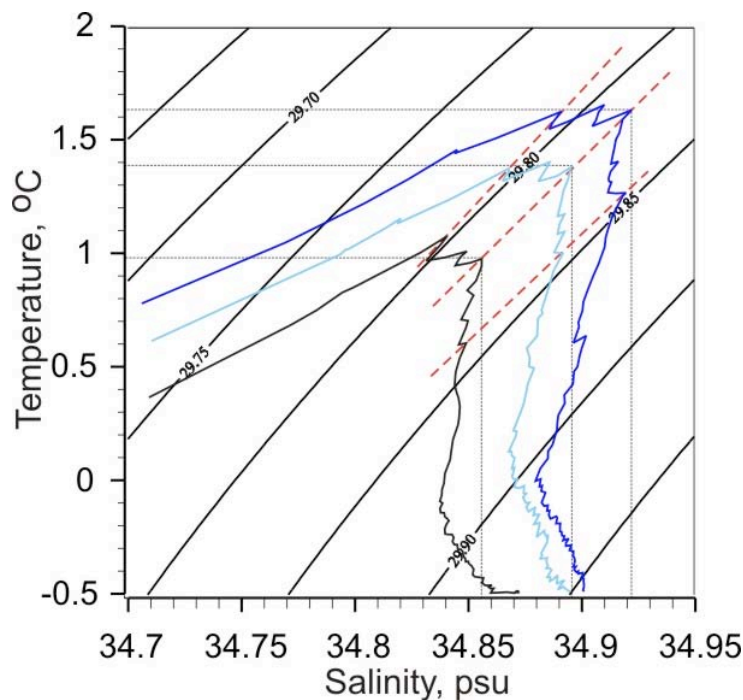


**Figure I.7.3.30:** Temperature versus salinity for three MMP profiles from mooring M1b: September 10, 2003 (black, profile #2), June 4, 2004 (light blue, #270), and September 3, 2004 (dark blue, #365). Thin solid black lines are isopycnals referenced to 300 db.

Like in 2002-2003, small-scale steps in stratification (Figures I.7.3.24 and I.7.3.25) were typical. The thickness of steps varied within 2-4 m. A striking feature of these records is that these steps were always found at the same isopycnal surfaces (Figure I.7.3.25, upper panel). Two warming events which started in February and August 2004 led to a shift of the entire water structure downward by about 50 m.

Temperature and salinity variabilities measured by the CTD SBE-37 (96 dbar, Figure I.7.3.31) are in reliable agreement with the MMP-based temperature and salinity variations (Figure I.7.3.27, upper panel). Two major warm/saltier events captured by the MMP in February and August 2004 were not found at this depth. Like in 2002-2003, the SBE-37 pressure sensor recorded pronounced tidal sea-level oscillations (Figure I.7.3.32, lower panel). Tidal constants may be found in the NABOS-03 report [Dmitrenko et al., 2004].

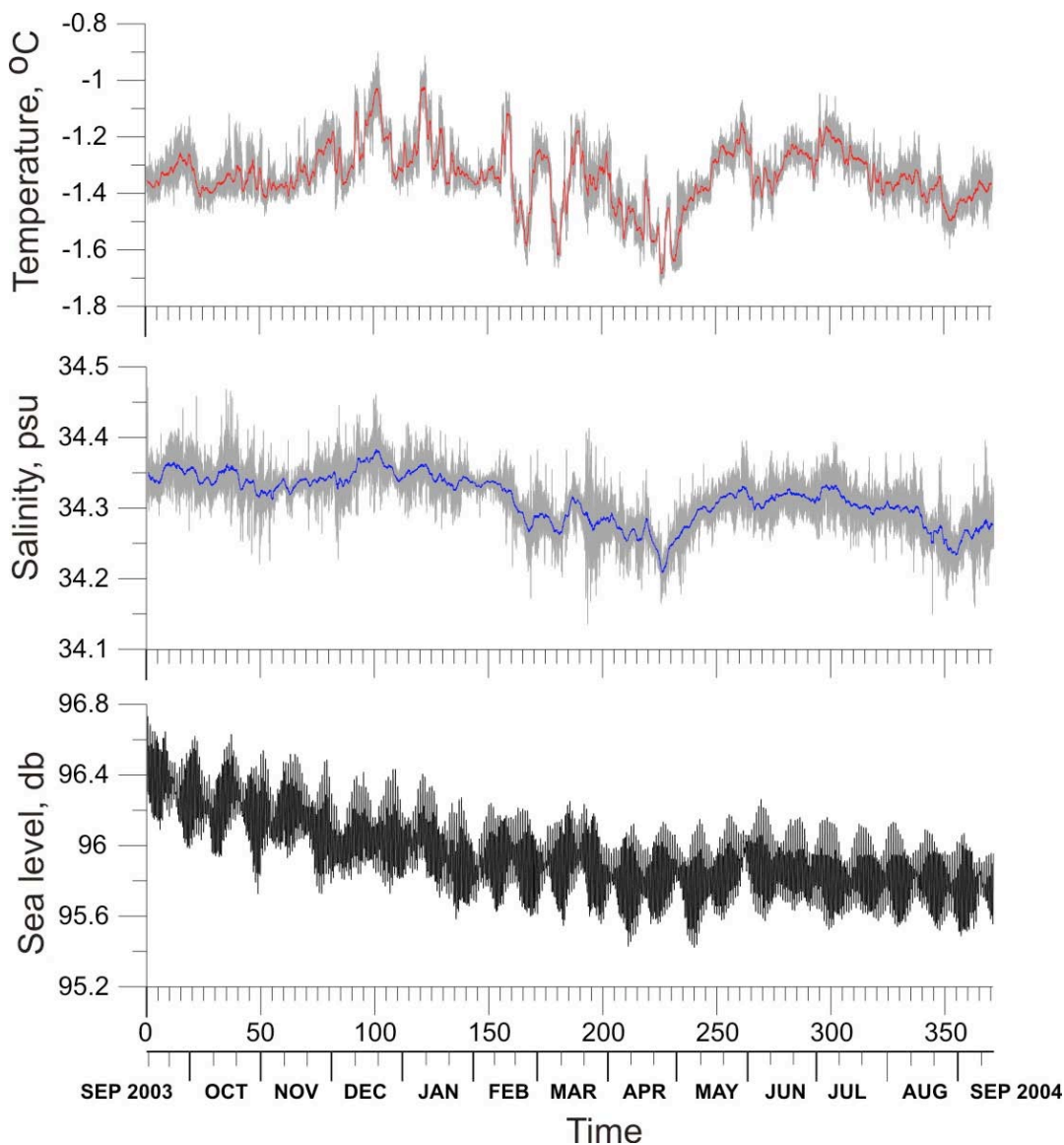


**Figure I.7.3.31:** Temperature, salinity and pressure records from SBE-37 (96 m depth). 24 h running mean is shown by red (temperature) and blue (salinity) lines.

#### **I.7.4. CHEMICAL OBSERVATIONS** (M.Nitishinskiy, AARI)

### **I.7.4.1. Objectives**

Exchange and interaction of water masses in the Laptev Sea have significant implications for the Arctic climatic system. In the past, dissolved oxygen (DO) and nutrients were used to identify specific water masses in the Arctic Ocean, although those chemical parameters are highly non-conservative due to biological activities in sea water and underlying sediments. Hydrochemical elements allow us to study and explain extremely complicated relationships between hydrophysical, biological and geochemical processes taking place both at the sea surface and beneath. Although there are substantial observational data for nutrients and DO on the shelf in the Laptev Sea, offshore hydrochemistry data in the central Laptev Sea are still scarce and gaps need to be filled. Regular monitoring of hydrochemical characteristics is also very important for understanding marine ecosystem functioning. DO is necessary for respiration of living organism. Nutrients (silicon, phosphates, nitrites, nitrates, and ammonium) are mineral substrates for primary production. Chlorophyll allows the amount of organic matter in sea water to be estimated. Knowledge of concentrations of different forms of carbon in sea water is essential for studying the carbon cycle and assessing its fluxes in the atmosphere-land-sea system.

Specific objectives of the NABOS-04 chemical observations were to fill gaps in existing observations of hydrochemical distributions in the Laptev Sea, leading to better understanding of the hydrochemical budget and major water mass mixing in this region.

### **I.7.4.2. Methods and Equipment**

Field experiments and laboratory analysis are complementary ways to conduct chemical observations. Field experiments included sampling along the icebreaker pathway and in the research area for determination of major chemical parameters like silicon, phosphates, oxygen, ammonium, and chlorophyll. These samples were analyzed first in icebreaker laboratories, and later in the laboratories of AARI and IO.

The laboratory phase included analysis of data, additional laboratory research, measurement of concentrations of phosphates, silicon, nitrites, nitrates, manganese, particulate matter (PM), particulate organic carbon (POC), dissolved organic carbon (DOC), and determining the group molecular composition of organic matter (OM).

Sampling of surface water was carried out along the pathway of the icebreaker every 3 or 6 hours (Figure I.7.4.1). At oceanographic stations samples were taken at 0, 20, 25 and 50 m by 8 l Niskin bottles (Figure I.7.4.2). Details of sampling at oceanographic stations are summarized in Table I.7.1 and also described in Appendix 1. The samples of surface water for PM, POC, DOC, and chlorophyll determination were collected at the stations and along the course of the icebreaker using a 10 l bucket. Water sampling was carried out using 8 l Niskin bottles at 20, 25, 48, and 50 m. The remainder of the water in the Niskin bottles comprised 6-7 l after water was taken for hydrochemical analysis. Water samples from 20 and 25 m levels and from 48 or 50 m levels were combined to get sufficient volume of water for PM filtration. Concentrations of oxygen, phosphates, silicon, ammonium, and chlorophyll "a" were measured onboard the vessel.

#### ***Analytical methods***

1. DO: Dissolved oxygen contents in seawater were analyzed onboard by using a modified Winkler titration method [Strickland and Parsons, 1968]. The typical precision of this method is 0.05 ml STP/liter. The detection limit is around 0.6 ml STP/liter. The analysis was completed within 24 hours after sampling.



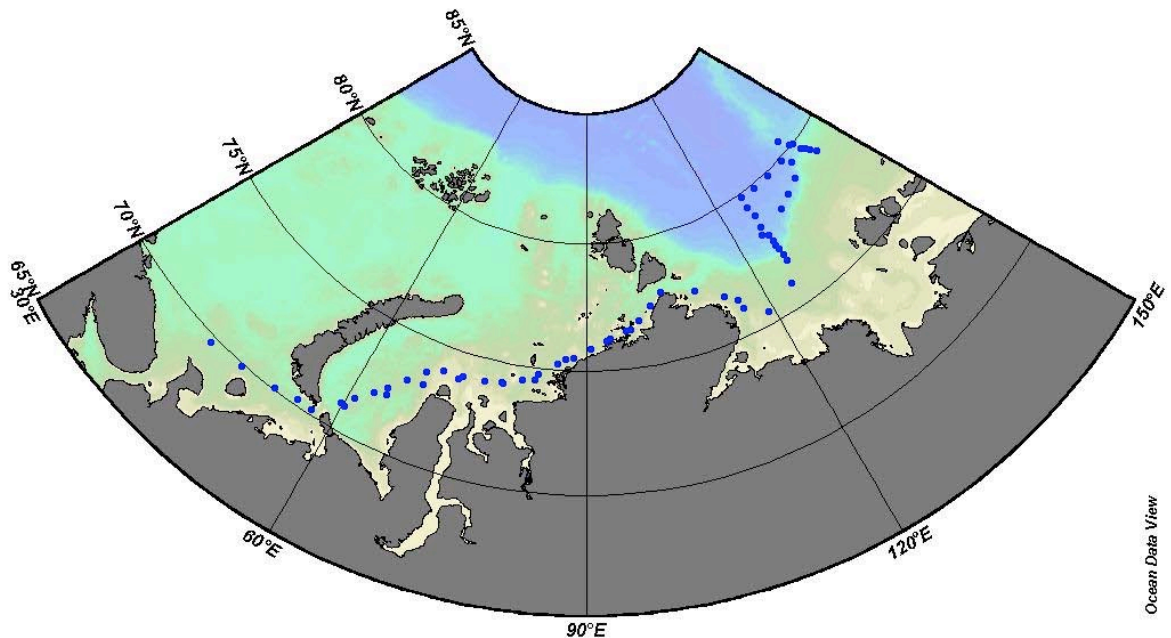


**Figure I.7.4.1:** Hydrochemical sampling along the icebreaker pathway and at the NABOS-04 research area.

2. Measurement of phosphates and silicon was carried out by the photocolorimetric method using a KFK-2M electrophotocolourimeter with accuracy  $\pm 2.5$  of obtained value.
3. Water sampling was used for ammonium concentration determination. It was planned to check for the possibility of using the analytic method proposed by Holmes et al. The method is based on a reagent containing ortho-phthaldialdehyde (OPA), which when it reacts with ammonium yields a fluorescent compound. This test is conducted immediately after sampling to eliminate the loss of ammonium or sample contamination during transportation, storage, and transfusion.
4. Fluorescence of the sample is measured by a TD-700 fluorometer after incubation in darkness at room temperature. Standards for calculation of the ammonium concentration in the sample are prepared directly during sampling, which guarantees that samples and standards are at the same stage of the reaction.
5. Filtration. Sea water filtration for PM content measurement was carried out through membrane (nuclear) filters. For reliability parallel 3-5 l samples of water were used for filtration. The water was passed through the filter by a pump creating an approx. 0.4-0.5 bar vacuum. A volume of water from 1 to 5 l was passed through a filter until filter saturation by PM was achieved. Filters with PM were washed by distilled water (75-100 ml) and were dried at 60°C. The water was passed through a GF/F filter (about 10 ml) and collected for DOC measurement. The samples were acidified by HCl down to pH 2-2.5 and were stored in a refrigerator. Chlorophyll "a" content was measured using 1/8 to 1/2 part of the filter. The same part was put into a freezer for chlorophyll determination in the laboratory.
6. Chlorophyll "a". The concentration of chlorophyll was determined using a "Fluorat-Panorama" spectrofluorometer by measuring both fluorescence and light absorption using three standard methods [Yentsch and Menzel, 1963; Holm-Hansen et al., 1965; Yentsch, 1965; Loftus and Carpenter, 1971; Yunev and Berseneva, 1986]. A glass fiber filter with collected chlorophyll was homogenized using a glass stick in a centrifuge tube with 5 ml of 90% acetone. After homogenization the tube was placed in the dark for one hour to allow complete extraction of the pigments. The suspension was then centrifuged at 8000 rot/min

for 15 minutes and the supernatant carefully decanted into a 10 ml tube. A new portion of 5 ml 90% acetone was added to the sediment and the process was repeated. Chlorophyll “a” was determined by light absorption spectra. Fluorometric determination of chlorophyll “a” was made by two methods: (i) by exciting the chlorophyll solution at 436 nm wavelength and measuring fluorescence at 680 nm, and (ii) by exciting the solution at 420 nm and measuring fluorescence at 667 nm. In the last case chlorophyll “a” concentration was determined by difference between fluorescence of chlorophyll solution before and after acidification by 0.25 N HCl. Acidification allows fluorescence of chlorophyll “a” to be quenched, and as a result the fraction of phaeophytin that does not take part in photosynthesis, which represents a product of chlorophyll degradation, can be determined. Dependence of fluorescence on chlorophyll concentration was determined by comparison with absorption spectra.

### I.7.4.3. Preliminary Results

The characterization of the sea water and PM samples collected on the expedition, including 30 samples of sea water for DOC measurement, 160 samples for PM determination, 82 samples of PM for POC measurement, and 82 samples of PM for chlorophyll analysis is shown in Table I.7.4.1. During the expedition 88 determinations of the concentrations of oxygen, phosphates, and silicon, 53 determinations of ammonium, and 82 determinations of chlorophyll were carried out. Thirty series of observations with surface water sampling were made along the icebreaker’s route. Sampling was done at selected depths at 21 oceanographic stations.

Distribution of silicon, oxygen, ammonium and phosphates along the pathway of the vessel is presented in Figure I.7.4.3. Silicon concentration was higher in the vicinity of big rivers (up to 30-35  $\text{mkmol l}^{-1}$ ). In the NABOS-04 research area located to the north of the river runoff impact the silicon concentration did not exceed 8.9  $\text{mkmol l}^{-1}$ .

**Table I.7.4.1:** Samples of water collected for measurement of particulate matter (PM), particulate organic carbon (POC), dissolved organic carbon (DOC), and chlorophyll concentration.

Station	Date	Latitude, N	Longitude,	Depth,	Level, m	PM	POC	DOC	Chlorophyll
KD01-04s	07.09.04	69°43.53'	43°45.27'	90	0	+	+		+
KD02-04s	07.09.04	69°53.063'	48°9.05'	65	0	+	+		+
KD03-04s	08.09.04	70°5.244'	52°54.384'	88	0	+	+		+
KD04-04s	08.09.04	70°7.2'	57°17.08'	85	0	+	+		+
KD05-04s	08.09.04	71°4.12'	59°49.57'	169	0	+	+		+
KD06-04s	08.09.04	71°29.529'	60°59.511'	80	0	+	+		+
KD07-04s	08.09.04	72°5.241'	62°42.714'	80	0	+	+		+
KD08-04s	08.09.04	72°27.6'	63°51.7'		0	+	+		+
KD09-04s	08.09.04	73°7'	65°51'		0	+	+		+
KD10-04s	09.09.04	73°42.6'	67°45.4'		0	+	+		+
KD11-04s	09.09.04	74°0.02'	69°55.43'		0	+	+		+
KD13-04s	09.09.04	74°5.41'	75°43.91'	21	0	+	+		+
KD14-04s	09.09.04	74°10.137'	78°8.652'	25	0	+	+		+
KD15-04s	09.09.04	74°24.37'	80°52.54'		0	+	+		+
KD16-04s	09.09.04	74°44.2'	83°5'		0	+	+		+
KD17-04s	10.09.04	75°14.42'	85°50.85'	25	0	+	+		+
KD18-04s	10.09.04	75°30.019'	88°11.171'	35	0	+	+		+

Station	Date	Latitude, N	Longitude,	Depth, m	Level, m	PM	POC	DOC	Chlorophyll
KD19-04s	10.09.04	75°49.9'	90°52.1'		0	+	+		+
KD20-04s	10.09.04	76°13.4'	93°56.7'		0	+	+		+
KD21-04s	10.09.04	76°29'	96°38'		0	+	+		+
KD22-04s	10.09.04	76°47.89'	98°52.6'	32	0	+	+		+
KD23-04s	10.09.04	77°19.3'	101°19.3'		0	+	+		+
KD24-04s	10.09.04	77°43.9'	103°34.3'		0	+	+		+
KD25-04s	11.09.04	77°23.5'	109°27.3'		0	+	+		+
KD26-04s	11.09.04	76°46'	113°45.8'		0	+	+		+
KD27-04s	11.09.04	76°23.77'	115°37'	46	0	+	+		+
KD28-04s	11.09.04	76°1.47'	115°49.08'		0	+	+		+
KD29-04s	11.09.04	75°28.5'	119°10.9'		0	+	+		+
KD30-04s	12.09.04	75°56.26'	124°25.2'		0	+	+		+
KD31-04s	15.09.04	78°27.707'	125°37.594'		0	+	+		+
KD01-04	12.09.04	76°45.8'	125°59.53'		0	+	+		+
KD02-04	12.09.04	77°3.153'	126°0.799'	52	0	+	+		+
KD03-04	12.09.04	77°19.29'	126°4.46'		0	+	+		+
KD-04-04	12.09.04	77°30.312'	125°58.127'	1800	0	+	+		+
KD05-04	13.09.04	77°44.391'	126°0.597'	2100	0	+	+		+
KD06-04	13.09.04	78°6.922'	126°4.678'	2100	0	+	+		+
KD07-04	15.09.04	78°56.86'	126°3.45'		0	+	+		+
					20	+	+		+
					30	+	+		+
					38	+	+		+
KD08-04	16.09.04	78°56.66'	126°3.42'	>3000	0	+	+		+
					20/25	+	+		+
					48/50	+	+		+
KD09-04	16.09.04	79°22.43'	125°40.99'	2000	0	+	+	+	+
					20/25	+	+	+	+
					48/50	+	+	+	+
KD10-04	16.09.04	79°48.57'	129°16.23'	>3000	0	+	+	+	+
					20/25	+	+	+	+
					48	+	+	+	+
KD11-04	17.09.04	79°78.7'	129°19.3'	>3000	0	+	+	+	+
					20/25	+	+	+	+
					48/50	+	+	+	+
KD12-04	17.09.04	79°49.75'	137°45.05'		0	+	+	+	+
					20/25	+	+	+	+
					48/50	+	+	+	+
KD13-04	18.09.04	79°50.07'	137°48.3'	2825	0	+	+	+	+
					20/25	+	+	+	+
					48/50	+	+	+	+
KD14-04	18.09.04	79°55'	143°16.4'	1300	0	+	+	+	+
					20/25	+	+	+	+
					48/50	+	+	+	+
KD19-04	19.09.04	79°26.1'	142°56.6'	500	0	+	+	+	+
					20/25	+	+	+	+
					48/50	+	+	+	+
KD21-04	19.09.04	79°0.04'	144°0.49'	98	0	+	+	+	+
					20/25	+	+	+	+
					48/50	+	+	+	+

Station	Date	Latitude, N	Longitude,	Depth, m	Level, m	PM	POC	DOC	Chlorophyll
KD22-04	19.09.04	79°30.52'	138°56.75'		0	+	+	+	+
					20/25	+	+	+	+
					48/50	+	+	+	+
KD23-04	19.09.04	78°59.7'	136°57.42'		0	+	+	+	+
					20/25	+	+	+	+
					48/50	+	+	+	+
KD24-04	20.09.04	78°45.3'	133°47.7'		0	+	+		+
					20/25	+	+		+
					48/50	+	+		+
KD25-04	20.09.04	78°29.92'	130°54.89'	1500	0	+	+		+
					20/25	+	+		+
					48/50	+	+		+
KD26-04	20.09.04	78°3.9'	124°55'	>2000	0	+	+		+
					20/25	+	+		+
					48/50	+	+		+

A maximum concentration of  $9 \text{ ml l}^{-1}$  oxygen has been observed in the northern parts of the Laptev Sea. This is due to the increase of oxygen solubility with temperature reduction and salinity rise.

Concentrations of ammonium and phosphates in surface water did not exceed  $1 \text{ mkmol l}^{-1}$  and were close to zero at almost all sites because of active consumption during photosynthesis, which endures up to the beginning of the winter.

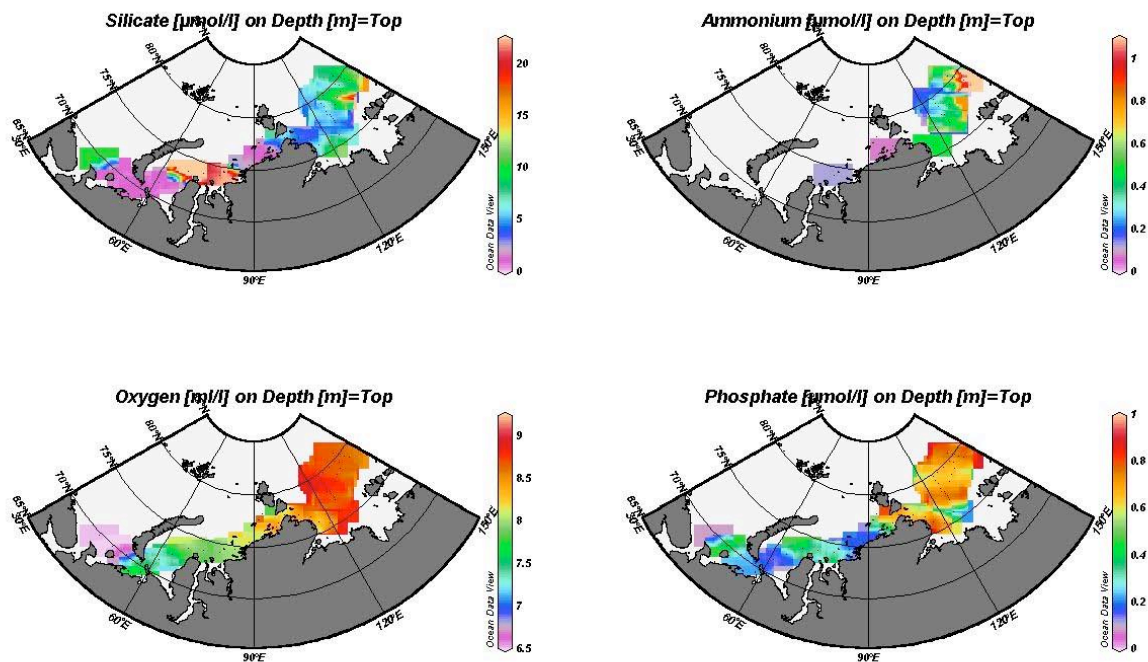


**Figure I.7.4.3:** Concentrations of silicon ( $\text{mkmol l}^{-1}$ ), oxygen ( $\text{ml l}^{-1}$ ), ammonium ( $\text{mkmol l}^{-1}$ ), and phosphates ( $\text{mkmol l}^{-1}$ ) in surface water along the pathway of the vessel.

The results of analysis of chlorophyll concentration in surface water along the icebreaker pathway are shown in Figure I.7.4.4. Chlorophyll concentration ranged from 0.26 to 6.0 mkg l<sup>-1</sup>. On the whole, these concentrations coincide with concentrations measured earlier. Near the Pechora Sea chlorophyll concentration in August-September was estimated at 0.5-1.5 mkg l<sup>-1</sup> [Vedernikov et al., 2001]. Determinations of hydrochemical characteristics along cross-sections A-D were limited to the upper 50 m.

The reduction of ammonium concentration with depth to almost zero at 30-40 m has been observed at all cross-sections. Phosphates concentration gradually increased with depth from 0.3 - 0.4 mkmol/l in surface water to 0.9-1.0 mkmol/l at the depth of 40-50 m (Figure I.7.4.5).

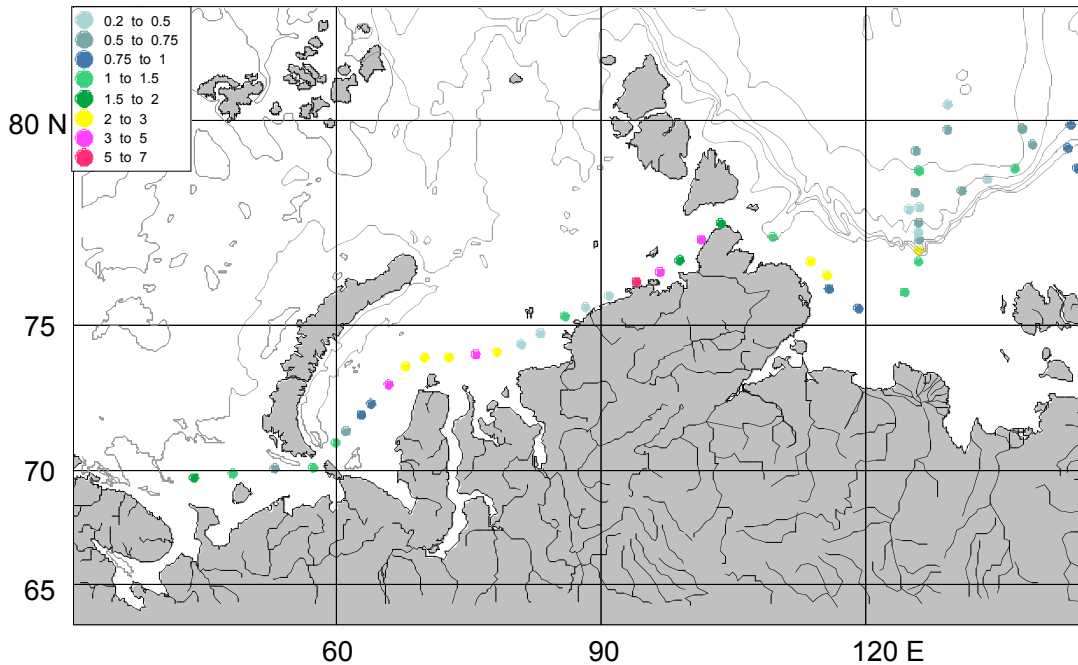


**Figure I.7.4.4:** Chlorophyll “a” concentration in surface water along the expedition pathway (mkg l<sup>-3</sup>).

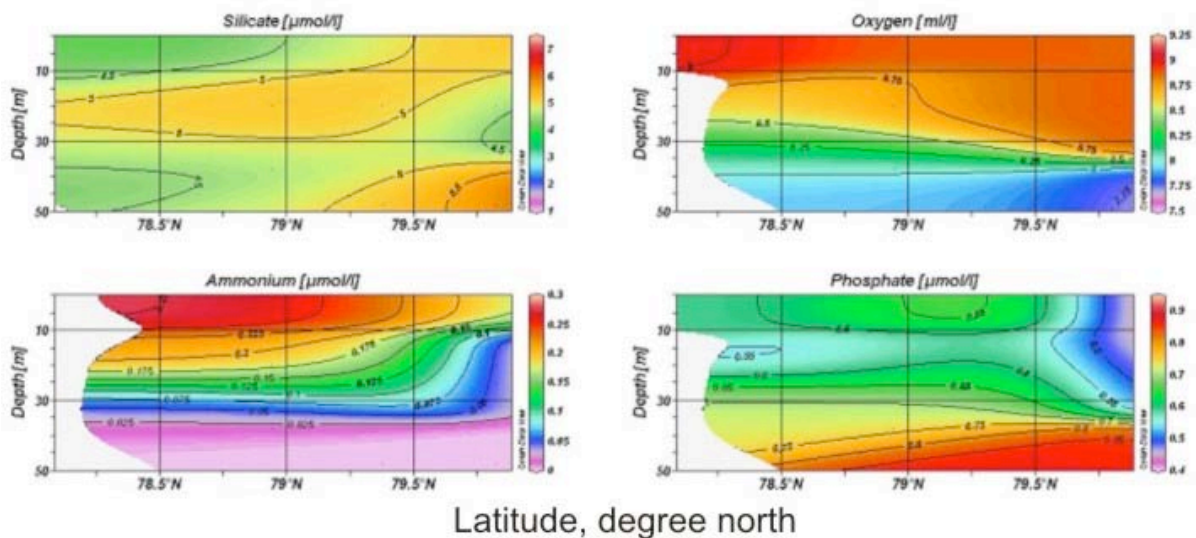


**Figure I.7.4.5:** Distribution of silicon (mkmol l<sup>-1</sup>), oxygen (ml l<sup>-1</sup>), ammonium (mkmol l<sup>-1</sup>), and phosphates (mkmol l<sup>-1</sup>) at cross-section C.

Maximum oxygen concentrations of about 9 ml l<sup>-1</sup> were observed in surface water, gradually decreasing to 8.2-8.6 ml l<sup>-1</sup> at a depth of 50 m.

Silicon concentration in surface water did not exceed 8.9 μmol l<sup>-1</sup>. In the water column from 0 to 50 m a reduction of silicon concentration with depth down to 4 μmol l<sup>-1</sup> was commonly observed. Chlorophyll concentration depended not only on the sea region but also on ice conditions. At neighbouring stations chlorophyll content could vary from low to high depending on development of photosynthesis. On the whole, there was a tendency for chlorophyll concentration to decrease toward central and northern parts of the sea (Figure I.7.4.4). However, richer chlorophyll content was found during earlier studies in the region of the continental slope during ice melting [Gleitz and Grossmann, 1997; Tuschling, 2000]. Chlorophyll concentration decreased with depth. At 50 m chlorophyll concentration was approximately one order of magnitude less than in the surface water (not shown).

## **I.7.5. BIOLOGICAL OBSERVATIONS** (*M. Ringuette, C. Bouchard, A. Forest, L. Fortier, LU*)

### **I.7.5.1. Objectives**

The main objective was the evaluation of the mesozooplankton population state by an estimation of the abundance and biomass of the Laptev sea community in the fall season. A sub-objective was to compare the population growth of the Laptev Sea mesozooplankton community with growth in the Beaufort Sea community by way of simultaneous cruises. The question here is: Are all the shelves and continental slopes equal? For years now, constant values were used to describe biological processes and build large scale models using the assumption that mechanisms should be equivalent throughout the Arctic. Those constants were often taken from various remote locations that sometimes have nothing in common. The comparison of the spatial distribution of the mesozooplankton community and its biomass variability along and across the shelf break area can be a serious test of the broad assumption that all the shelves are analogous throughout the entire Arctic Ocean. This can also be an interesting complement to the work done during previous studies of the Laptev Sea (Kosobokova et al. 1998; Abramova 1999; Kosobokova and Hirche 2001).

Secondly, the Arctic cod represent a funnel through which the carbon cycle must pass in order to sustain the higher trophic levels (birds, seals and polar bears) (Welch et al. 1992). Apart from the very first weeks of life, we know little about the life cycle of this important species. It is believed that the adult cod use the disturbed pack ice as a habitat, and several observations tend to corroborate that belief. In summer the cod aggregate in large schools whose biomass can attain several tons (Welch et al. 1992). The rest of the life cycle is poorly described, including reproductive activities and egg development in the natural environment. By comparing different habitats and ecosystems we aim to distinguish between local factors that can promote growth and survival, and general species adaptation to the cold Arctic environment. Study of genetic differentiation in different fish stocks across the Arctic holds potential for defining the structure of the whole arctic population.

Finally, the sequential sampling of the vertical flux using a sediment trap mooring will primarily compare the upper ocean biological processes to the deep ocean sinking particles. This study will also serve as a comparison with long-term sediment traps deployed on the same schedule within the ArticNet framework in the Beaufort Sea. This will constitute the first effort for a dual long-term arctic monitoring program of biological processes occurring in two different coastal regions.

### **I.7.5.2. Methods**

Sampling area is shown in Figure I.7.5.1. A conical net of 1 m diameter and 250µm mesh, equipped with a TSK flowmeter towed from 500 m to the surface, or from the bottom at shallower stations, was used to estimate the mesozooplankton community and biomass. On the side, a small net of 10 cm diameter with 50µm mesh was installed, allowing the capture of the smaller species of interest along with the young nauplii stages. This setup allows us to uniformly sample all the target species. All samples were preserved in a 4% buffered formalin solution. Samples will be counted and organisms will be identified at the lowest taxonomic level possible in the coming fall at Laval University.

Individual copepods from the dominant species of the Arctic Ocean (*Calanus hyperboreus*, *C. glacialis* and *Metridia longa*) were sorted and placed into a pre-weighed boat. Plates are maintained in desiccant until our return to the lab in Québec where they will be re-weighed to provide a dry-weight and eventually a CHN composition. Again the same procedure is performed with the Beaufort Sea samples. In addition we will measure a reproductive index (RI) in order to compare the reproductive state of the two populations.

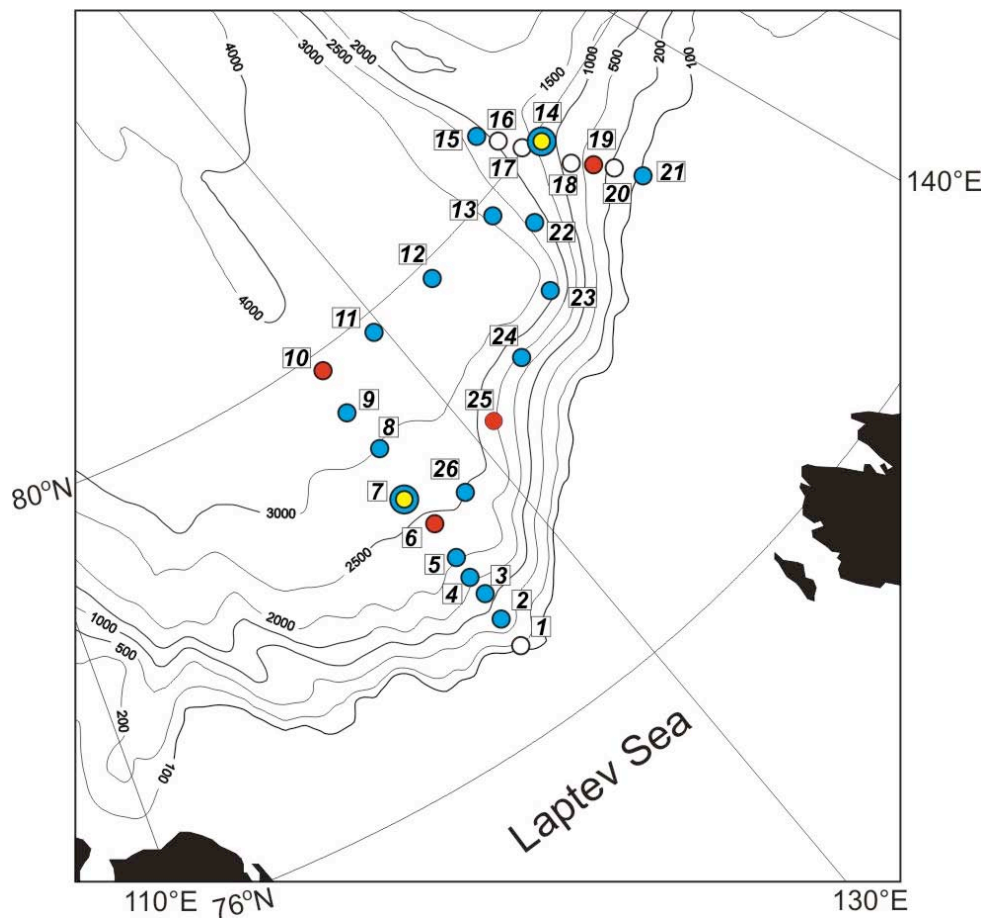


**Figure I.7.5.1:** Spatial distribution of the stations sampled for taxonomic composition and biomass and individual dry weight (red circles). Blue circles show the stations with vertical conical net sampling. Yellow circles are mooring stations.

A double Tucker-like net of 1 m<sup>2</sup> with 500µm and 750µm mesh net was used to catch Juvenile Arctic cod with a double Tucker-like trawl. This trawl consists of two 1m<sup>2</sup> nets installed side by side on a rectangular frame and equipped with a flowmeter. Juveniles caught were individually measured fresh and preserved in 95% ethanol. Otoliths will be removed in the lab, and will be used to estimate individual daily growth. Stomach contents will also be analyzed.

**Table I.7.5.1:** Technicap PPS/3 opening/closing sequence at the NABOS 2004 M3 mooring in the Laptev sea.

Sample cup No.	Open	Close	Collection days
1	21 Sept., 2004	31 Oct., 2004	40
2	1 Nov., 2004	31 Dec., 2004	61
3	1 Jan., 2005	31 Mar., 2005	90
4	1 Apr., 2005	30 Apr., 2005	30
5	1 May, 2005	15 May, 2005	15
6	16 May, 2005	31 May, 2005	16
7	1 Jun., 2005	15 Jun., 2005	15
8	16 Jun., 2005	30 Jun., 2005	15
9	1 Jul., 2005	15 Jul., 2005	15
10	15 Jul., 2005	31 Jul., 2005	16
11	1 Aug., 2005	15 Aug., 2005	15
12	16 Aug., 2005	5 Sept., 2005	21
<b>Total (days)</b>			<b>349</b>

Measurement of the particle fluxes in the Laptev sea will be possible by using two sediment traps installed at 135m and 860m on the mooring line M3 (Station KD1404 in Figure I.7.5.1). The mooring line is also equipped with 2 Aanderaa current meters (RCM-11), 2 Microcat SBE37 and 1 RDI ADCP. See Chadwell and Dempsey, section I.7.3.3.2, "Mooring design and equipment" of this report for complete details on mooring design and technical information. The time sequence of the traps designed to shorten the sampling interval at the maximum of the particle fluxes in spring and summer is presented in Table I.7.5.1. Cups were filled with hyper-saline 5% formalin solution. Microscopic observations and chemical analysis will both be performed on future samples after retrieval in 2005. Biogenic elements (POC, PON, BioSi, carbonates), planktonic organisms (swimmers, algae cells) and derivate materials (marine snow and fecal pellets) are major targets that will be analyzed. All those measurements will be performed in our Québec laboratory. However, the M3 mooring line is located in a complex hydrographic environment along the Laptev Sea slope characterized by variable transport processes. Thus, a considerable quantity of the biological and lithographic particles (C13, C15, Pb210) will also be analyzed by our Japanese colleagues at the National Institute of Polar Research (NIPR) in Japan in order to assess the origin of the particles.

### I.7.5.3. Preliminary results

Mesozooplankton sampling for taxonomic composition and biomass estimation requires rather long work back in the laboratory. Results will be available hopefully in the coming year. A total of 21 stations were sampled from 500 m to the surface (Figure I.7.5.1). In addition, 4 stations were sub-sampled to obtain individual dry weight and CHN.

Unfortunately the heavy ice concentration encountered this year in the Laptev Sea [Smolianitsky, this report] prevented us from deploying the double Tucker-like net. However, based on observations made from the deck of the ship, distribution of the Arctic cod appeared similar to last year. While the icebreaker is sailing, fish simply get cut on returned ice flows. This phenomenon was observed solely in the southern stations of line A. The more southerly the



location the smaller the fish were, meaning the juveniles seems to be distributed closer to the ice edge than the adults at this time of the year.

### **I.7.6. ICE BUOYS DEPLOYMENTS** (*I.Dmitrenko, IARC*)

Ice buoys have been used extensively in Arctic and Antarctic regions to track ice movement and are available commercially for deployment by ships or aircraft. Such buoys are equipped with low temperature electronics and lithium batteries that can operate at temperatures down to  $-50^{\circ}\text{C}$ . Data is transmitted by the NOAA Argos satellite. The description of AWI buoys can be found on:

<http://iabp.apl.washington.edu/gpsbuoy.gif> and

<http://iabp.apl.washington.edu/awiaari.gif>.

Information about buoy deployments is presented in Table I.7.1 and Appendix 1. The stations where the buoys were deployed are referenced as ice stations (ICE##04) in chronological order.



**Figure I.7.6.2:** AWI ARGOS ice buoy deployed during station ICE0204.

The buoy with ARGOS ID # 25887 was deployed at the oceanographic transect A, and a second buoy was deployed at transect B (Figures I.7.3.1 and I.7.6.2). Both AWI buoys were deployed from the icebreaker in the vicinity of the oceanographic stations on two-year-old ice in 150-200 m (Figure I.7.6.1). Distance from ice floe edges was at least 400-500 m. Due to unknown reasons we did not receive any response from the second buoy. The drift of buoy #25887 during two months starting September 14 is shown in Figure I.7.6.2.

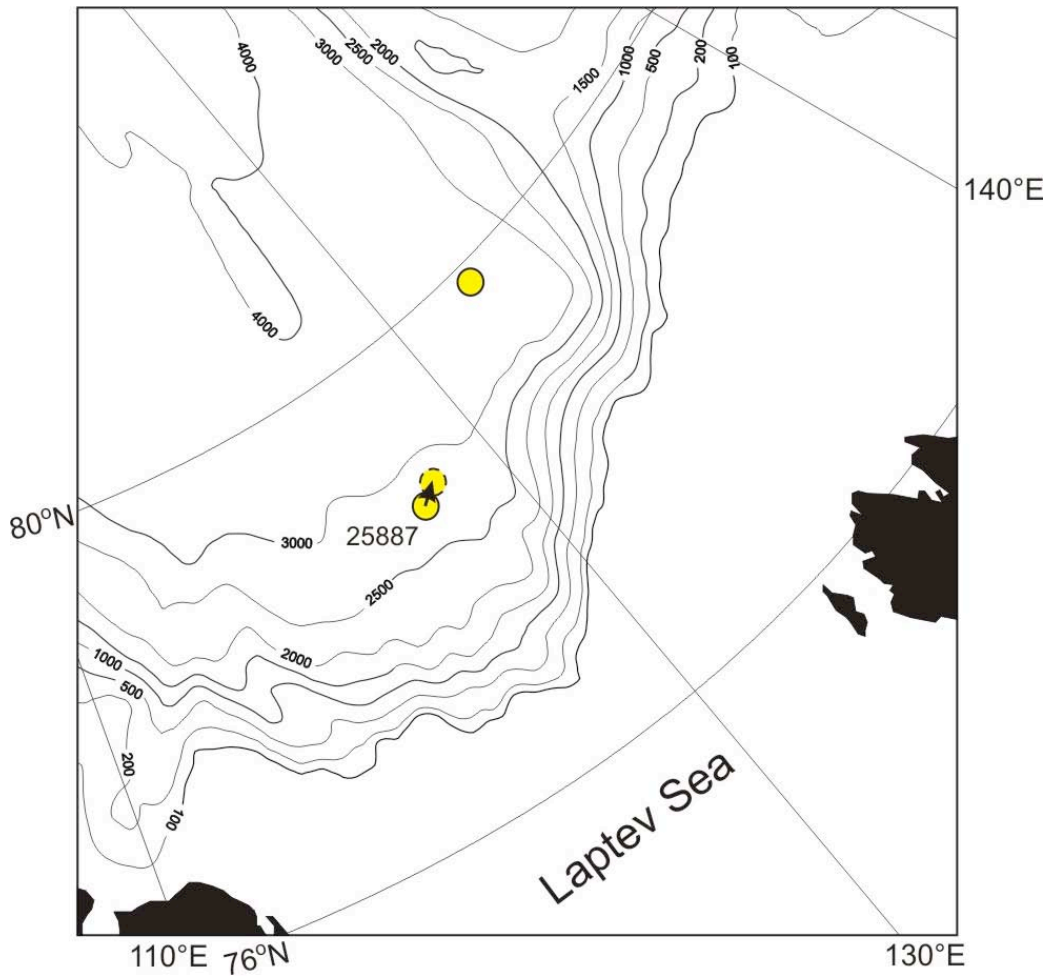
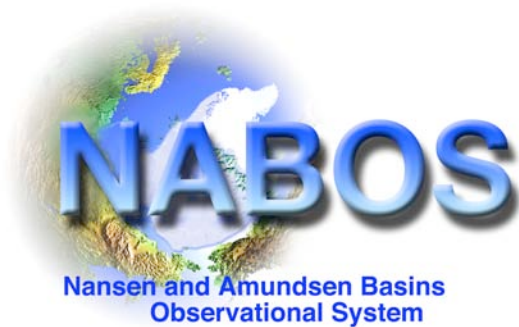


**Figure I.7.6.2:** Positions of deployment and drift from September 14 to November 15, 2004 of AWI ARGOS ice buoys. The buoy number is presented according to ARGOS ID. From November 15, 2004 the buoy positions have been taken from <http://iabp.apl.washington.edu>.



## **SECTION II**

### **Expedition to the western Nansen Basin aboard R/V Lance in September 2004**

Vladimir Ivanov<sup>1</sup> and Edmond Hansen<sup>2</sup>

1 - International Arctic Research Center  
University of Alaska Fairbanks  
Fairbanks, Alaska, USA

2 – Norwegian Polar Institute  
Tromsø, Norway

## II.1. INTRODUCTION

The scope of the NABOS project calls for international cooperation/coordination, which is commensurate with the IARC general objectives. The advantages of such cooperation were clearly demonstrated during the Lance cruise in 2004, when the huge cost of the ship time and scientific equipment was shared by NPI and IARC while the expected scientific outcome might be beneficial to both involved parties.

The cruise was conducted by the Norwegian Polar Institute (chief scientist Dr. Edmond Hansen) in the framework of the ASOF project. The main purpose was to maintain the NPI mooring array in the western Fram Strait and to acquire CTD and ADCP data at the standard monitoring lines. The NABOS-related task was to deploy the long-term mooring on the continental slope between Svalbard and Franz Joseph Land and to carry out CTD observations at the site of deployment.

## II.2. RESEARCH VESSEL

R/V Lance (Figure II.2.1) is the research facility of the Norwegian state scientific agency routinely employed by the NPI for carrying out oceanographic studies in the Nordic Seas and an adjacent part of the Arctic Basin. Her main technical characteristics are presented in Table II.2.1. The ship may navigate through the pack ice with concentration up to 70%. There are three research laboratories in the front part of the ship and enough space for placement of additional container-laboratories on the working deck. Routine oceanographic equipment includes a CTD-profiler mounted on a 12-bottle rosette. The rosette is deployed using a hydraulic winch with a 9-mm cable wire. On-deck handling of the rosette is facilitated by the A-frame. Another winch in conjunction with a 10-ton crane is used for mooring deployment and recovery. Both winches are located on the working deck in the front part of the ship. There is a helicopter deck in the rear part of the ship (a helicopter was not employed during this cruise).

**Table II.2.1:** Main technical characteristics of R/V Lance.

Gross tonnage	1334 GRT
Max draft	6.5 m
Breadth	12.6 m
Length	60.80 m
Freeboard to working deck	3 m
Cruising speed	10.5 knots
Range	21000 nm
Endurance	85 days
Ice breaking ability	Yes, DnV ICE 1A certificate
Max crew and scientists	13 and 25



**Figure II.2.1:** R/V Lance, general view.

### **II.3. CRUISE TRACK**

The cruise started from Longyearbyen, Svalbard on August 31, 2004. The program activities commenced on September 1 with the CTD section across the continental slope in the western Fram Strait (Fig. II.3.1). Within the following 10 days 7 moorings were recovered/redeployed in the western Fram Strait and 49 CTD stations were taken. Ice thickness measurements were carried out at 6 ice stations. On September 11 Lance made a brief call to Ny-Alesund, Svalbard, where two members of the scientific crew disembarked. On September 13 Lance reached the site of the NABOS mooring. The CTD section, including 8 stations across the continental slope and the bottom topography survey, preceded the mooring deployment, which took place on September 13. By the next day the ship returned to the northeastern Fram Strait and continued with CTD sections across the continental slope (27 stations). Program operations were completed on September 16. The cruise terminated in Tromsø, Norway on September 19, 2004. The complete cruise log is presented in Appendix 3.

### **II.4. SCIENTIFIC PARTY**

Edmond Hansen, NPI, chief scientist  
Jürgen Holfort, NPI  
Kristen Fossan, NPI  
Terje Brinck Løyning, NPI  
Sebastian Gerland, NPI (left in Ny-Alesund)  
Richard Hall, NPI (left in Ny-Alesund)  
Vladmir Ivanov, IARC

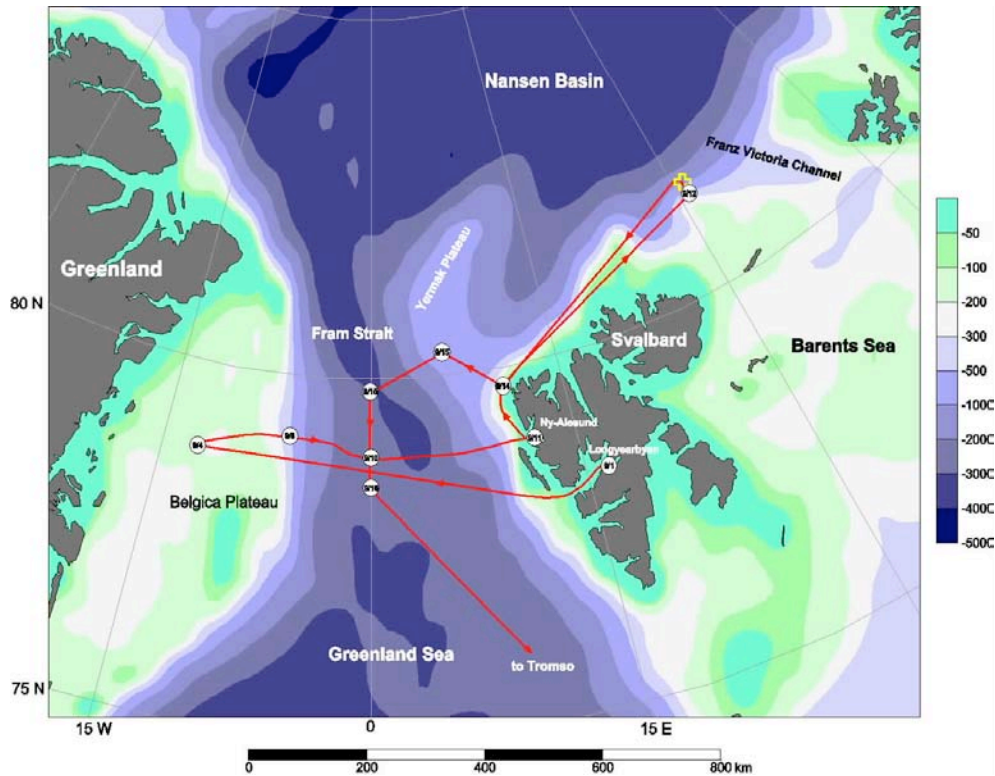


Figure II.3.1: Cruise track.

## II.5. WEATHER AND ICE CONDITIONS

In general, the synoptic regime over the study area during the period of the cruise was characterized by low cyclonic activity. This caused moderate southeasterly winds, about 5-10 m/s, and air temperature around zero centigrade. The wave/swell height was 1.5 – 2 meters on the average and did not seriously impede outboard operations.

The drifting ice was observed in the western part of the Fram Strait. Maximal ice concentration was 70-80%. The average ice thickness was 3-4 meters (according to the direct measurements from the ice floes). Several huge icebergs up to 20 meters in height above the water and with an overall size of hundreds of meters were met in the western part of the Fram Strait. The area to the north and northeast of Svalbard was practically ice-free. In the area of the NABOS mooring deployment ice concentration did not exceed 10-15% (Figure II.5.1).

## II.6. OCEANOGRAPHIC OBSERVATIONS

### II.6.1. Background information

Two major inflows supply the Arctic Ocean interior with Atlantic Water (AW) - the Fram Strait AW branch and the Barents Sea AW branch (Rudels et al., 1994). The Fram Strait AW enters the Nansen Basin with the West-Spitsbergen current and follows the continental slope eastwards. On its way around Svalbard the upper portion of this flow rapidly loses heat due to strong exchange with the atmosphere and mixing with the westward moving Arctic surface

water and sea ice (Aagaard et al., 1987). On reaching the western flank of Franz-Victoria Channel the core of AW is already shielded from direct contact with the atmosphere and sea ice by a cold and fresh surface layer with a thickness of about 50-100 m (EWG, 1997).

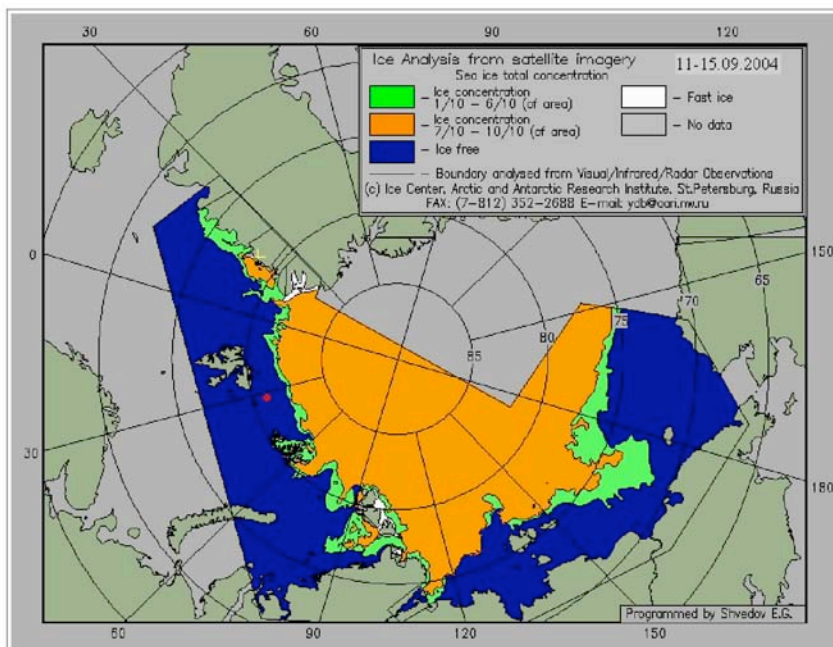


**Figure II.5.1:** Ice conditions on September 11-15/2004. Location of M4 is shown by a red circle ([http://www.aari.nw.ru/index\\_en.html](http://www.aari.nw.ru/index_en.html)).

Below this thin upper layer AW presumably keeps its thermohaline properties close to what they were in the Fram Strait, since there is no intensive lateral mixing, which is the case further downstream (Ivanov, 2002; Schauer et al., 2002). Owing to this fact, the area straight to the west of Franz-Victoria Channel is expected to be quite appropriate for tracing the advective signals in the AW entering with the West Spitsbergen current and spreading along the continental slope towards the main NABOS moorings in the Laptev Sea. The density of observations in this part of the Nansen Basin is not very high. Available historical surveys close to the site of the mooring deployment demonstrate a large difference in thermohaline properties, which cannot be unambiguously attributed to either seasonal or interannual variation (see section II.6.2.3). The annual (and hopefully multi-year) mooring record at this site would allow the mechanisms behind the observed variability of thermohaline properties to be elucidated, and would complement the data obtained at the NABOS moorings in the Laptev Sea with valuable upstream information.

## II.6.2. CTD measurements

The objective of CTD measurements was to take a snapshot of a cross-slope thermohaline structure at the site of mooring deployment for further analysis along with the long-term mooring data.

### **II.6.2.1. Methods**

The bottom slope at the site of the NABOS mooring is rather steep, about 0.07 or 5°. Hence, the spatial resolution of CTD stations was taken to be about 2 miles on the average. The section was completed in 7 hours, starting from the shallowest station at 187 m depth. The distance between this station and the deepest one (at 2500 m) appeared to be 17 miles. The casts were run from about 1-2 m below the surface to 7-10 m above the bottom. The speed of descent was close to 1 m/s. Approach to the seabed was indicated by a bottom-alarm device. Temperature and conductivity sensors operated steadily. Water samples near the bottom were taken for onshore calibration of salinity data.

SBE SEASOFT software for Windows was used for data acquisition and processing. Derived variables include pressure (in db), water temperature (in °C), and conductivity (S/m). The processed data (depth, temperature and salinity) with 1 m vertical resolution were added to the IARC database.

### **II.6.2.2. Equipment**

CTD profiles were recorded using the Seabird profiler SBE911plus. This system continuously measures conductivity, temperature and pressure at 0.25 m intervals in the vertical. Technical specifications for the device are available at the web-site [http://www.seabird.com/products/spec\\_sheets/911data.htm](http://www.seabird.com/products/spec_sheets/911data.htm). The water sampling was carried out using General Oceanic Rosette Model SBE 32 with five five-liter Niskin bottles.

### **II.6.2.3. Preliminary Results**

Vertical sections of temperature, salinity and potential density along the M4 line are presented in Figure II.6.1. Water temperature is positive from the ocean surface to about 850-m depth throughout the entire section, except at the two deepest stations, 57 and 58, where a thin and cold subsurface layer is present. Absolute temperature maximum is equal to 4.22 °C at 79 m depth. Salinity abruptly increases from 32.51 at the surface to 35.01 between 300 and 400 m, and then slowly decreases to 34.92 in the deep water. Absolute salinity maximum is equal to 35.015 psu at 300 m depth. In the cross-slope direction temperature and salinity increase seaward, reaching maximums at different locations inside the section, and then decrease further on. The upper 150-200 m layer is marked by multiple, density-compensated thermohaline intrusions.

Depicted features of thermohaline structure point out that the M4 line has crossed the Fram Strait branch of Atlantic Water (AW). The core of the current, which may be distinguished by maximums in temperature and salinity, is located in the middle of the section between stations 55 and 56. This confirms that the chosen depth for mooring deployment, 1000 m, is quite reasonable, considering the priority task to record variation of properties inside the core of the AW flow.

A possible range of the AW properties temporal variation can be derived from historical data around the M4 site. Locations of available historical surveys are presented in Figure II.6.2. Cross-slope temperature sections in the upper 1000 m layer are shown in Figures II.6.3 and II.6.4.

The most remarkable feature that follows from the presented plots is that in September 2004 the highest ever temperature (4.22 °C) was measured at the M4 site. Obviously, this fact cannot be attributed to incompatible horizontal and/or vertical resolution of measurements in the cruises mentioned. Neither can it be linked with spatial shift between specific surveys. Maximal along-slope shift between the analyzed sections does not exceed 10 km, which is negligible compared with the along-flow variation of temperature in the AW (Aagaard et al., 1987). Taking into account that all data were obtained by the same sensors and in a similar fashion we have to admit large temporal variation of temperature at the M4 site. A set of numerical parameters quantifying this variation is calculated in Table II.6.1.



**Table II.6.1:** Parameters of the vertical water structure for the surveys presented in Figure II.6.2

	$T_{max}$ , °C/ S, PSU	$Z_{Tmax}$ / H, m	$S_{max}$ , PSU/ T°C	$Z_{Smax}$ / H, m	$Z_{up+}$ , m	$Z_{dw+}$ , m	$\Delta Z_{+}$ , m	$\bar{T}_{+}$ , °C	$\bar{S}_{+}$ , PSU
07/87	1.616/ 34.944	266/ 3014	34.969/ 1.528	402/ 3014	79	897	818	1.023	34.930
07/91	2.900/ 34.978	113/ 740	34.984/ 2.850	125/ 740	42	730	688	1.780	34.931
08/93	3.075/ 34.983	191/ 912	35.020/ 2.778	316/ 912	46	883	837	1.631	34.927
09/04	4.221/ 34.948	76/ 1011	35.015/ 3.303	297/ 809	0	828	828	2.153	34.889

Detailed discussion of the calculated parameters is beyond the scope of this brief technical report. However, it is worth mentioning an important difference between the 2004 survey and all the others. In July 1987, 1991 and in August 1993 there was a near-to-freezing-point surface mixed layer, which is a typical element of the vertical structure in the studied area (Aagaard et al., 1987; Rudels et al., 1996; EWG, 1997). In September 2004 this surface mixed layer was also distinguished, but with a temperature well above zero. As a result there is a continuous layer of positive temperature from the ocean surface to approx 850 m depth; this situation is quite unusual for the Nansen Basin, 500 km to the east of the Fram Strait (e.g. EWG, 1997). The probable reason behind this is the fact that in summer 2004 this area was almost ice-free starting from the beginning of August (see Figure II.5.1). Negative ice anomaly enhanced accumulation of short wave radiation in the mixed layer and reduced heat loss due to fusion. Elevated heat content in the mixed layer, in turn, decreased the upward heat flux, which is considered to be the major cooling agent for the upper portion of AW in the studied area (Aagaard et al., 1987). Observed warming below the upper few tens of meters cannot be explained by the local atmospheric forcing, but implies some kind of advective signal, and hence, requires the joint analyses of M4 data with the data upstream (Fram Strait, Nordic Seas). It is important to stress that the maximal measured temperature at the M4 site is more than 1 °C higher than the maximal AW temperature at the same location in 1993, during the “warming in the Arctic” of 1990s (Quadfasel et al., 1991).

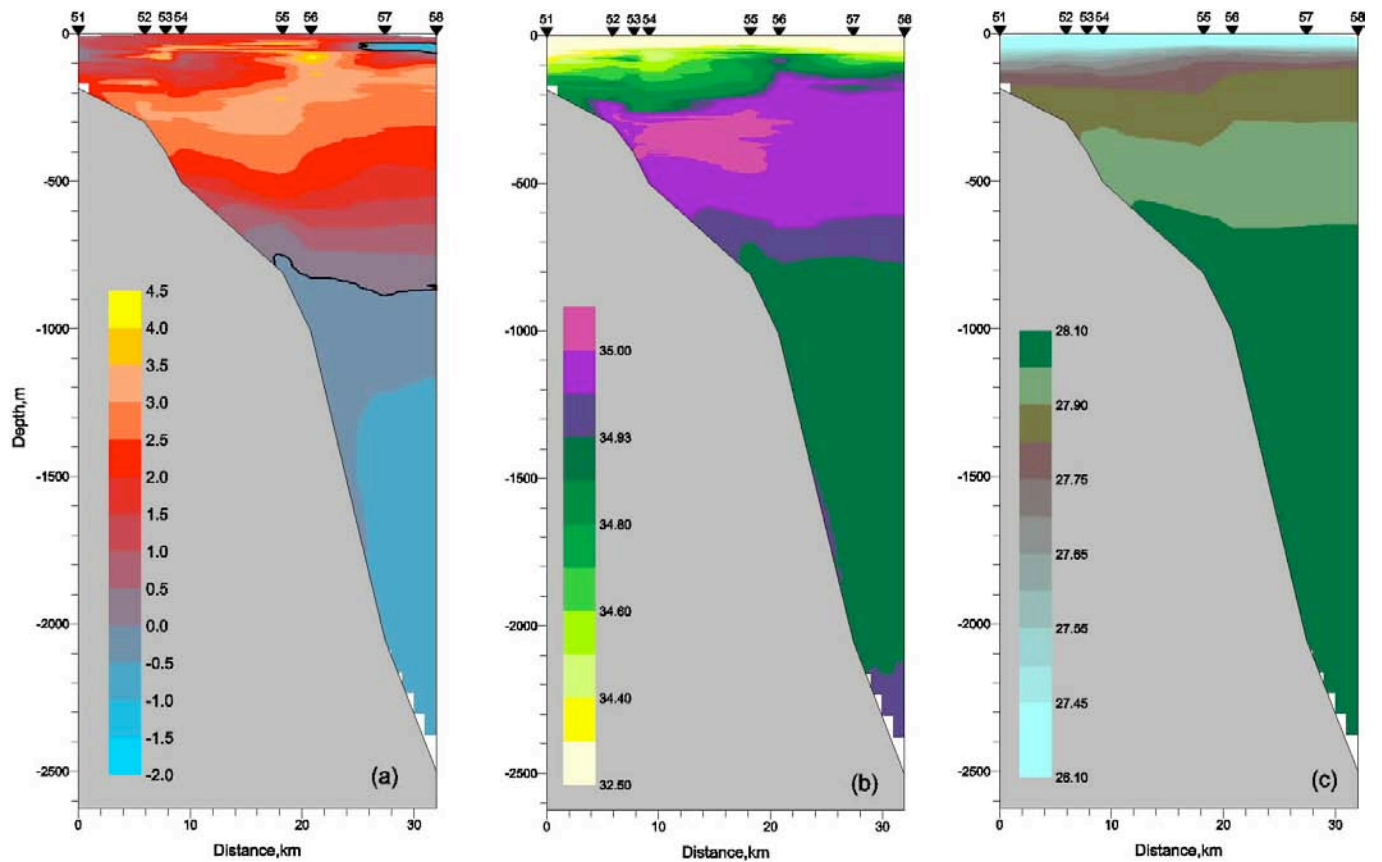


**Figure II.6.1:** M4 section: (a) temperature ( $^{\circ}\text{C}$ ); (b) salinity (psu); (c) potential density (units).

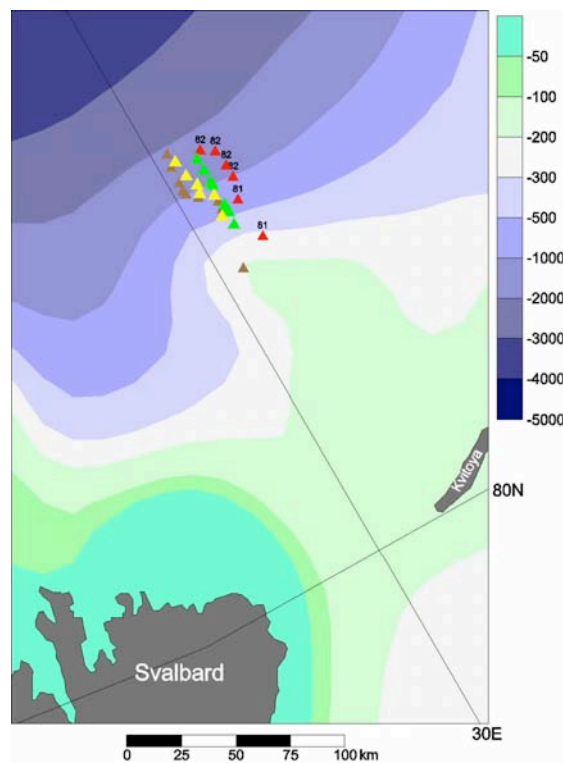


**Figure II.6.2:** Historical surveys around the M4 site: 07/87- Polarstern (red); 07/91- Polarstern (yellow); 08/93 – Polarstern (brown); 09/04 – Lance (green).

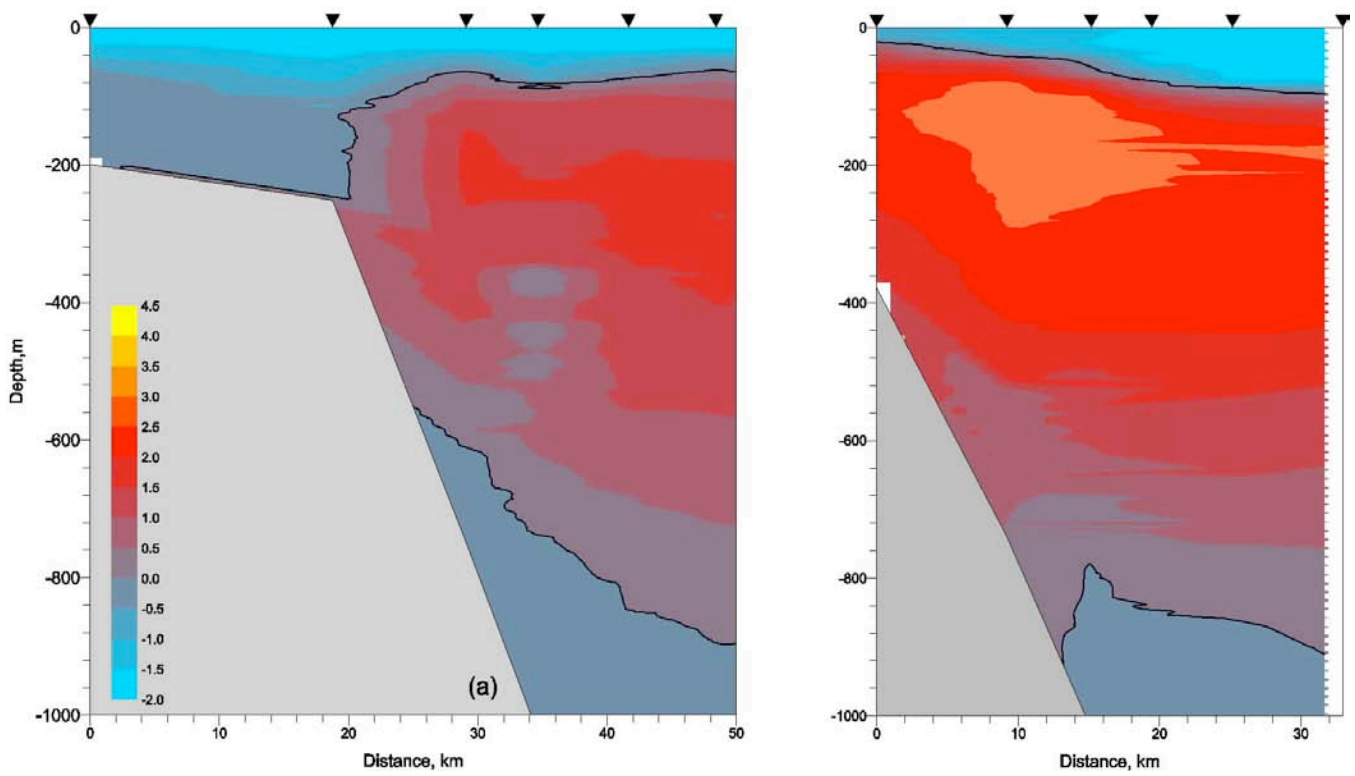


**Figure II.6.3:** Vertical temperature sections around M4 site: (a) Polarstern 07/87; (b) Polarstern 07/91.

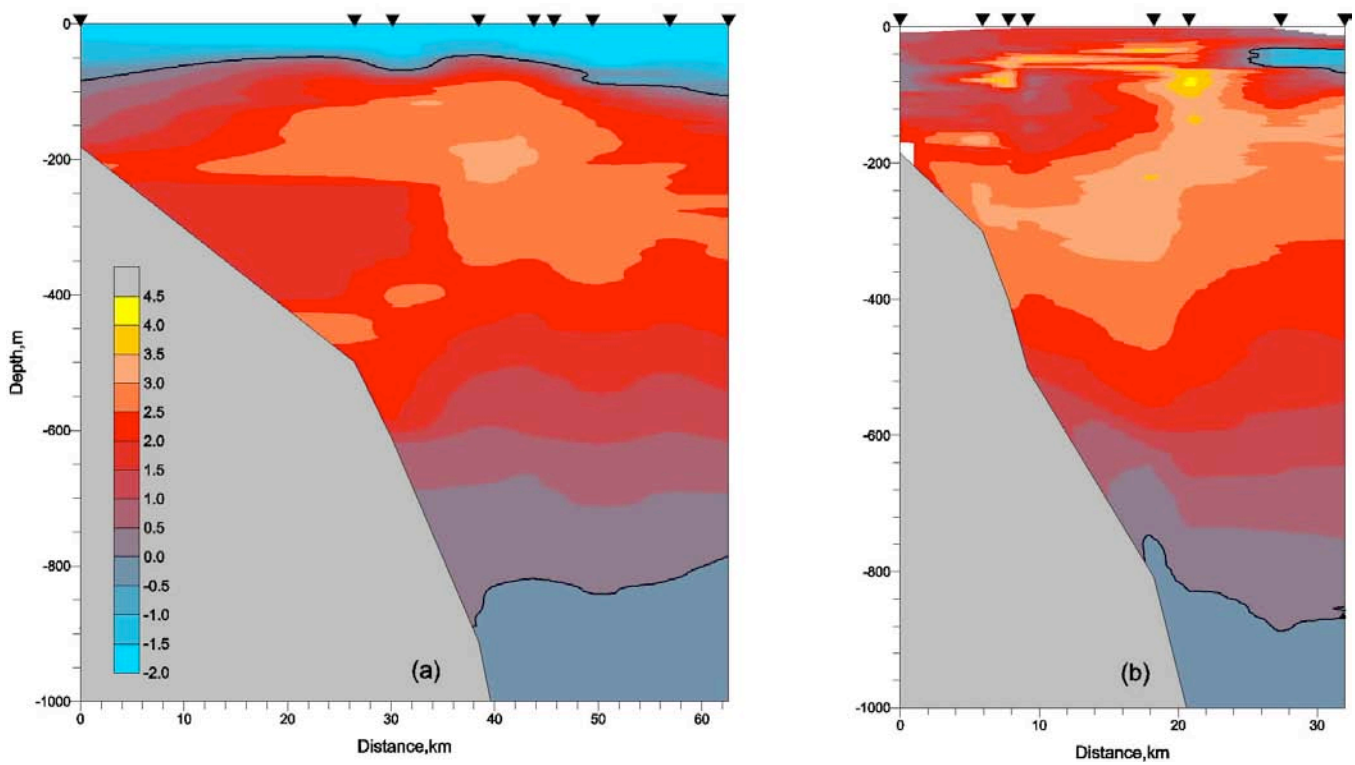


**Figure II.6.4:** Vertical temperature sections around M4 site: (a) Polarstern 08/93; (b) Lance 09/04.

### **II.6.3. Mooring observations**

The purpose of mooring observations is to provide a long-term record of thermohaline properties and water motion on the continental slope of the western Nansen Basin.

#### **II.6.3.1. Mooring design and equipment**

Mooring design and oceanographic equipment is presented in Figure II.6.5. The type and the number of employed sensors (SBE37 and RCM9) were determined by the scientific objective of the M4 deployment and by the available funds for equipping it. Location of sensors was chosen in order to provide maximal coverage of the AW, which is the major target at this mooring. Hence, 4 SBEs and 2 RCMs were placed within the upper half of the water column. Two upper SBEs (59 and 100 m) match well with the location (79 m) of the absolute maximum in the water temperature measured at the section. The 3<sup>rd</sup> SBE (at 209 m) and the second RCM (at 210 m) are expected to record thermohaline and dynamical conditions close to the climatic core of AW, while the 4<sup>th</sup> SBE (450 m) will record thermohaline conditions below the core. Two deepest sensors are required to obtain the data near the bottom. Technical specifications of the applied sensors are available at web sites:

[http://www.seabird.com/products/spec\\_sheets/37smdata.htm](http://www.seabird.com/products/spec_sheets/37smdata.htm) and <http://www.aanderaa.com/frameaset.asp>.

#### **II.6.3.2. Mooring deployment**

Mooring deployment was completed at 11:48 GMT on September 13 in the position 81°33'.761 N, 30°55'.390 E at a depth 1012 m. One day prior to the deployment all the instruments were connected with the batteries and sampling was switched on and checked. The Kevlar rope of required length was put on the drum. The deployment operation was an anchor-first one. Fixing of SBE devices, which do not require cutting the rope, was done directly when the calculated length of rope was reached. To attach the RCM current meters, which required cutting the rope, the weight of the mooring already overboard was transferred from the crane to the iron ring welded to the deck of the ship, the RCM was connected by short Kevlar pieces passed through shackles to the main rope at both sides of the place where the cut would occur, and the weight was transferred back to the main string. After all instruments were placed on the rope the ship moved to the target depth of deployment and the mooring was released. The entire procedure took about an hour and a half.

We would like to express deep gratitude to Kristen Fossan, whose experience and excellent technical skills greatly contributed to trouble-free and successful deployment of the M4 mooring.

# Norwegian Mooring M4A

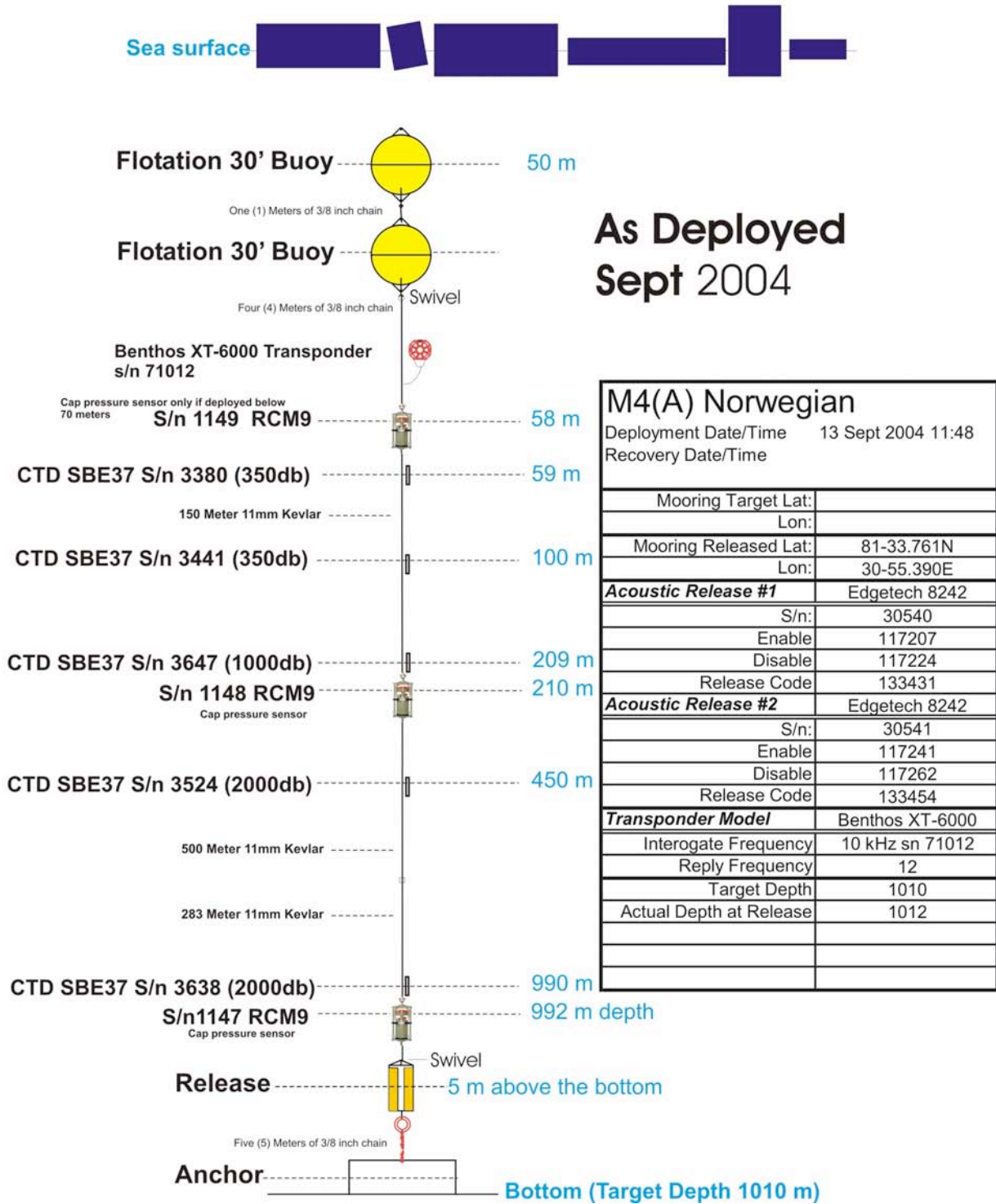


Figure II.6.5: M4 design and equipment.





## SECTION III

### Cruise Report of the CABOS-04 Expedition to the Beaufort Sea aboard Canadian Coast Guard Icebreaker *Louis S. St-Laurent*, September 2004

David Walsh<sup>1</sup>, Sarah Zimmerman<sup>2</sup>, Eddy Carmack<sup>2</sup>, and Igor Polyakov<sup>3</sup>

1 – Naval Research Lab, USA

2 – Institute of Ocean Sciences, Sidney  
British Columbia, Canada

3 - International Arctic Research Center  
University of Alaska Fairbanks  
Fairbanks, Alaska, USA

### III.1. INTRODUCTION

The CABOS mooring is the first devoted to the planned long-term monitoring program of the Canadian Basin of the Arctic Ocean. The goal of CABOS is to monitor the internal temperature, salinity, and velocity structure of the basin and assess how these parameters change over time. The plan calls for inflows and outflows from the basin to be monitored as well, using moorings placed at critical topographic "choke" points, allowing the integrated heat and freshwater budgets of the Canadian Basin to be studied. The program is in some respects similar to NABOS, but given the very different characters of the Canadian and Eurasian Basins, the design of and motivation for the observing system is different.

The Canada Basin - the largest of the Arctic Basins - has the capacity to store vast quantities of heat and fresh water, and the eventual fate of this stored energy may have important consequences for Arctic climate (Aagaard and Carmack, 1989). Current knowledge of the circulation within the Canada Basin, while sketchy, holds that narrow boundary currents carry warm water of Atlantic origin cyclonically around the basin at depths of ~150-600m, but the near-surface circulation, exposed to wind forcing, moves in the opposite direction. Some fraction of the water leaving the Canada Basin exits through the Canadian Archipelago to the Labrador Sea, a major global deep-water formation site critical to the world ocean thermohaline circulation. Aagaard and Carmack (1989) proposed that relatively fresh waters leaving the Arctic may have a strong effect on deep convection within the Labrador Sea and elsewhere, hence influencing production of dense "deep waters." If this is true, the flow through the archipelago could be of global climatic significance and its monitoring is a key scientific challenge.

Many changes in the Canada Basin are presumably transmitted from "upstream" locations in the Eurasian Basin, where warm Atlantic waters enter (McLaughlin et al., 2002). As an example, the effects of an influx of anomalously warm Atlantic water which entered the Nansen Basin in or around 1989 have been followed around the Arctic Basin, the signal having recently arrived in the Alaskan Beaufort Sea. Atlantic waters flow in narrow topographically trapped currents, and are known to be strongly modified by mixing processes as they make their way around the basin (Carmack et al., 1997). Therefore, in order to understand the integrated effect of climatically induced fluctuations in Atlantic water inflow it is necessary to monitor not only the point of entry of anomalous water masses, but also how these masses are modified as they transit the basin. The net oceanic heat flux coming into the Arctic depends upon the balance between the heat content of inflowing waters and that of waters exiting the basin. Similarly, the net effect will depend on how long the anomalous heat energy is stored, and how it eventually leaves.

Our hope is for CABOS to evolve into a long-term observational program (distinct from NABOS, providing invaluable complementary information), and it is sensible to plan it in a way that complements on-going work in the Beaufort Sea. Rather than focusing on a particular area, we propose to deploy five additional moorings dispersed along the margins of the Canada Basin (e.g., three placed along the Alpha-Mendeleev Ridge, and two north of Siberia towards the head of the basin). This would allow measurement of large-scale internal variability, including basin-scale "tilting" of temperature, salinity, and density surfaces - critical to our understanding of the Canada Basin's role as a reservoir for storage of heat and fresh water. The CABOS moorings would also provide detailed information regarding small-scale processes at the mooring locations, but their primary purpose would be to isolate large-scale modes of variability within the Canada Basin. This widely spaced array will sacrifice some of the finer horizontal resolution provided by regional studies (like NABOS), emphasizing the largest-scale modes of variability.

An expanded CABOS would extend and complement the Japan/Canada JWACS (Joint Western Arctic Climate Studies) and the USA/Canada BGEP (Beaufort Gyre Exploration Program) programs, and could provide an upstream reference for other measurement programs [e.g., the Arctic and Subarctic Ocean Fluxes (ASOF) program]. Indeed, the growing list of Arctic programs is demonstrating an important "value added" property, with each complementing the others.




### III.2. RESEARCH VESSEL AND CRUISE PLAN

A brief description of the ship CCGS *Louis S. St.-Laurent* used for mooring deployment and recovery can be found below in Table III.1, copied from the Canadian Department of Fisheries and Oceans web-site:

[http://www.ccg-gcc.gc.ca/vessels-navires/details\\_e.asp?id=A-1](http://www.ccg-gcc.gc.ca/vessels-navires/details_e.asp?id=A-1).

**Table III.1:** Canadian Coast Guard CCGS LOUIS S. ST-LAURENT

Official No:	328095		
Type:	Heavy Gulf Icebreaker		
Port of Registry:	Ottawa		
Region:	Maritimes		
Home Port:	Dartmouth, Nova Scotia, Canada		
Call Sign:	CGBN		
When Built:	1969		
Builder:	Canadian Vickers, Montreal, Québec, Canada		
Modernized:	1988 - 1993 - Halifax Shipyard & 2000 new props		
Certificates		Complement	
Class of Voyage:	Home Trade I	Officers:	13
Ice Class:	100 A	Crew:	33
MARPOL:	Yes	Total:	46
IMO:	6705937	Crewing Regime:	Lay Day
		Available Berths:	53

The cruise of the icebreaker CCGS *Louis S. St.-Laurent* started on July 29, 2004 and ended on September 2, 2004. The cruise program included several mooring deployments and recoveries for a number of science programs as well as a detailed CTD survey. The CABOS mooring locations are shown in Figure III.1. For additional information, including the cruise track, see: <http://www.whoi.edu/beaufortgyre/dispatch2004/position.html>.

### III.3. MOORING RECOVERY AND DEPLOYMENT

Sarah Zimmerman, who led the Arctic-2004 expedition aboard the Canadian icebreaker CCGS *Louis S. St.-Laurent*, wrote from the ship: "From AG5 we decided to try for the CABOS-2 recovery. The mooring was in 9+ tenths ice, but just on the edge of this pack. We made our way up, ranged on the mooring with great help from the WHOI team, performed the rosette cast and then worked on making a hole. The ship was able to crunch the ice into smaller pieces but

pushing them out of the way to make a clear opening was difficult. We decided to wait for a natural opening 600m away to come over the top of the mooring. It didn't quite drift over, so we broke more ice to widen this hole and released the mooring. We didn't see it come up and worried that it had lodged under the ice. After some nosing around without sighting the mooring and a transponder reading showing the mooring was pretty much at its original location we decided to open the second release in case there had been some fouling. Sure enough the mooring popped up a minute later in the now perfectly open hole. A grappling line was thrown and the recovery went smoothly. The Lebus winch that WHOI brought out worked for pulling in and spooling the cable. When the dual release was brought on deck and given a shake, the bar that should have opened from the first release, unstuck and fell away. This same problem - of a jammed release on the Edgetech dual release - was seen on a UW mooring last summer in the Chukchi Sea. In that case, a dragging line was put out and with a nudge to the mooring line was able to un-stick the jammed bar and free the mooring from the anchor. The WHOI moorings use a cable instead of a bar, and the hope is that this system prevents this type of jamming. Well - maybe more than you wanted to hear but the adrenaline is still wearing off! Rick downloaded the data and the quick look shows the monkey was operating up to the day of recovery although after day ~200 the monkey progressively stopped climbing as high or as deep so that by the end it was only moving between ~250 and 200m. The guide wheels on the monkey show deep grooves off of center, indicating the monkey was not aligned vertically. The spring to the climbing wheel was fully intact and still springy (which I guess was a problem last year). Many thanks to the ships crew and WHOI team for their help!"

### III.3.1. Mooring Recovery

Near the mooring site, a CTD cast was performed. We then moved to the mooring site and ranged on the mooring and calculated its exact position. Ice was broken slightly up-drift of the mooring site, and then the mooring released. Although we had confirmation of release the mooring did not surface. We were fearful the mooring had come up under some of the old ice surrounding our created hole; however ranging on the transducer showed the mooring was still in its original spot. The second release was triggered and the mooring successfully surfaced. When brought out of the water, the bar of the dual release finally fell away from the first stuck release. The lost bar was replaced by a cable from WHOI for the CABOS mooring deployment.

Ice Conditions:	5/10 of old ice
Wind Conditions:	10-20 knt SExE
Drift:	To the East
Air Temperature:	5°C

CTD cast #16 taken at this site.

CTD cast gives average sound speed of full depth: 1457 m/s; 50m 1436 m/s; 100m 1438 m/s.

Location survey: Calculated position is 71° 46.6722'N, 131° 53.1952'W, 60m from the anchor drop position.

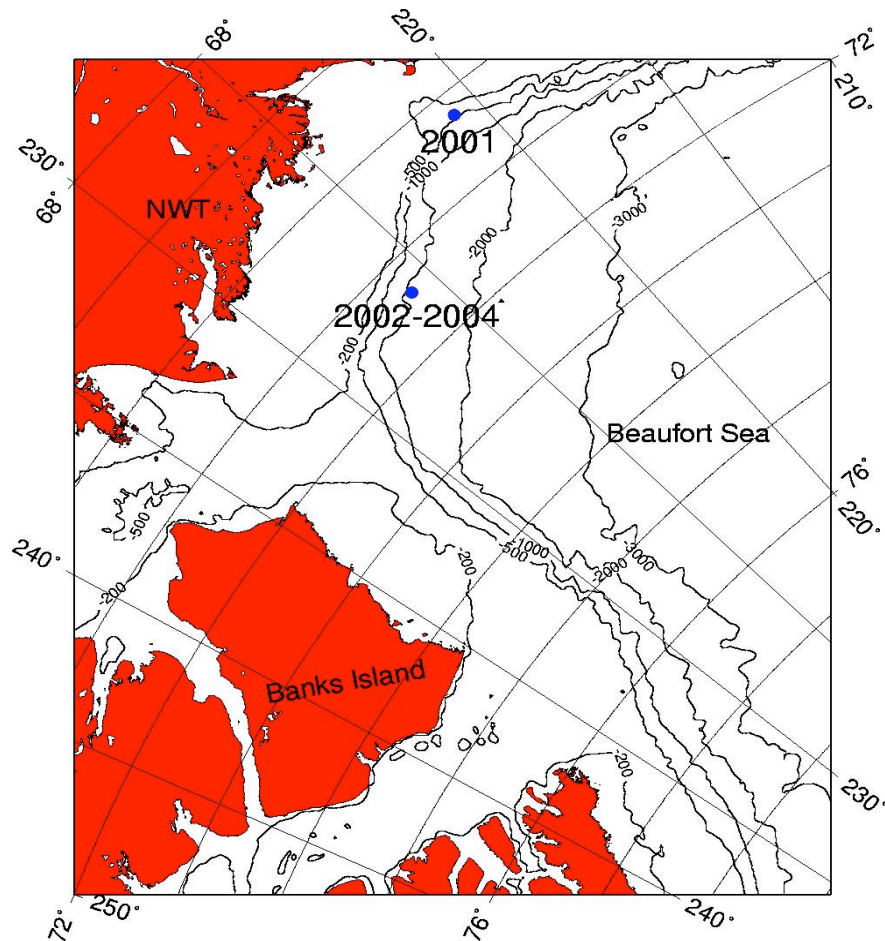


**Figure III.1:** Map showing locations of the moorings deployed in 2001, 2002, 2003, and 2004.

UTC	Position	Depth	Comments
19:37	71°46.675'N, 131° 53.258'W	1120m	Mooring Release Code Sent
19:39	71°46.691'N, 131° 53.247'W	1120m	No confirmation of release
19:47	71°46.739'N, 131°53.314'W	1120m	Mooring has released 470ft to starboard
19:54	71° 46.767'N, 131° 53.320'W	1120m	Transducer on board, read 175m horizontal
20:02	71° 46.69'N, 131° 53.14'W	1120m	Transducer in water, reads 64m
20:09	71° 46.72'N, 131° 53.01'W	1120m	Transducer in water, reads 72m
20:13	71° 46.75'N, 131° 53.01'W	1120m	Transducer in water, reads 192m
20:25	71° 46.66'N, 131° 53.08'W	1120m	Transducer in water, reads 101m
20:26	71° 46.66'N, 131° 53.08'W	1120m	Transducer in water, reads 106m
20:31	71° 46.66'N, 131° 53.00'W	1120m	Second release triggered
20:32	71° 46.66'N, 131° 53.00'W	1120m	Surface
20:47	71° 46.69'N, 131° 53.19'W	1120m	Alongside, top buoy hooked and recovery commenced
20:48	71° 46.69'N, 131° 53.18'W	1120m	Top buoy at rail
21:50	71° 46.81'N, 131° 52.72'W	1120m	Mooring release on board

Notes on recovered equipment:

MMP: Actual time is 23:20, MMP time reads 22:55.

## Canadian Mooring- As Deployed 2003

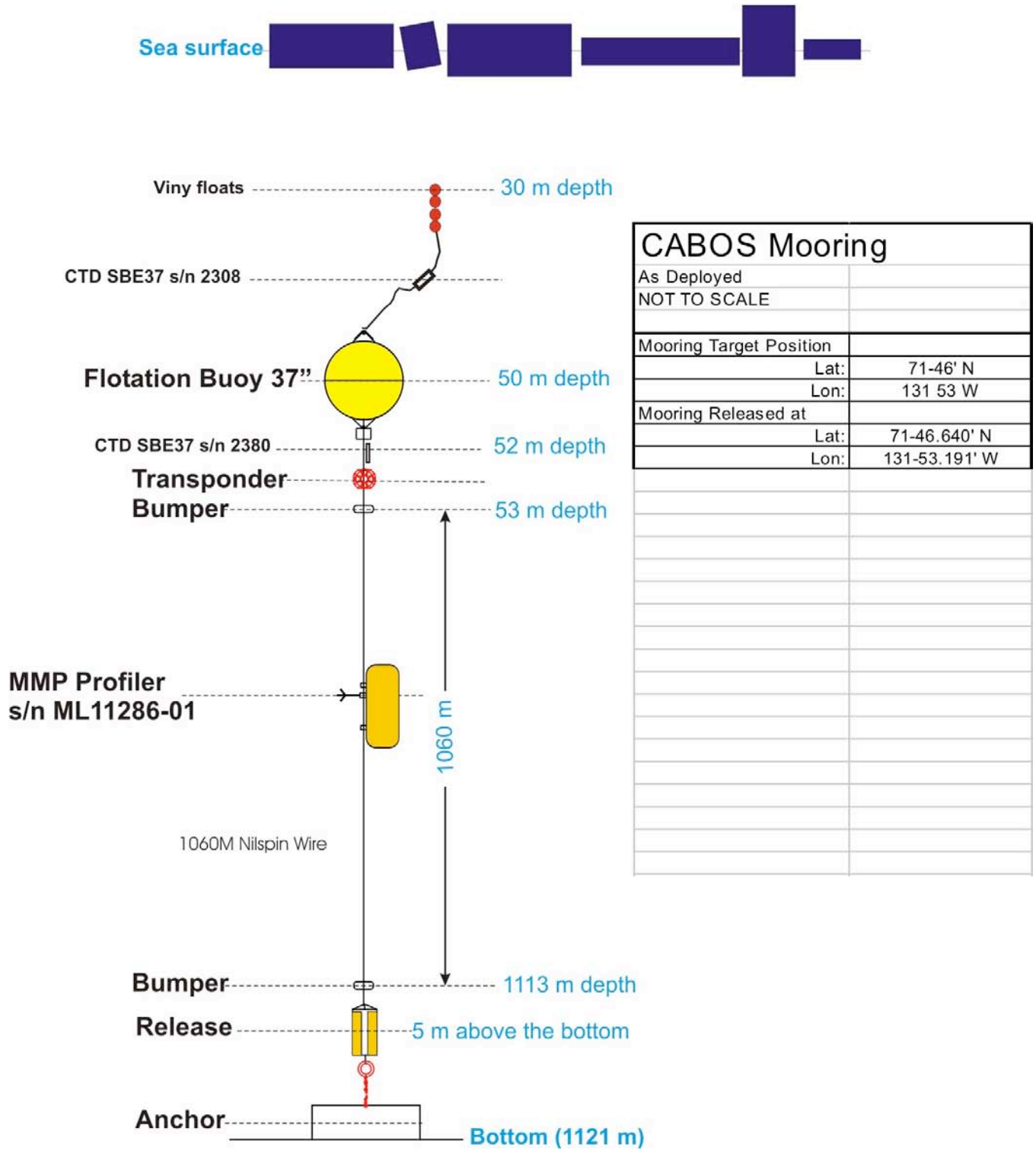


Figure III.2: Recovered (2003-04) CABOS mooring design and equipment.

The motor turns up.

The watchdog check has regular interruptions of “Transponder IRQ Acknowledge”. It appears the release or pinger may have been talking to the MMP?

Last data set written ~1200 GMT 7 August, the day of recovery.

Top ~100m of Nilspin wire covered in a layer of light slime.

Guide wheels have worn groove. The top wheel has the groove on the outside edge. The bottom wheel has the groove on the inside edge. Top and bottom are defined by the MMP standing vertically with the current profiler above the CTD.

Data show roughly 200 days of operation and then the MMP started slipping.

CTD S/N 2360: Actual time is 15:45, CTD time reads 15:47

CTD S/N 2308: Actual time is 20:00, CTD time reads 20:02

### III.3.2. Mooring Deployment

A bottom survey was performed in August 30, 2004, followed by a CTD cast (Cast #50) and then the deployment. We sought to place the mooring in water depth of 1117 to 1125m to match the configuration depth of the MMP. The MMP has been configured with the intent to stop profiling before hitting the bumpers. It was thought that repeatedly hitting the bumpers could have contributed to the reduced profiling of last years deployment. We began deployment of the mooring expecting to drift over the right depth by the time the mooring was ready to be lowered. Instead the ship’s drift slowed and stopped leaving us in water too deep. The mooring was brought back on deck, the ship relocated and the mooring re-deployed.

The final deployment depth was 1121m. We believe the top bumper is located between 54 and 57m and the bottom bumper is between 1110 and 1113m. The MMP was programmed to run from 60m to 1110m. After deployment, the range distance was 116m, indicating the mooring landed 60 to 65m from where it was dropped.

Ice Conditions: 5/10 with mostly first year frozen around pieces of multiyear

Wind Conditions: 10 knt or less, 305° True

Drift: 0.5 knt to SE, changed to 0.3 knt to S, chaged to 0knt.

Air Temperature: 1°C

**Table III.1:** Sensors for CABOS Mooring deployed in 2004.

Equipment	Serial #	Parameters	Last Calibration	Sampling Rate	Depth (db)	Comments
Top Microcat CTD SBE-37SM	2368	Conductivity Temperature Pressure	Oct 14, 2003	15 Minutes	54	Pressure sensor rated to 3500db
McLane Moored Profiler (MMP)	11494	Current Conductivity Temperature Pressure	N/A	Two profiles per day	55 to 1100	
MMP FSI ACM Sensor	1589	Current	N/A	-	N/A	MMP sub-sensor
MMP FSI EMCTD Sensors	1335	Conductivity Temperature Pressure	Fall 2004	-	N/A	MMP sub-senor

### Canadian Mooring- As Deployed 2004

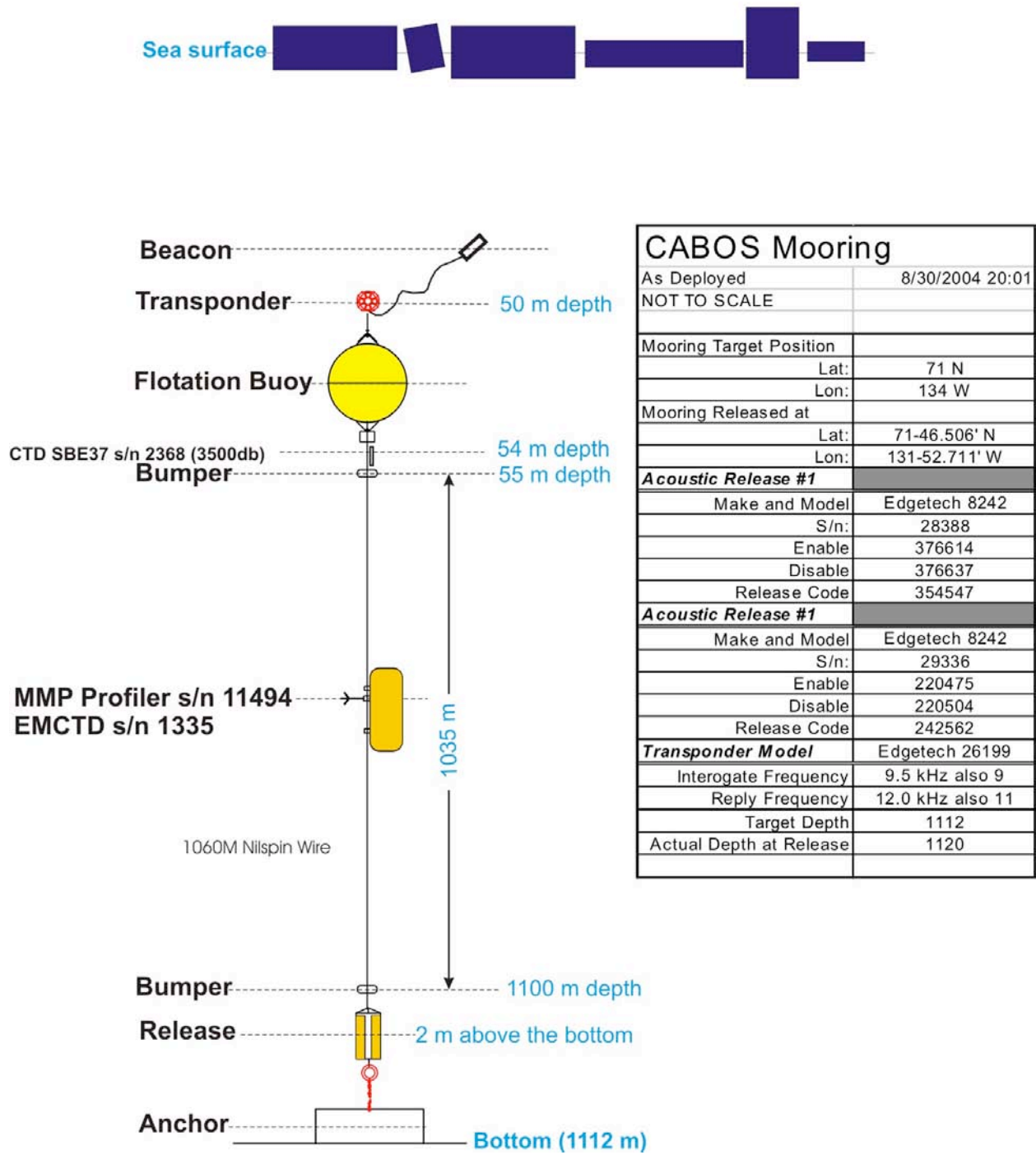
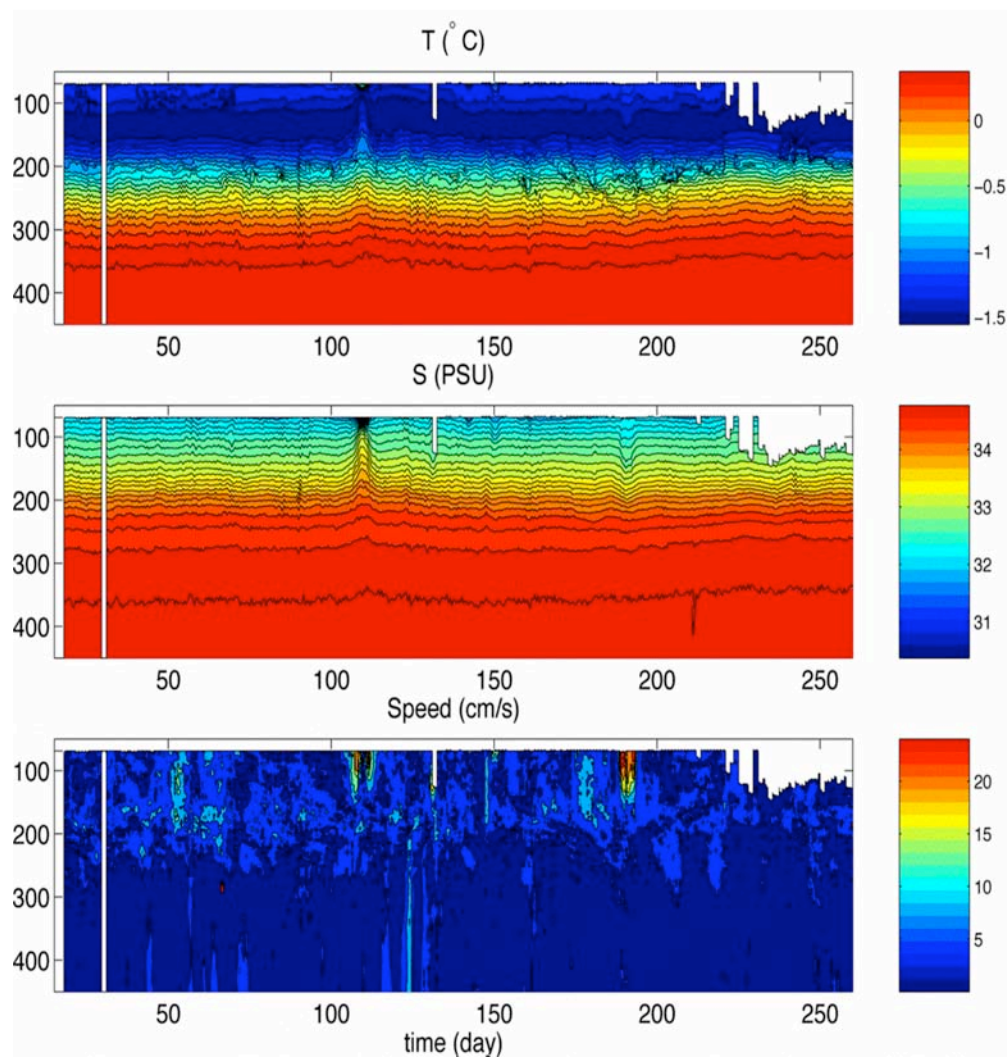


Figure III.3: Deployed (2004-05) CABOS mooring design and equipment.

### III.4. A PRELIMINARY LOOK AT THE LATEST MMP DATA

A first look at MMP data obtained by the 2003-2004 CABOS mooring is shown in Figure III.4.

We were lucky to capture the passage of several eddies past the mooring location. Of the two strongest, one was found to be cyclonic (characterized by compression of isopycnals) and the other anticyclonic. The cyclone (see expanded view in Figure III.5) produced a strong disturbance in temperature, salinity, and velocity fields, with classical doming of iso-surfaces and two strong maxima in velocity magnitude. Both vortices were observed close to the surface, above 150 m depth. Just visible at the bottom of the velocity contour (third panel) is the signature of strong waves which propagated past the mooring site - we speculate that these are coastal trapped waves propagating along the basin boundary. By providing a detailed view of velocity, temperature, and salinity fields and how they evolve over time, these and other similar data will allow us to accurately estimate the time-mean structure of these fields, and elucidate mechanisms of variability occurring on time scales from days to years. Comparing these new data with data from the previous year will provide a first detailed look at interannual variability of full-depth velocity, temperature, and salinity structure in this part of the Arctic Ocean.



**Figure III.4:** Temperature (upper panel), salinity (middle panel) and current speed (lower panel) during 255 days of measurements from September 2003 to June 2004 from McLane Moored Profiler (MMP) data. Blank spaces represent missing data.

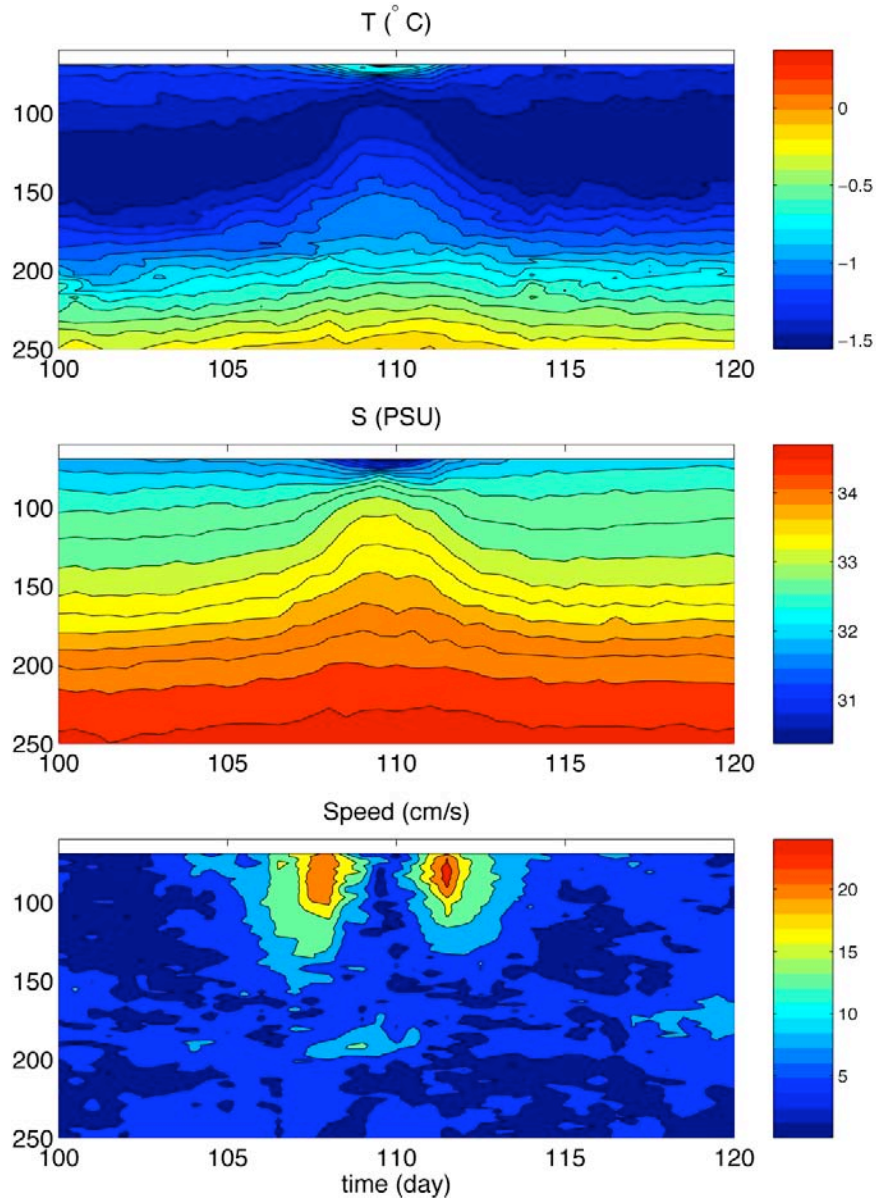


**Figure III.5:** Depth-time diagram of the MMP record of water temperature (top), salinity (middle), and current speed (bottom) measured in the Canada Basin in 2003-04. Note the clear signature of an eddy passing through the mooring location with domed isopycnal surfaces and increased speed.

Temperature, salinity and sea level records from the surface floating and 52 m depth SBE-37 CTDs are shown in Figure III.6 (serial #2308) and Figure III.7 (serial #2360).



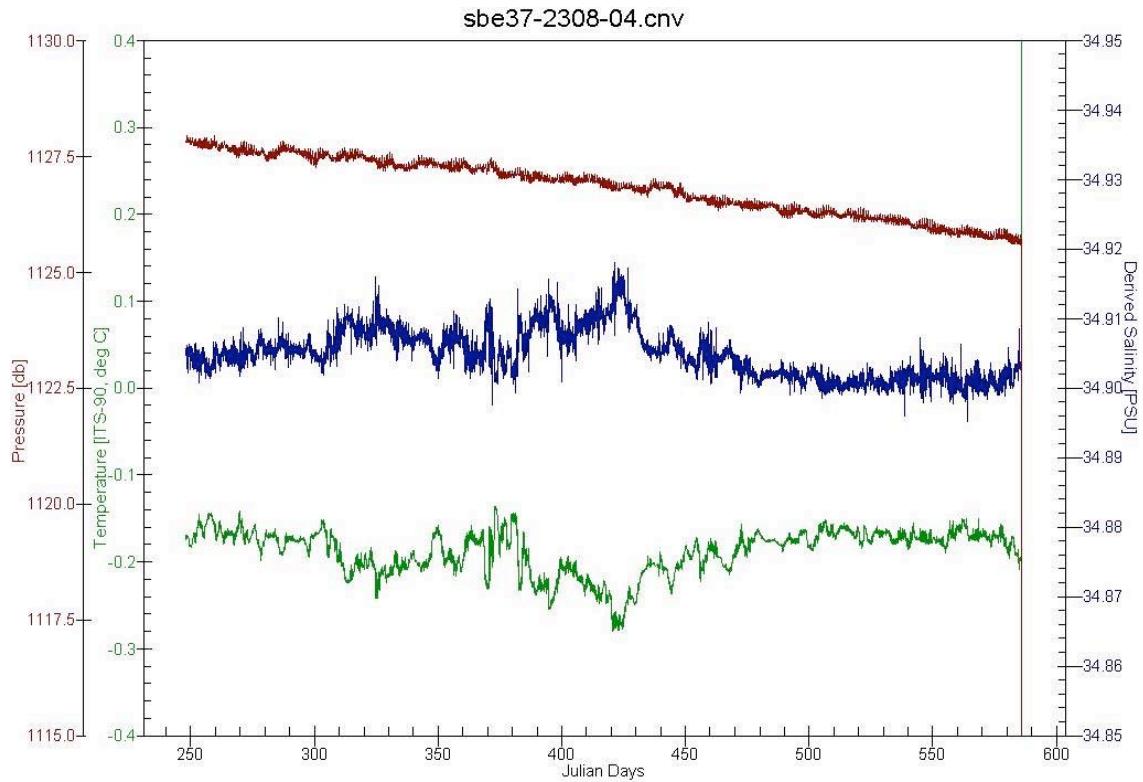


**Figure III.6:** Time series of sea level (red), salinity (blue) and temperature (green) from the surface floating CTD SBE-37 #2308. Raw data were shown.

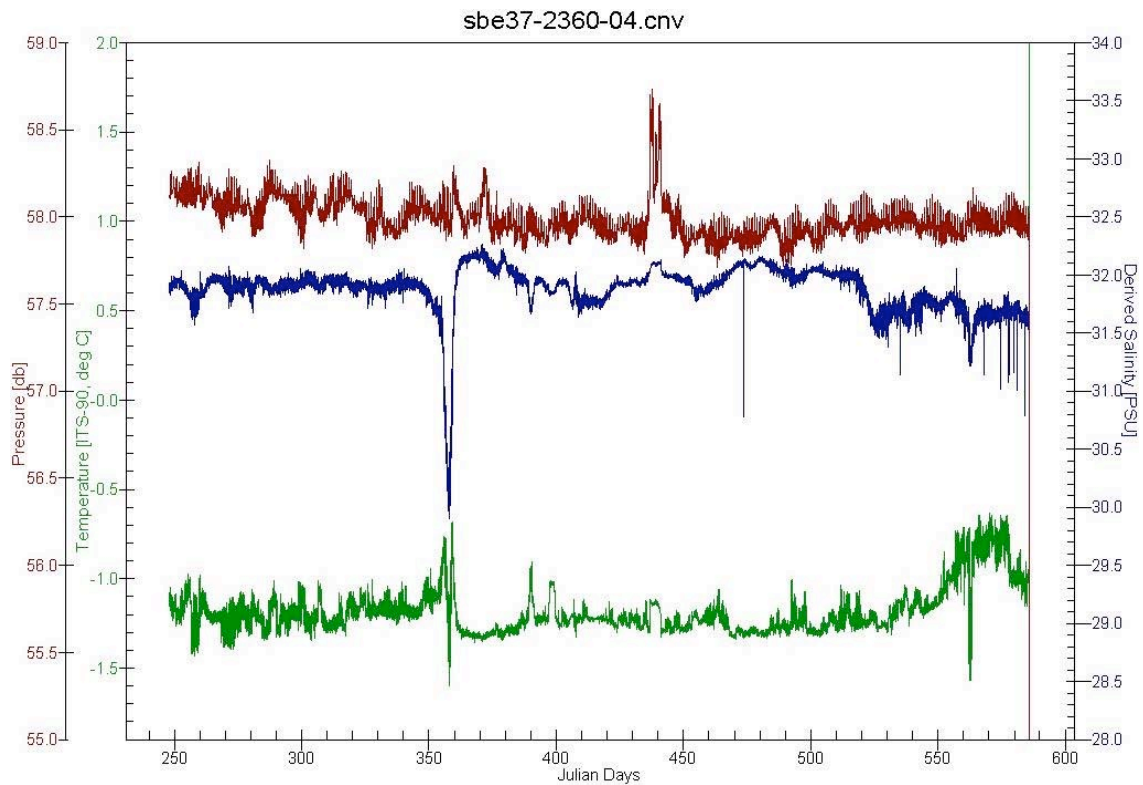


**Figure III.7:** Time series of sea level (red), salinity (blue) and temperature (green) from the 52 m depth CTD SBE-37 #2360. Raw data were shown.

## REFERENCE

- Aagaard, K., A synthesis of the Arctic Ocean circulation, P.-V. Reun. Cons. Int. Explor. Mer., 188, 11-22, 1989.
- Aagaard, K. and E. C. Carmack, The role of sea ice and other fresh water in the Arctic circulation. *J. Geophys. Res.*, 94, 14485-14498, 1989.
- Aagaard, K., A. Foldvik and S.R. Hillman. The West Spitsbergen Current: Disposition and Water Mass Transformation, *J. Geophys. Res.*, 92(C4), 3778-3784, 1987.
- Abramova, E.N., Composition, abundance and population structure of spring-time zooplankton in the shelf-zone of Laptev Sea. In: *Land-Ocean systems in the Siberian Arctic: Dynamics and history*. Springer, New York, 161-168, 1999.
- Andreas, E.L., Parameterizing scalar transfer over snow and ice: a review. *Journal of Hydrometeorology*, 3, 417-431, 2002.
- Andreas, E.L., and B.A. Cash, Convective heat transfer over wintertime leads and polynyas. *J. Geophys. Res.*, 104(C11), 25721-25734, 1999.
- Carmack, E., K. Aagaard, J. Swift, R. Perkin, F. McLaughlin, R. Macdonald, P. Jones, J. Smith, K. Ellis, and L. Kilius, Changes in temperature and tracer distributions within the Arctic Ocean: Results from the 1994 Arctic Ocean Section, *Deep-Sea Research*, 44, 1487-1502, 1997.
- Coachman, L. K., and C. A. Barnes, The movement of Atlantic Water in the Arctic Ocean, *Arctic*, 16, 8-16, 1963.
- Dmitrenko I., L. Timokhov, O. Andreev, R. Chadwell, M. Dempsey, H. Eicken, S. Kirillov, A. Klein, S. Mastrukov, M. Nitishinskiy, I. Polyakov, M. Ringuette, N. Tanaka, and D. Walsh, Cruise Report of the NABOS-03 Expedition to the Northern Laptev Sea aboard the Icebreaker Kapitan Dranitsyn, September 2003, IARC Technical Report 1, Fairbanks, Alaska, 2004.
- Environmental Working Group (EWG), Joint U.S. - Russian Atlas of the Arctic Ocean [CD-ROM], Natl. Snow and Ice Data Cent., Boulder, Colorado, 1997.
- Fairal C.W., and S.E. Larsen, Inertial-dissipation method and turbulent fluxes at the air-ocean interface, *Boundary-layer Meteorol.*, 34, 287-301, 1986.
- Gleitz, M., and S. Grossmann, Phytoplankton primary production and bacterial production, *Ber. Polarforschung*, 226, 92-94, 1997.
- Grachev, A.A., C.W. Fairal, and S.E. Larsen, On the determination of the neutral drag coefficient in the convective boundary layer, *Boundary Layer Meteorology*, 86, 257-278, 1998.
- Holm-Hansen, O., C.J. Lorenzen, R.W. Holmes, and J.D.H. Strickland, Fluorometric determination of chlorophyll, *J. Cons. Int. Explor. Mer.* 30(1), 3-15, 1965.
- Ice Chart Color Standard, WMO/Td, 1215, 2004.
- Ivanov, B.V., S. Gerland, J.-G. Winther, and H. Goodwin, Energy exchange processes in the marginal ice zone of the Barents Sea, Arctic Ocean, during spring 1999, *Journal of Glaciology*, 49(166), 415-419, 2003.
- Ivanov V.V., Atlantic Water in the western Arctic, Experience of structured oceanographic investigations in the Arctic Ocean, A.P. Lisitzin, M.E. Vinogradov and E.A. Romankevich (Eds.), Moscow, Nauchny Mir, 76-91, 2002. (in Russian)
- Jones, E.P., Circulation in the Arctic Ocean. *Polar Research*, 29(2), 139-146, 2001.

Karcher, M. J., R. Gerdes, F. Kauker, and C. Koberle, Arctic warming - Evolution and spreading of the 1990s warm event in the Nordic Seas and the Arctic Ocean, *J. Geophys. Res.*, 108, C2,10.1029/2001JC001265, 2003.

Kosobokova, K.N., H. Hanssen, H.J. Hirche, and K. Knickmeier, Composition and distribution of zooplankton in the Laptev Sea and adjacent Nansen Basin during summer, 1993. *Polar Biology* 19, 63-76, 1998

Kosobokova, K.N., and H.-J., Hirche, Reproduction of *Calanus glacialis* in the Laptev Sea, Arctic Ocean. *Polar Biology* 24, 33-43, 2001.

Loftus, M.E., and J.H. Carpenter, A fluorometric method for determining chlorophylls a, b, and c, *J. of Marine Research*, 29(3), 319-338, 1971.

McLaughlin, F.A., E.C. Carmack, R.W. Macdonald, A. Weaver, J. N. Smith, and K. Aagaard, The Canada Basin 1989-1995: Upstream change and far-field effects of the Barents Sea Branch. *J. Geophys. Res.*, 107(C7), 10.1029/2001JC000904, 19-1 - 19-20, 2002.

Makshtas, A.P., The heat budget of Arctic ice in the winter, Leningrad, AARI, 1991.

Morison, J. H., K. Aagaard, K. K. Falkner, K. Hatakeyama, R. Moritz, J. E. Overland, D. Perovich, K. Shimada, M. Steele, T. Takizawa, and R. Woodgate, North Pole Environmental Observatory delivers early results, *Eos, AGU Transactions*, 83, 241,244-245,249, 2002.

National Snow and Ice Data Center (NSIDC), Bootstrap sea ice concentrations for NIMBUS-7 SMMR and DMSP SSM/I. Boulder, CO, USA. 2003. Internet: <http://nsidc.org>

Pfirman, S. L., D. Bauch, and T. Gammelsrod. The Northern Barents Sea: Water mass distribution and modification. In: *The Polar Oceans and Their Role in Shaping the Global Environment*, 77-94, 1994.

Polyakov, I. V., D. Walsh, I. A. Dmitrenko, R. L. Colony, and L. A. Timokhov, Arctic Ocean variability derived from historical observations, *Geophys. Res. Lett.*, 30(6), 1298, doi:10.1029/2002GL0164412003, 2003.

Quadfasel, D., A. Sy, and B. Rudels, A ship of opportunity section to the North Pole: upper ocean temperature observations, *Deep- Sea Res.*, 40, 777-789, 1993.

Quadfasel, D., A. Sy, D. Wells and A. Tunik, Warming in the Arctic, *Nature*, 350, 385, 1991.

Repina I.A., and A.S. Smirnov, Heat and momentum exchange between the atmosphere and ice from the observational data obtained in the region of Franz Josef land, *Atmospheric and Oceanic Physics*, 36(5), 618-626, 2000.

Repina I.A., Smirnov A.S., and Volkov Yu.A. The influence of surface structure in polar regions on heat and momentum exchange between atmosphere and ocean. *Surface and internal waves in Arctic seas*, 2002, pp. 189-214. (In Russian).

Rigor, I. G., J. M. Wallace, and R. L. Colony, Response of sea ice to the Arctic Oscillation, *J. Climate*, 15, 2648-2663, 2002.

Rudels, B., L.G. Anderson, and E.P.Jones, Formation and evolution of surface mixed layer and halocline of the Arctic Ocean, *J. Geophys. Res.*, 101(C4), 8807-8821, 1996.

Rudels, B., G. Björk, R. D. Muench, and U. Schauer, Double-diffusive layering in the Eurasian Basin of the Arctic Ocean, *J. Mar. Syst.*, 21, 3-27, 1999.

Rudels, B., E. P. Jones, L. G. Anderson, and G. Kattner, On the intermediate depth waters of the Arctic Ocean, in: *The Polar Oceans and Their Role in Shaping the Global Environment: The Nansen Centennial Volume*, *Geophys. Monogr. Ser.* vol. 85, edited by O. M. Johannessen, R. D. Muench, and J. E. Overland, pp. 33-46, AGU, Washington, D.C., 1994.

- Rudels, B., R. Meyer, E. Fahrbach, V. Ivanov, S. Osterhus, D. Quadfasel, U. Schauer, V. Tverberg, and R. A. Woodgate, Water mass distribution in Fram Strait and over the Yermak Plateau in summer 1997, *Annales Geophysicae*, 18, 687-705, 2000.
- Schauer, U., R. D. Muench, B. Rudels, and L. Timokhov, Impact of eastern Arctic shelf waters on the Nansen Basin intermediate layers, *J. Geophys. Res.*, 102(C2), 3371-3382, 1997.
- Schauer, U., B. Rudels, E.P. Jones, L.G. Anderson, R.D. Muench, G. Björk, J.H. Swift, V. Ivanov, A.-M. and Larsson, Confluence and redistribution of Atlantic water in the Nansen, Amundsen and Makarov basins, *Annales Geophysicae*, 20 (2), 257 – 273, 2002.
- Smolyanitsky, V., Arctic sea ice climatology for 1950-1994 assessed on the basis of WMO project 'Global Digital Sea Ice Data Bank' Proceedings of the Conference "Mapping and Archiving of Sea Ice Data - the expanding role of radar". WMO/TD, 1027, 2000.
- Strickland, J.D.H., and T.R. Parsons, A Practical Handbook of Seawater Analysis. Fisheries Research Board of Canada, Bulletin 167, 1968.
- Timofeev, V. T., Vodniye Massy Arkticheskogo Basseina (Water masses of the Arctic Basin), *GydroMeteolzdats, Leningrad*, 1960.
- Tuschling, K., Phytoplankton ecology in the arctic Laptev Sea – a comparison of three seasons, *Ber. Polarforschung*, 347, 2000.
- Vedernikov, V.I., V.I. Gagarin, and V.I. Burenkov, Features of distribution of primary production and chlorophyll in the Pechora Sea in August–September 1998, *Oceanology* 41, 64–74, 2001. (in Russian).
- Welch, H.E., M.A. Bergmann, T.D. Siferd, K.A. Martin, M.F. Curtis, R.E. Crawford, R.J. Conover, and H. Hop, Energy flow through the marine ecosystem of the Lancaster Sound region, arctic Canada, *Arctic* 45, 343-357, 1992.
- WMO, WMO Sea Ice Nomenclature, Suppl. \_ 4, WMO/OMM/\_\_\_, 259, 1989.
- Woodgate, R. A., K. Aagaard, R. D. Muench, J. Gunn, G. Bjork, B. Rudels, A. T. Roach, and U. Schauer, The Arctic Ocean boundary current along the Eurasian slope and the adjacent Lomonosov Ridge: Water mass properties, transports and transformations from moored instruments, *Deep-Sea Research, Part 1*, 48, 1757-1792, 2001.
- Yentsch, C.H., and D.W. Menzel, A method for the determination of phytoplankton chlorophyll and phaeophytin by fluorescence, *Deep-Sea Research*, 10, 221-231, 1963.
- Yentsch, C.S., Distribution of chlorophyll and phaeophytin in the open ocean, *Deep-Sea Research*, 12, 653-666, 1965.
- Yunev, O.A., and G.P. Berseneva, Fluorometric method for determining chlorophyll "a" in phytoplankton, *Hidrobiologicheskii jurnal*. 22(2), 89-95, 1986. (in Russian).

**Appendix 1: NABOS-04 STATION LIST** (I.Dmitrenko, IARC, and S.Mastrykov, SRNHI)

Station Number: KD0104 Data: 12/09/04 Time of beginning: 04:00  
dd/mm/yy hh:mm (GMT)  
 Latitude: 76°44.6'N Longitude: 125°59.8'E Depth: 67 m Ice: 90%  
(navigation chart)

#	Research Activity	Time, GMT		GPS Position		Comments 1	Comments 2
		beginning	end	beginning	end		
1	CTD	04:05	04:10	<u>= 76°44.0'</u> <u>=125°59.7'</u>	<u>= 76°44.6'</u> <u>=125°59.7'</u>		Up to: 67 m

Station Number: KD0204 Data: 12/09/04 Time of beginning: 6:25  
dd/mm/yy hh:mm (GMT)  
 Latitude: 77°03.2'N Longitude: 125°59.6'E Depth: 112 m Ice: 90%  
(navigation chart)

#	Research Activity	Time, GMT		GPS Position		Comments 1	Comments 2
		beginning	end	beginning	end		
2	CTD	06:34	6:38	<u>= 77°03.2'</u> <u>=125°59.6'</u>	<u>= 77°03.2'</u> <u>=126°00.4'</u>		Up to: 106m
3	Rosette	07:10	07:25	<u>= 77°03.1'</u> <u>=126°00.4'</u>	<u>= 77°03.2'</u> <u>=126°00.6'</u>		No samples
4	Net	06:49	07:02	<u>= 77°03.1'</u> <u>=126°00.3'</u>	<u>= 77°03.1'</u> <u>=126°00.3'</u>		Sampling levels: up to 500m

Station Number: KD0304 Data: 12/09/04 Time of beginning: 16:00  
dd/mm/yy hh:mm (GMT)  
 Latitude: 77°19.3'N Longitude: 126°04.4'E Depth: 1420 m Ice: 90%  
(navigation chart)

#	Research Activity	Time, GMT		GPS Position		Comments 1	Comments 2
		beginning	end	beginning	end		
1	CTD	16:00	16:55	<u>= 77°19.3'</u> <u>=126°04.4'</u>	<u>= 77°19.5'</u> <u>=126°03.4'</u>		Up to: 1360 m
2	Rosette	16:50	16:50	<u>= 77°19.2'</u> <u>=126°03.4'</u>	<u>= 77°19.2'</u> <u>=125°03.4'</u>		Sampling levels: 0 m
3	Net	17:01	17:48	<u>= 77°19.6'</u> <u>=126°03.3'</u>	<u>= 77°19.8'</u> <u>=126°02.8'</u>		Up to: 500 m

Station Number: KD0404 Data: 12/09/04 Time of beginning: 19:56  
dd/mm/yy hh:mm (GMT)  
 Latitude: 77°30.7'N Longitude: 125°58.7'E Depth: 1810 m Ice: 90%  
(navigation chart)

#	Research Activity	Time, GMT		GPS Position		Comments 1	Comments 2
		beginning	End	beginning	end		
1	CTD	20:18	21:30	= 77°30.9'	= 77°31.4'		Up to: 1760 m
				=125°58.0'	=125°58.8'		
2	Rosette	21:30	21:30	= 77°31.4'	= 77°31.4'		Sampling levels: 0 m
				=125°58.8'	=125°58.8'		
3	Net	21:31	22:14	= 77°31.4'	= 77°31.7'		Up to: 500 m
				=125°58.8'	=125°59.3'		

Station Number: KD0503 Data: 12/09/04 Time of beginning: 23:45  
dd/mm/yy hh:mm (GMT)  
 Latitude: 77°44.4'N Longitude: 126°00.6'E Depth: 1700 m Ice: 90%  
(navigation chart)

#	Research Activity	Time, GMT		GPS Position		Comments 1	Comments 2
		beginning	end	beginning	end		
1	CTD	23:51	00:50	= 77°44.4'	= 77°44.8'		Up to: 1600 m
			13/09	=126°00.6'	=126°01.9'		
2	Net	00:57	1:39	= 77°44.9'	= 77°45.1'		Up to: 500 m
			13/09	13/09	=126°02.1'		

Station Number: KD0604 Data: 13/09/04 Time of beginning: 04:08  
dd/mm/yy hh:mm (GMT)  
 Latitude: 78°06.2'N Longitude: 126°04.5'E Depth: 2400 m Ice: 90%  
(navigation chart)

#	Research Activity	Time, GMT		GPS Position		Comments 1	Comments 2
		beginning	end	beginning	end		
1	CTD	4:11	5:30	= 78°06.2'	= 78°06.6'		Up to: 2100 m
				=126°04.5'	=126°05.5'		
2	Rosette	4:20	4:25	= 78°06.9'	= 78°06.9'		Sampling levels: 0 m
				=126°04.7'	=126°04.7'		
3	Net	5:37	6:20	= 78°06.6'	= 78°06.8'		Up to: 500 m
				=126°05.5'	=126°05.9'		

Station Number: KD0704 Data: 13/09/04 Time of beginning: 12:14  
dd/mm/yy hh:mm (GMT)  
 Latitude: 78°26.4'N Longitude: 125°38.6'E Depth: 2700 Ice: 90%  
(navigation chart)

#	Research Activity	Time, GMT		GPS Position		Comments 1	Comments 2
		beginning	end	beginning	end		
1	Echo-sounder	01:41 14/09	01:45 14/09	<u>= 78°26.7'</u>	<u>= 78°26.7'</u>		Depth: 2700 m
				<u>=125°40.2'</u>	<u>=125°40.2'</u>		
2	CTD	12:23	13:56	<u>= 78°26.5'</u>	<u>= 78°27.0'</u>		Up to: 2450 m
				<u>=125°38.5'</u>	<u>=125°39.0'</u>		
3	Net	14:20	14:58	<u>= 78°27.0'</u>	<u>= 78°27.3'</u>		Up to: 500 m
				<u>=125°39.0'</u>	<u>=125°39.3'</u>		
6	Mooring deployment	17:24 14/09	11:11 15/09	<u>= 78°26.0'</u>	<u>= 78°25.8'</u>		
				<u>=125°34.7'</u>	<u>=125°36.7'</u>		
7	Mooring recovering	04:00 14/09	07:30 14/09	<u>= 78°26.6'</u>	<u>= 78°27.1'</u>		
				<u>=125°39.8'</u>	<u>=125°40.4'</u>		

Station Number: ICE0104 Data: 14/09/04 Time of beginning: 08:06  
dd/mm/yy hh:mm (GMT)  
 Latitude: 78°25.9'N Longitude: 125°38.4'E Depth: >2000 m Ice: 90%  
(navigation chart)

#	Research Activity	Time, GMT*		GPS Position		Comments 1	Comments 2
		beginning	end	beginning	end		
1	Ice station	08:06	10:30	<u>= 78°25.9'</u>	<u>= 78°26.6'</u>		Sampling list: ice core: 3+4
				<u>=125°38.4'</u>	<u>=125°40.7'</u>		
2	Ice buoy	08:20	08:45	<u>= 78°25.9'</u>	<u>= 78°26.6'</u>	#25887	<u>=78°26.049'</u> <u>=125°38.900'</u>
				<u>=125°38.4'</u>	<u>=125°38.9'</u>		

Station Number: KD0804 Data: 15/09/04 Time of beginning: 16:10  
dd/mm/yy hh:mm (GMT)  
 Latitude: 78°56.9'N Longitude: 126°03.6'E Depth: >3000m Ice: 90%  
(navigation chart)

#	Research Activity	Time, GMT		GPS Position		Comments 1	Comments 2
		beginning	end	beginning	end		
1	CTD	16:15	17:30	<u>= 78°56.9'</u>	<u>= 78°56.9'</u>		Up to: 2000 m
				<u>=126°03.6'</u>	<u>=126°03.5'</u>		
2	Rosette	18:27	19:09	<u>= 78°56.8'</u>	<u>= 80°04.6'</u>		Sampling levels: 20, 30, 38 m
				<u>=126°03.4'</u>	<u>=126°03.4'</u>		
3	Net	17:34	18:16	<u>= 78°56.9'</u>	<u>= 78°56.8'</u>		Up to: 500 m
				<u>=126°03.5'</u>	<u>=126°03.4'</u>		

Station Number: KD0904 Data: 15/09/04 Time of beginning: 23:04  
dd/mm/yy hh:mm (GMT)  
 Latitude: 79°23.2'N Longitude: 125°47.6'E Depth: >3000 m Ice: 90%  
(navigation chart)

#	Research Activity	Time, GMT		GPS Position		Comments 1	Comments 2
		beginning	end	beginning	end		
1	CTD	23:04 16/09	0:31 16/09	<u>= 79°23.2'</u>	<u>= 79°22.6'</u>		Up to: 2000 m
				<u>=125°47.6'</u>	<u>=125°43.9'</u>		
2	Rosette	01:50 16/09	2:29 16/09	<u>= 79°22.4'</u>	<u>= 79°22.4'</u>		Sampling levels: 20, 25, 48, 50m
				<u>=125°40.4'</u>	<u>=125°39.9'</u>		
3	Net	01:02 16/09	1:45 16/09	<u>= 79°22.5'</u>	<u>= 79°22.4'</u>		Up to: 500 m
				<u>=125°42.7'</u>	<u>=125°41.0'</u>		
4	ADCP	00:37:30 16/09	00:52 16/09	<u>= 79°22.6'</u>	<u>= 79°22.5'</u>		Up to 150 m
				<u>=125°43.7'</u>	<u>=125°43.1'</u>		

Station Number: KD1004 Data: 16/09/04 Time of beginning: 5:57  
dd/mm/yy hh:mm (GMT)  
 Latitude: 79°49.6'N Longitude: 126°05.2'E Depth: >3000 m Ice: 80%  
(navigation chart)

#	Research Activity	Time, GMT		GPS Position		Comments 1	Comments 2
		beginning	end	beginning	end		
1	Echo-sounder	6:00	6:10	<u>= 79°49.6'</u>	<u>= 79°49.6'</u>		Depth: 3340m
				<u>=126°05.2'</u>	<u>=126°05.2'</u>		
2	CTD	05:58	07:19	<u>= 79°49.6'</u>	<u>= 79°49.0'</u>		Up to: 2000 m
				<u>=126°05.2'</u>	<u>=126°05.4'</u>		
3	Rosette	08:25	08:55	<u>= 79°48.8'</u>	<u>= 79°48.6'</u>		Sampling levels: 0, 20, 25, 48, 50 m
				<u>=126°05.2'</u>	<u>=126°04.9'</u>		
4	Net	07:46	08:22	<u>= 79°49.0'</u>	<u>= 79°48.8'</u>		Up to: 500 m
				<u>=126°05.3'</u>	<u>=126°05.2'</u>		
5	ADCP	7:20:38	7:35:00	<u>= 79°49.1'</u>	<u>= 79°49.0'</u>		Up to: 150 m
				<u>=126°05.4'</u>	<u>=126°05.4'</u>		



Station Number: KD1104 Data: 16/09/04 Time of beginning: 13:30  
dd/mm/yy hh:mm (GMT)  
 Latitude: 79°48.8'N Longitude: 129°19.5'E Depth: 3280 m Ice: 90%  
(navigation chart)

#	Research Activity	Time, GMT		GPS Position		Comments 1	Comments 2
		beginning	end	beginning	end		
1	CTD	13:34	14:54	<u>= 79°48.8'</u>	<u>= 79°48.6'</u>		Up to: 2200 m
				<u>=129°19.3'</u>	<u>=129°16.9'</u>		
2	Rosette	16:04	16:33	<u>= 79°48.6'</u>	<u>= 79°48.6'</u>		Sampling levels: 0, 20, 25, 48 50m
				<u>=129°15.3'</u>	<u>=129°14.9'</u>		
3	Net	15:20	16:01	<u>= 79°48.6'</u>	<u>= 79°48.6'</u>		Up to: 500 m
				<u>=129°16.3'</u>	<u>=129°15.4'</u>		
4	ADCP	15:00	15:15	<u>= 79°48.6'</u>	<u>= 79°48.6'</u>		Up to 150 m
				<u>=129°16.8'</u>	<u>=129°16.4'</u>		

Station Number: KD1204 Data: 16/09/04 Time of beginning: 22:10  
dd/mm/yy hh:mm (GMT)  
 Latitude: 79°49.8'N Longitude: 133°23.8'E Depth: >3000m Ice: 90%  
(navigation chart)

#	Research Activity	Time, GMT		GPS Position		Comments 1	Comments 2
		beginning	end	beginning	end		
1	CTD	22:13	22:32	<u>= 79°49.8'</u>	<u>= 79°49.5'</u>		Up to: 2000 m
				<u>=133°23.8'</u>	<u>=133°22.1'</u>		
2	Rosette	00:22 17/09	00:53 17/09	<u>= 79°49.3'</u>	<u>= 79°49.3'</u>		Sampling levels: 0, 20, 25, 48 50m
				<u>=133°20.9'</u>	<u>=133°20.0'</u>		
3	Net	23:38	00:19 17/09	<u>= 79°49.5'</u>	<u>= 79°49.3'</u>		Up to: 500 m
				<u>=133°22.1'</u>	<u>=133°20.9'</u>		

Station Number: ICE0204 Data: 17/09/04 Time of beginning: 03:59  
dd/mm/yy hh:mm (GMT)  
 Latitude: 79°50.3'N Longitude: 134°50.0'E Depth: >2000 m Ice: 90%  
(navigation chart)

#	Research Activity	Time, GMT		GPS Position		Comments 1	Comments 2
		beginning	end	beginning	end		
1	Ice station	04:10	06:55	<u>= 79°50.3'</u>	<u>= 79°50.3'</u>		Sampling list: ice core: 2+2
				<u>=134°50.0'</u>	<u>=134°48.8'</u>		
2	Ice buoy	05:00	05:15	<u>=79°50.3'</u>	<u>=79°50.3'</u>	# ?	<u>=79°50.3'</u>

				<u>  =134<sup>0</sup>49.4'</u>	<u>  =134<sup>0</sup>49.4'</u>		<u>  =134<sup>0</sup>49.4'</u>
--	--	--	--	--------------------------------	--------------------------------	--	--------------------------------

Station Number: KD1304 Data: 17/09/04 Time of beginning: 10:53  
dd/mm/yy hh:mm (GMT)  
Latitude: 79<sup>0</sup>50.1'N Longitude: 137<sup>0</sup>48.3'E Depth: 2800 m Ice: 9%  
(navigation chart)

#	Research Activity	Time, GMT		GPS Position		Comments 1	Comments 2
		beginning	end	beginning	end		
1	Echo-sounder	11:00	11:10	<u>  = 79<sup>0</sup>50.0'</u>	<u>  = 79<sup>0</sup>50.0'</u>		Depth: 2825m
				<u>  =137<sup>0</sup>48.2'</u>	<u>  =137<sup>0</sup>47.9'</u>		
2	CTD	11:03	12:19	<u>  = 79<sup>0</sup>50.0'</u>	<u>  = 79<sup>0</sup>49.8'</u>		Up to: 2000 m
				<u>  =137<sup>0</sup>48.2'</u>	<u>  =137<sup>0</sup>46.3'</u>		
3	Rosette	13:07	13:30	<u>  = 79<sup>0</sup>49.7'</u>	<u>  = 79<sup>0</sup>49.6'</u>		Sampling levels: 0, 20, 25, 48 50m
				<u>  =137<sup>0</sup>45.0'</u>	<u>  =137<sup>0</sup>44.8'</u>		
4	Net	12:22	12:57	<u>  = 79<sup>0</sup>49.8'</u>	<u>  = 79<sup>0</sup>49.8'</u>		Up to: 500 m
				<u>  =137<sup>0</sup>46.3'</u>	<u>  =137<sup>0</sup>45.3'</u>		

Station Number: KD1404 Data: 17/09/04 Time of beginning: 18:55  
dd/mm/yy hh:mm (GMT)  
Latitude: 79<sup>0</sup>55.4'N Longitude: 142<sup>0</sup>20.2'E Depth: 1300 m Ice: 80%  
(navigation chart)

#	Research Activity	Time, GMT		GPS Position		Comments 1	Comments 2
		beginning	end	beginning	end		
1	Echo-sounder	18:55	19:00	<u>  = 79<sup>0</sup>55.4'</u>	<u>  = 79<sup>0</sup>55.4'</u>		Depth: 1320m according to echogram
				<u>  =142<sup>0</sup>20.2'</u>	<u>  =142<sup>0</sup>20.2'</u>		
2	CTD	18:59	19:50	<u>  = 79<sup>0</sup>55.4'</u>	<u>  = 79<sup>0</sup>55.2'</u>		Up to: 1200m
				<u>  =142<sup>0</sup>20.2'</u>	<u>  =142<sup>0</sup>18.7'</u>		
3	Rosette	20:43	21:09	<u>  = 79<sup>0</sup>55.1'</u>	<u>  = 79<sup>0</sup>55.0'</u>		Sampling levels: 0, 20, 25, 48 50m
				<u>  =142<sup>0</sup>17.2'</u>	<u>  =142<sup>0</sup>16.4'</u>		
4	Net	19:54	20:40	<u>  = 79<sup>0</sup>55.2'</u>	<u>  = 79<sup>0</sup>55.1'</u>		Up to: 500 m
				<u>  =142<sup>0</sup>18.7'</u>	<u>  =142<sup>0</sup>17.2'</u>		
6	Mooring deployment	01:40	06:35	<u>  = 79<sup>0</sup>55.3'</u>	<u>  = 79<sup>0</sup>55.1'</u>		
		18/09	18/09	<u>  =142<sup>0</sup>26.7'</u>	<u>  =142<sup>0</sup>21.1'</u>		

Station Number: KD1504 Data: 18/09/04 Time of beginning: 10:00  
dd/mm/yy hh:mm (GMT)  
 Latitude: 80°25.8'N Longitude: 140°26.2'E Depth: 1600 m Ice: 90%  
(navigation chart)

#	Research Activity	Time, GMT		GPS Position		Comments 1	Comments 2
		beginning	end	beginning	end		
1	CTD	10:51	11:53	= 80°26.0'	= 80°26.1'		Up to: 1500m
				=140°25.0'	=140°23.8'		
2	Rosette	12:58	13:23	= 80°26.1'	= 80°26.1'		Sampling levels: 0, 20, 25, 48 50m
				=140°22.4'	=140°21.7'		
3	Net	11:55	12:34	= 80°26.1'	= 80°26.1'		Up to: 500 m
				=140°23.8'	=140°22.9'		

Station Number: KD1603 Data: 18/09/04 Time of beginning: 14:55  
dd/mm/yy hh:mm (GMT)  
 Latitude: 80°14.1'N Longitude: 140°58.4'E Depth: 1700 m Ice: 90%  
(navigation chart)

#	Research Activity	Time, GMT		GPS Position		Comments 1	Comments 2
		beginning	end	beginning	end		
1	CTD	14:58	16:00	= 80°14.1'	= 80°14.2'		Up to:1600 m
				=140°58.4'	=140°56.7'		

Station Number: KD1704 Data: 18/09/04 Time of beginning: 17:34  
dd/mm/yy hh:mm (GMT)  
 Latitude: 80°01.7'N Longitude: 141°27.9'E Depth: 1600 m Ice: 90%  
(navigation chart)

#	Research Activity	Time, GMT		GPS Position		Comments 1	Comments 2
		beginning	end	beginning	end		
2	CTD	17:40	18:34	= 80°01.7'	= 80°01.7'		Up to: 1500 m
				=141°27.8'	=141°26.8'		

Station Number: KD1804 Data: 18/09/04 Time of beginning: 20:51  
dd/mm/yy hh:mm (GMT)  
 Latitude: 79°35.3'N Longitude: 142°24.0'E Depth: 1170 m Ice: 90%  
(navigation chart)

#	Research Activity	Time, GMT		GPS Position		Comments 1	Comments 2
		beginning	end	beginning	end		
1	CTD	20:57	21:37	= 79°35.3'	= 79°35.3'		Up to: 1100 m

				<u>  </u> =142 <sup>0</sup> 23.8'	<u>  </u> =142 <sup>0</sup> 22.0'	
--	--	--	--	-----------------------------------	-----------------------------------	--

Station Number: KD1904 Data: 18/09/04 Time of beginning: 23:10  
dd/mm/yy hh:mm (GMT)  
Latitude: 79<sup>0</sup>25.4'N Longitude: 143<sup>0</sup>01.1'E Depth: 500 m Ice: 90%  
(navigation chart)

#	Research Activity	Time, GMT		GPS Position		Comments 1	Comments 2
		beginning	end	beginning	end		
1	CTD	23:12	23:31	<u>  </u> = 79 <sup>0</sup> 25.4'	<u>  </u> = 79 <sup>0</sup> 25.5'		Up to: 450 m
				<u>  </u> =143 <sup>0</sup> 01.1'	<u>  </u> =143 <sup>0</sup> 00.5'		
2	Rosette	00:33 19/09	00:58 19/09	<u>  </u> = 79 <sup>0</sup> 25.9'	<u>  </u> = 79 <sup>0</sup> 26.1'		Sampling levels: 0, 20, 25, 48 50m
				<u>  </u> =142 <sup>0</sup> 57.3'	<u>  </u> =142 <sup>0</sup> 56.6'		
3	Net	23:42	00:26 19/09	<u>  </u> = 79 <sup>0</sup> 25.5'	<u>  </u> = 79 <sup>0</sup> 25.8'		Up to: 500 m
				<u>  </u> =143 <sup>0</sup> 00.5'	<u>  </u> =142 <sup>0</sup> 57.5'		

Station Number: KD2004 Data: 19/09/04 Time of beginning: 02:07  
dd/mm/yy hh:mm (GMT)  
Latitude: 79<sup>0</sup>15.2'N Longitude: 143<sup>0</sup>29.2'E Depth: 218 m Ice: 90%  
(navigation chart)

#	Research Activity	Time, GMT		GPS Position		Comments 1	Comments 2
		beginning	end	beginning	end		
2	CTD	02:12	02:20	<u>  </u> = 79 <sup>0</sup> 15.2'	<u>  </u> = 79 <sup>0</sup> 15.3'		Up to: 200 m
				<u>  </u> =143 <sup>0</sup> 29.0'	<u>  </u> =143 <sup>0</sup> 29.0'		

Station Number: KD2104 Data: 19/09/04 Time of beginning: 04:22  
dd/mm/yy hh:mm (GMT)  
Latitude: 79<sup>0</sup>00.0'N Longitude: 143<sup>0</sup>59.8'E Depth: 98m Ice: 90%  
(navigation chart)

#	Research Activity	Time, GMT*		GPS Position		Comments 1	Comments 2
		beginning	end	beginning	end		
1	CTD	04:31	04:40	<u>  </u> = 79 <sup>0</sup> 00.0'	<u>  </u> = 79 <sup>0</sup> 00.0'		Up to: 90 m
				<u>  </u> =144 <sup>0</sup> 00.0'	<u>  </u> =144 <sup>0</sup> 00.2'		
2	Rosette	05:02	05:32	<u>  </u> = 79 <sup>0</sup> 00.0'	<u>  </u> = 79 <sup>0</sup> 00.0'		Sampling levels: 0, 20, 25, 48 50m
				<u>  </u> =144 <sup>0</sup> 00.5'	<u>  </u> =144 <sup>0</sup> 00.5'		
3	Net	04:42	04:59	<u>  </u> = 79 <sup>0</sup> 00.0'	<u>  </u> = 79 <sup>0</sup> 00.0'		Up to: 90 m
				<u>  </u> =144 <sup>0</sup> 00.2'	<u>  </u> =144 <sup>0</sup> 00.0'		

Station Number: KD2204 Data: 19/09/04 Time of beginning: 10:30  
dd/mm/yy hh:mm (GMT)  
 Latitude: 79°30.4'N Longitude: 138°59.4'E Depth: >2000m Ice: 80%  
(navigation chart)

#	Research Activity	Time, GMT		GPS Position		Comments 1	Comments 2
		beginning	end	beginning	end		
1	CTD	10:33	11:50	<u>= 79°30.4'</u>	<u>= 79°30.5'</u>		Up to: 1900 m
				<u>=138°59.4'</u>	<u>=138°56.8'</u>		
2	Rosette	12:35	13:21	<u>= 79°30.6'</u>	<u>= 79°30.6'</u>		Sampling levels: 0, 20, 25, 48 50m
				<u>=138°55.4'</u>	<u>=138°53.8'</u>		
3	Net	11:53	12:28	<u>= 79°30.5'</u>	<u>= 79°30.6'</u>		Up to: 500 m
				<u>=138°56.8'</u>	<u>=138°55.7'</u>		

Station Number: KD2304 Data: 19/09/04 Time of beginning: 16:45  
dd/mm/yy hh:mm (GMT)  
 Latitude: 78°59.7'N Longitude: 137°02.0'E Depth: 1920m Ice: 90%  
(navigation chart)

#	Research Activity	Time, GMT		GPS Position		Comments 1	Comments 2
		beginning	end	beginning	end		
1	CTD	16:46	17:56	<u>= 78°59.7'</u>	<u>= 78°59.7'</u>		Up to: 1810 m
				<u>=137°02.0'</u>	<u>=136°59.7'</u>		
2	Rosette	18:46	19:01	<u>= 78°59.7'</u>	<u>= 78°59.7'</u>		Sampling levels: 0, 20, 25, 48 50m
				<u>=136°58.4'</u>	<u>=136°57.4'</u>		
3	Net	18:00	18:35	<u>= 78°59.7'</u>	<u>= 78°59.7'</u>		Up to: 500 m
				<u>=136°59.6'</u>	<u>=136°58.4'</u>		

Station Number: KD2404 Data: 19/09/04 Time of beginning: 22:45  
dd/mm/yy hh:mm (GMT)  
 Latitude: 78°45.2'N Longitude: 133°53.3'E Depth: >2000m Ice: 90%  
(navigation chart)

#	Research Activity	Time, GMT		GPS Position		Comments 1	Comments 2
		beginning	end	beginning	end		
1	CTD	22:47	00:04 20/09	<u>= 79°45.2'</u>	<u>= 78°45.3'</u>		Up to: 2000 m
				<u>=133°53.3'</u>	<u>=133°50.4'</u>		
2	Rosette	00:55 20/09	01:22 20/09	<u>= 78°45.3'</u>	<u>= 78°45.3'</u>		Sampling levels: 0, 20, 25, 48 50m
				<u>=133°48.8'</u>	<u>=133°48.7'</u>		

3	Net	00:06	00:51	<u>= 78°45.3'</u>	<u>= 78°45.3'</u>	Up to: 500 m
		20/09	20/09	<u>=133°50.4'</u>	<u>=133°48.8'</u>	

Station Number: KD2504 Data: 20/09/04 Time of beginning: 06:18  
dd/mm/yy hh:mm (GMT)  
Latitude: 78°30.1'N Longitude: 131°00.0'E Depth: 2500m Ice: 100%  
(navigation chart)

#	Research Activity	Time, GMT		GPS Position		Comments 1	Comments 2
		beginning	end	beginning	end		
1	CTD	06:26	07:42	<u>= 78°30.1'</u> <u>=130°59.7'</u>	<u>= 78°29.9'</u> <u>=130°57.1'</u>		Up to: 2000 m
2	Rosette	08:25	08:49	<u>= 78°29.9'</u> <u>=130°55.6'</u>	<u>= 78°29.9'</u> <u>=130°54.9'</u>		Sampling levels: 0, 20, 25, 48 50m
3	Net	07:45	08:25	<u>= 78°29.9'</u> <u>=130°57.1'</u>	<u>= 78°29.9'</u> <u>=130°55.6'</u>		Up to: 500 m

Station Number: KD2604 Data: 20/09/04 Time of beginning: 14:33  
dd/mm/yy hh:mm (GMT)  
Latitude: 78°09.7'N Longitude: 127°59.9'E Depth: >2000m Ice: 100%  
(navigation chart)

#	Research Activity	Time, GMT		GPS Position		Comments 1	Comments 2
		beginning	end	beginning	end		
1	CTD	14:45	16:06	<u>= 78°09.6'</u> <u>=127°59.4'</u>	<u>= 78°09.3'</u> <u>=127°57.4'</u>		Up to: 2000 m
2	Rosette	17:03	17:27	<u>= 78°09.0'</u> <u>=127°55.7'</u>	<u>= 78°08.9'</u> <u>=127°55.0'</u>		Sampling levels: 0, 20, 25, 48, 50m
3	Net	16:16	16:55	<u>= 78°09.3'</u> <u>=127°57.1'</u>	<u>= 78°09.1'</u> <u>=127°56.0'</u>		Up to: 500 m

**Appendix 2: Ship track of icebreaker Kapitan Dranirsyn during NABOS-04 expedition  
(V.Smolianitsky, AARI)**

Latitude	longitude	date	time (UTC)	SOG(knots)	COG(deg)
70.00257	31.89018 2	05.09.2004	12:00:00	13.125	90.0
69.30717	34.44471 2	05.09.2004	18:00:00	6.750	225.0
69.30217	34.36685 1	06.09.2004	18:00:00	1.100	90.0
69.49003	38.22707 2	07.09.2004	00:00:00	13.300	83.5
69.65997	41.88467 2	07.09.2004	06:00:00	15.200	78.7
69.83191	46.38154 2	07.09.2004	12:00:00	16.333	81.5
70.00843	50.98858 2	07.09.2004	18:00:00	16.467	87.0
70.19633	55.52201 2	08.09.2004	00:00:00	15.100	90.0
70.86548	59.26991 2	08.09.2004	06:00:00	14.767	41.3
71.98436	62.39992 2	08.09.2004	12:00:00	15.346	42.9
73.11775	65.83890 2	08.09.2004	18:00:00	15.500	41.7
74.00058	69.82170 2	09.09.2004	00:00:00	14.856	90.0
74.06882	75.19663 2	09.09.2004	06:00:00	14.872	82.8
74.35501	80.54445 2	09.09.2004	12:00:00	15.494	59.6
75.13059	85.43494 2	09.09.2004	18:00:00	15.400	43.1
75.81926	90.75986 2	10.09.2004	00:00:00	15.126	61.1
76.48042	96.21661 2	10.09.2004	06:00:00	14.163	63.6
77.25847	101.02500 2	10.09.2004	12:00:00	13.797	49.6
77.67043	106.51550 2	10.09.2004	18:00:00	14.400	102.2
77.09881	111.26510 2	11.09.2004	00:00:00	12.596	130.7
76.48162	115.24340 2	11.09.2004	06:00:00	12.760	165.4
75.70497	116.75130 2	11.09.2004	12:00:00	14.200	93.3
75.48540	122.11820 2	11.09.2004	18:00:00	15.685	76.1
76.46690	125.84770 2	12.09.2004	00:00:00	7.462	14.7
77.01391	125.95670 2	12.09.2004	06:00:00	7.329	5.4
77.32878	126.11610 2	12.09.2004	12:00:00	4.450	217.8
77.33138	126.04810 2	12.09.2004	18:00:00	5.100	149.7
77.74075	126.01210 2	13.09.2004	00:00:00	.500	340.5
78.11110	126.09300 2	13.09.2004	06:00:00	.500	270.0
78.43872	125.66830 2	13.09.2004	12:00:00	1.000	141.3
78.46505	125.68930 2	13.09.2004	18:00:00	.400	90.0
78.44592	125.63880 2	14.09.2004	00:00:00	.453	31.0
78.44980	125.66800 2	14.09.2004	06:00:00	.500	.0
78.45086	125.69730 2	14.09.2004	12:00:00	.600	16.7
78.43369	125.57220 2	14.09.2004	18:00:00	2.075	20.4
78.44728	125.63160 2	15.09.2004	00:00:00	.133	90.0
78.41838	125.63370 2	15.09.2004	06:00:00	.200	321.2
78.42973	125.58940 2	15.09.2004	12:00:00	.300	343.3
78.94682	126.05770 2	15.09.2004	18:00:00	.000	270.0
79.37970	125.75820 2	16.09.2004	00:00:00	.550	270.0
79.82667	126.08820 2	16.09.2004	06:00:00	.400	270.0
79.80587	128.27440 2	16.09.2004	12:00:00	10.067	65.5
79.82928	130.06000 2	16.09.2004	18:00:00	10.167	82.8
79.82372	133.36320 2	17.09.2004	00:00:00	.300	270.0
79.83869	134.81250 2	17.09.2004	06:00:00	.100	340.6
79.83075	137.78470 2	17.09.2004	12:00:00	.200	270.0
79.89356	141.60660 2	17.09.2004	18:00:00	17.333	46.5
79.92613	142.31250 2	18.09.2004	00:00:00	.300	270.0
79.91953	142.36980 2	18.09.2004	06:00:00	.360	90.0
80.43433	140.39610 2	18.09.2004	12:00:00	.300	180.0
80.02862	141.45830 2	18.09.2004	18:00:00	.200	270.0
79.42765	142.98140 2	19.09.2004	00:00:00	.700	270.0
79.00176	143.79680 2	19.09.2004	06:00:00	9.547	301.7
79.50837	138.94630 2	19.09.2004	12:00:00	.321	270.0
78.99537	136.99550 2	19.09.2004	18:00:00	.400	270.0
78.75438	133.84590 2	20.09.2004	00:00:00	.600	270.0
78.51658	131.15240 2	20.09.2004	06:00:00	9.300	237.5
78.29075	129.24230 2	20.09.2004	12:00:00	5.600	232.8
78.12406	127.86580 2	20.09.2004	18:00:00	11.623	201.2
77.31667	126.09220 2	21.09.2004	00:00:00	.983	270.0
77.32220	126.23660 2	21.09.2004	06:00:00	.620	270.0
76.30400	124.07840 2	21.09.2004	12:00:00	15.744	245.6
75.62843	119.70730 2	21.09.2004	18:00:00	7.930	212.8
76.07693	117.65130 2	22.09.2004	00:00:00	6.700	354.7

76.52735	117.35310	2	22.09.2004	06:00:00	5.600	341.4
76.93540	116.17010	2	22.09.2004	12:00:00	8.900	.0
77.28230	113.70680	2	22.09.2004	18:00:00	12.667	277.2
77.25735	112.79770	2	23.09.2004	00:00:00	.100	90.0
77.40064	112.11230	2	23.09.2004	06:00:00	13.161	310.5
77.89133	107.97400	2	23.09.2004	12:00:00	15.461	276.3
77.90711	102.05660	2	23.09.2004	18:00:00	18.752	242.2
76.72872	98.66253	2	24.09.2004	00:00:00	18.461	227.4
75.95973	91.85540	2	24.09.2004	06:00:00	17.160	241.9
75.24268	85.82764	2	24.09.2004	12:00:00	16.758	222.3
74.35771	80.61433	2	24.09.2004	18:00:00	16.334	240.8

### Appendix 3: RV Lance cruise log

Date	Activity (UTC time)
Tue 31/8	0400 departure LYB to Billefjorden/Brucebyen for field equipment pickup. 1125 RADNOR water sampling outside Adventfjorden. 1130 steaming toward F11-6.
Wed 1/9	1030 arrival F11-6. Mooring on deck 1215. CTD no 1-4.
Thu 2/9	0630 arrival F12-6. Remnants of F12 on deck 0720. 0840 arrival F13-6. Mooring on deck 1135. 1250 arrival F14-6. Mooring on deck 1315. 1845 arrival F17-1. Mooring on deck 1900. 1915 arrival F18-1. F18-1 does not respond or release. Engine maintenance, drifting for two hours. CTD no 5-13.
Fri 3/9	0800 arrival F19-1. Ice cover to dense, can not release. Sea ice work. 1200 retrying F19-1 recovery. Mooring under very large ice floe, can not release. CTD no 13-14.
Sat 4/9	0615 releasing F19-1. Mooring on deck 0700. Dismantling F19-1 (tube). Assembling F19-2 (new tube with RDCP600). CTD no 15.
Sun 5/9	Bad weather, not possible to work on deck, to much wind for CTDs because of fast drift of ship and ice. Waiting. 1500: Trying to do CTDs westward, but reaches the fast ice edge after one station. Can not penetrate further. CTD no 16.
Mon 6/9	0950 deploying F19-2 at N 78°49.832' W 012°30.074', depth 192 m. Assembling F17-2 (ADCP) and F18-2 (tube). Sea ice work.
Tue 7/9	07-0800 dredging for F18-1. Mooring not found. 1000 deploying F18-2 at N 78°49.981' W 008°04.646', depth 226 m.



	1215 deploying F17-2 at N 78°49.888' W 007°59.274', depth 215 m. Assembling F14-7. 1725 deploying F14-7 at N 78°48.992' W 006°26.834', depth 282 m. CTD no 17-20.
Wed 8/9	Assembling F13-7 (deep mooring with tube and iceberg protecting cone around ULS, very time consuming). 1745 deploying F13-7 at N 78°50.700' W 005°00.926', depth 1028 m. CTD no 21-27.
Thu 9/9	Assembling F12-7. 1210 deploying F12-7 at N 78°49.765' W 004°01.528', depth 1855 m. Assembling F11-7. Sea ice work. 1850 deploying F11-7 at N 78°49.917' W 003°15.415', depth 2378 m. CTD no 28-30.
Fri 10/9	CTDs toward Ny-Ålesund. CTD no 31-40.
Sat 11/9	CTDs toward Ny-Ålesund. CTD no 41-50. Arrival Ny-Ålesund 1000. Offloading/loading. Departure Ny-Ålesund 1600. Steaming toward NABOS M4 mooring.
Sun 12/9	2000 arrival first M4 CTD station. CTD section and depth survey. CTD no 51-54.
Mon 13/9	CTD no 55-58, finishing section. 1145 deploying NABOS M4 mooring at N 81°33.761' E 030°55.391' depth 1012 m. Steaming toward Yermak plateau.
Tue 14/9	1000 arrival Virgohamna. Dismantling equipment and tools from mooring work while in lee, packing. 1610 starting on the Yermak plateau sections. CTD no 59-63.
Wed 15/9	CTD no 54-73.
Thu 16/9	CTD no 74-79. 2030 starting steaming toward Tromsø
Fri 17/9	Steaming toward Tromsø
Sat 18/9	Steaming toward Tromsø
Sun 19/9	0900 arrival Tromsø

#### Appendix 4: RV Lance stations list

Station	YYYY MM DD	HH(UTC) MIN	Lat, deg	Lon, deg	Depth, m
51	2004 9 12	20 13	81.373	30.963	184
52	2004 9 12	21 17	81.428	31.003	300
53	2004 9 12	22 41	81.445	31.000	400
54	2004 9 12	23 22	81.455	31.000	501
55	2004 9 13	00 18	81.535	31.000	809
56	2004 9 13	01 19	81.562	31.000	1000
57	2004 9 13	02 24	81.617	31.000	2038
58	2004 9 13	04 16	81.663	31.000	2500